EMID-701996

DEPARTMENT OF ENERGY

Environmental Management Los Alamos Field Office (EM-LA)
Los Alamos, New Mexico 87544

EMLA-2022-BF077-02-001

RECEIVED
APR 21 2022
NMED Hazardous
Waste Bureau

April 21, 2022

Mr. Rick Shean
Bureau Chief
Hazardous Waste Bureau
New Mexico Environment Department
2905 Rodeo Park Drive East, Building 1
Santa Fe, NM 87505-6313

Subject: Submittal of the 2021 Sandia Wetland Performance Report

Dear Mr. Shean:

Enclosed please find two hard copies with electronic files of the "2021 Sandia Wetland Performance Report." The U.S. Department of Energy (DOE) Environmental Management Los Alamos Field Office (EM-LA) and Newport News Nuclear BWXT-Los Alamos, LLC (N3B) have prepared this report in response to requirements set forth in the "Work Plan and Final Design for Stabilization of the Sandia Canyon Wetland." The requirement to design a Sandia wetland monitoring program was previously set forth in the New Mexico Environment Department's (NMED's) "Approval with Modification, Interim Measures Work Plan for Stabilization of the Sandia Canyon Wetland," in response to the previously submitted "Interim Measures Work Plan for Stabilization of the Sandia Canyon Wetland." The "2020 Sandia Wetland Performance Report" was approved with comments by NMED on May 3, 2021.

Pursuant to Section XXIII.C of the Compliance Order on Consent, EM-LA, N3B, and NMED met in a pre-submission review meeting on December 7, 2021, to discuss changes in monitoring requirements for 2022. EM-LA, N3B, and NMED met in a follow-up meeting on January 26, 2022. The enclosed report captures the changes discussed.

If you have any questions, please contact Amanda White at (505) 309-1366 (amanda.white@em-la.doe.gov) or Cheryl Rodriguez at (505) 414-0450 (cheryl.rodriguez@em.doe.gov).

Sincerely,

ARTURO DURAN

Digitally signed by ARTURO DURAN
Date: 2022.04.20 17:34:29 -06'00'

Arturo Q. Duran
Compliance and Permitting Manager
U.S. Department of Energy
Environmental Management
Los Alamos Field Office

Enclosures:

1. Two hard copies with electronic files – 2021 Sandia Wetland Performance Report (EM2022-0012)

cc (letter with hard-copy enclosure[s]):
Cheryl Rodriguez, EM-LA

cc (letter with CD/DVD enclosure[s]):
Laurie King, EPA Region 6, Dallas, TX
Raymond Martinez, San Ildefonso Pueblo, NM
Dino Chavarria, Santa Clara Pueblo, NM
Steve Yanicak, NMED-DOE-OB
Chris Catechis, NMED-RPD

cc (letter emailed):
Jennifer Payne, LANL
Stephen Hoffman, NA-LA
William Alexander, N3B
Allison Chan, N3B
Bryan Dail, N3B
Emily Day, N3B
Audrey Krehlik, N3B
Kim Lebak, N3B
Joseph Legare, N3B
Pamela Maestas, N3B
Keith McIntyre, N3B
Joseph Murdock, N3B
Karly Rodriguez, N3B
Joseph Sena, N3B
Steve Veenis, N3B
Amanda White, N3B
M. Lee Bishop, EM-LA
Michael Mikolanis, EM-LA
David Nickless, EM-LA
emla.docs@em.doe.gov
n3brecords@em-la.doe.gov
Public Reading Room (EPRR)
PRS Website

April 2022
EM2022-0012

2021 Sandia Wetland Performance Report

EM2022-0012

2021 Sandia Wetland Performance Report

April 2022

Responsible project director:

Printed Name	Signature	Title	Organization	Date
Steve Veenis	Steve Veenis	Project Director	Water Program	4/6/22

Responsible N3B representative:

Printed Name	Signature	Title	Organization	Date
Troy Thomson	Troy Thomson	Program Manager	N3B Environmental Remediation Program	4/6/22

Responsible DOE EM-LA representative:

Printed Name	Signature	Title	Organization	Date
Arturo Q. Duran	ARTURO DURAN Digitally signed by ARTURO DURAN Date: 2022.04.20 17:35:26 -06'00'	Compliance and Permitting Manager	Office of Quality and Regulatory Compliance	

EXECUTIVE SUMMARY

The 2021 Sandia wetland performance report is the eighth annual performance report following the 2012 to 2014 baseline that assessed the overall condition of the wetland at the head of Sandia Canyon. Sandia wetland monitoring was performed in the context of the wetland's ability to mitigate migration of contaminants of concern (i.e., chromium, polychlorinated biphenyls [PCBs], and polycyclic aromatic hydrocarbons) detected in wetland sediments as a result of historical releases at Los Alamos National Laboratory (the Laboratory). The geochemistry and physical stability of wetland sediments, along with the extent of wetland vegetation, are the key indicators of wetland conditions. The condition of the wetland is assessed to evaluate the effectiveness of the grade-control structure (GCS) completed in 2013 at the terminus of the wetland and to monitor changes to the Laboratory's operational practices that have affected outfall volumes discharging to the wetland. This report presents the results of monitoring conducted for surface water, alluvial groundwater, and geomorphology between January and December 2021, in the context of the baseline conditions presented in the "Sandia Wetland Performance Report, Baseline Conditions 2012–2014."

The monitoring conducted during the performance period indicates the Sandia wetland remains stable following the installation of the GCS, even with generally lower, but variable effluent volumes entering the wetland. The GCS continues to be effective in arresting headcutting at the terminus of the wetland. Groundwater within the shallow alluvium remains in a reducing condition, with no obvious detrimental temporal trends in chemistry observed. Sampling of hexavalent chromium in the base flow and alluvial groundwater indicates concentrations at or near the method detection limit and below the appropriate New Mexico water quality criteria. Water levels in the wetland remained similar over the last 8 yr, with temporary drops in the easternmost transect during summer months. Despite the observed decreases after the Sanitary Effluent Reclamation Facility came online in 2012, water levels remained sufficiently high to sustain obligate wetland vegetation, and analytical results of iron and manganese indicate alluvial groundwater remained in strongly reducing conditions in most wells upgradient of the GCS. Chloride, generally considered a conservative tracer and highly mobile, nonreactive chemical species, indicates similar trends upgradient (E121) and downgradient (E123) at gaging stations along the wetland. Storm water data also indicate that the GCS has had a positive effect in reducing contaminant mobility, and this trend continued through 2021. Storm flow suspended sediment and chromium concentrations have decreased compared with pre- and post-GCS data immediately downgradient of the wetland at gaging station E123, presumably from eliminating headcutting at the terminus of the wetland and from sediment-trapping efficiency of the dense vegetation within the wetland. Historically, total PCB concentrations in base flow and storm flow have been lower post-GCS, but in 2020 and 2021, total PCB concentrations appear to be more varied in both flow conditions, especially at E122. Fewer storm flow samples were collected in 2020 compared with 2021 because of the drought in 2020, but PCB concentrations were similar at E121 in both years, slightly higher at E122 in 2021, and lower at E123 in 2021.

Geomorphic-change detection studies indicate the wetland remains stable, with no significant geomorphic change experienced between years. Beginning in 2019, ground-based survey techniques were replaced by aerial-based survey techniques, which provide a more accurate and robust data set for both geomorphic and vegetation data. The initial results of the aerial-based geomorphic survey conducted in 2021, along with visual inspections of the wetland area, suggest that no significant geomorphic changes have occurred. Additional ground surveys and an aerial-based vegetation survey in 2022 will allow for a more comprehensive assessment of the physical stability of the wetland area.

Surface water and alluvial groundwater analytical data collected in 2021 were compared with New Mexico surface water quality criteria (20.6.4 New Mexico Administrative Code [NMAC]) and groundwater standards (20.6.2 NMAC), respectively. Exceedances of water quality criteria are presented in this report and are determined to be associated with historical Laboratory releases, runoff from developed areas in the upper watershed, naturally occurring chemicals, and/or the natural reducing conditions of the wetland within the alluvial system.

CONTENTS

Figures

Tables

Appendices

1.0 INTRODUCTION

This report addresses performance of the Sandia wetland for calendar year (CY) 2021. Section 1 of this report describes the Sandia wetland and contaminants in the wetland sediment and discusses Sandia wetland monitoring goals. Section 2 discusses Sandia wetland monitoring methods and summarizes monitoring conducted in 2021. Section 3 discusses monitoring results, and section 4 presents conclusions. Appendixes include acronyms, a metric conversion table, and definitions of data qualifiers (Appendix A); an evaluation of geomorphic changes in 2021 (Appendix B); a summary of watershed mitigation inspections in 2021 (Appendix C); and analytical gaging station, alluvial well, and sediment data; water-level data; and 5-min stage, discharge, and precipitation data (Appendix D, on CD included with this document).

The Sandia wetland, located at the head of Sandia Canyon, has expanded from a relatively small footprint in the early 1950s to its current size in response to liquid effluent released by Los Alamos National Laboratory (LANL or the Laboratory). Throughout the course of Laboratory operations, the wetland has been perpetuated by sustained effluent releases to the canyon from outfalls located in Technical Area 03 (TA-03). Contaminants, namely chromium, polychlorinated biphenyls (PCBs), and polycyclic aromatic hydrocarbons (PAHs), are present in wetland sediments because of historical releases from Laboratory operations (LANL 2009, 107453). Ensuring the stability of the wetland has become an important aspect of managing the inventory of contaminants entrained in wetland sediments. Information on radioactive materials and radionuclides, including the results of sampling and analysis of radioactive constituents, is voluntarily provided to the New Mexico Environment Department (NMED) in accordance with DOE policy.

Through monitoring and reporting, the performance of the wetland has been studied since 2014, following initial baseline monitoring that occurred between 2012 and 2014. Monitoring efforts have been designed to evaluate the physical and chemical stability of the wetland that provide insight regarding the ability of the wetland to contain contaminants of concern and prevent migration past the grade-control structure (GCS) that was installed in 2013 (Figure 1.0-1).

1.1 Wetland Description

The Sandia wetland is a cattail-dominated wetland primarily sustained by effluent from the National Pollutant Discharge Elimination System ([NPDES] Permit No. NM002835)-permitted outfalls 001 and 03A199. An additional NPDES-permitted outfall, 03A027, discharged effluent from 2012 to 2016 (EPA 2014, 600257; EPA 2015, 701237). Operational changes occurring at the Sanitary Effluent Reclamation Facility (SERF) since mid-2012 have influenced the outfall volumes and the chemical makeup of the effluent (Figures 1.1-1 to 1.1-5). The wetland has experienced generally decreased liquid outfall effluent volumes (both daily and annually) from NPDES-permitted Outfalls 001 and 03A027 as part of the SERF expansion project and water reuse programs at the Laboratory. However, since the initial decrease in effluent volume, Outfall 001 has shown a slight increasing trend in volume over the period of monitoring in the Sandia wetland (Figure 1.1-1). As part of the SERF expansion, a portion of the effluent previously released to Sandia Canyon is now being rerouted to cooling towers at various facilities, including the Strategic Computing Complex (SCC) and the Trinity supercomputer. In September 2019, a temperature limit of 20°C was imposed on all discharges to Outfall 001. In the warmer months, this requirement necessitates rerouting some of the water to the power plant cooling towers before being discharged, to ensure compliance with the temperature limit (Griffin 2021, 701199). No operational changes that would affect the quantity or quality of water being discharged to the wetland occurred in 2021 (LANL 2022, 701910). Descriptions of earlier operational changes at SERF can be found in previous years' Sandia wetland performance reports (LANL 2015, 600399; LANL 2016, 601432; LANL 2017, 602341; LANL 2018, 603022; N3B 2019, 700415).

The 2019 draft discharge permit, NPDES Permit No. NM0028355, contemplated additional reuse by the SCC, rerouting cooling tower blowdown, and recycling to SERF, which may impact discharge from the dominant outfall (001). Discharge is recommended to be maintained at a minimum of 40,000 gallons per day (gpd) during months when evapotranspiration is highest. This discharge level is believed to be sufficient to maintain the ecologic, hydrologic, and geochemical functioning of the wetland, as described in the "100% Design Memorandum for Sandia Wetlands Stabilization Project" (LANL 2012, 240016). If future changes to effluent volume or chemistry are shown to adversely impact the wetland, or wetland evapotranspiration increases appreciably, adaptive management will be used to ensure wetland stability (e.g., engineered controls to manage sediment and water distribution to increase the area of wetland saturation). Currently, there is continuous discharge from the outfall to the wetland area. The average daily outfall volume for 2021 (209,000 gpd) exceeds the 40,000 gpd recommended discharge by a significant amount. Snowmelt and precipitation (direct and indirect) augment discharge flows necessary to support the wetland.

Surface water is generally present in a discrete channel (though in some areas surface water spreads from bank to bank) and passes through the wetland with a short residence time relative to alluvial groundwater (LANL 2009, 107453; LANL 2014, 257590). Wetland sediments are underlain by Bandelier Tuff, upon which alluvial groundwater is perched. A water-balance analysis conducted in 2007 and 2008 showed little surface water loss (approximately 2% of both effluent and runoff) occurs through the wetland (LANL 2009, 107453). A direct-current (DC) electrical-resistivity-based geophysical survey found that large continuous areas of the wetland are underlain by highly resistive welded tuffs (Qbt 2 of the Tshirege Member of the Bandelier Tuff) that represent a significant barrier to the infiltration of alluvial groundwater into the subsurface (LANL 2012, 228624). In several areas, the survey also identified subvertical conductive zones that penetrate the upper bedrock units and, in some cases, appear to correlate with mapped fault and/or fracture zones. These conductive zones may represent present-day or historical infiltration pathways. However, the DC resistivity data do not differentiate between conductive zones that contain higher water content (possibly representing active infiltration) and wetted clay-rich fracture fill that may hinder infiltration.

A GCS was installed in the lower portion of the wetland in 2013 to arrest an active headcut (up to 3 m high) and to help maintain favorable hydrologic and geochemical conditions that would minimize contaminant migration (LANL 2011, 203454). The GCS was designed to meet the following objectives:

- Minimize erosion during large flow events
- Provide an even grade to allow wetland expansion and further stabilization
- Be sufficiently impervious to prevent the draining of alluvial soils and promote a high water table
- Facilitate nonchannelized flow
- Support wetland function under potentially reduced effluent conditions

The GCS transitions the grade approximately 11 vertical ft from the elevation of the wetland just upgradient of the former headcut location to the natural streambed just upstream of gaging station E123. To maintain grade and to reduce the overall fill and size of a single structure, a set of three steel sheet-pile walls was installed with decreasing elevation drops. Downstream of the third sheet-pile wall, a cascade pool was constructed of boulders and cobbles to transition to the final grade. The transition from the wetland above the GCS to the stream channel below is gradual, smooth, and stepped to prevent erosive flows that could scour and destabilize the stream reach below the structure (LANL 2013, 251743).

The design of the GCS should allow for a reduction of outfall effluent discharge into the wetland without compromising the physical and geochemical function of the wetland, particularly of the eastern terminus where the GCS more intimately controls wetland water levels. The area behind the GCS was backfilled and wetland vegetation was planted to allow expansion of the wetland area. These measures physically stabilize the wetland by reducing sediment and associated contaminant transport into the lower sections of the canyon and should also maintain reducing conditions within the sediment near the terminus of the wetland, thus contributing to the goal of reducing potential contaminant transport (LANL 2013, 251743). A set of as-built diagrams for the GCS is presented in Appendix C of the completion report for the construction of the GCS (LANL 2013, 251743).

Installation of the GCS has led to cessation of headcutting at the terminus of the wetland and has created an impermeable barrier to subsurface flow, such that alluvial groundwater must resurface before exiting the wetland. Given the impermeable nature of this barrier and the largely impermeable tuff underlying the wetland, the system can conceptually be thought of as a bathtub that effectively holds water with excess water spilling over the GCS at the wetland terminus. Annual evaluation of base flow rates confirms this “bathtub” assumption as rates entering and exiting the wetland are similar, although this assumption breaks down during storm events because of additional flow from tributaries, e.g., from the former Los Alamos County landfill. However, as long as water inputs from the outfalls exceed wetland evapotranspiration, even significantly reduced outfall discharge may sustain water levels and sufficient saturation within wetland sediments. Extreme decreases in effluent input volumes into the wetland, however, could potentially result in wetland dewatering. The wetland sediment is typically saturated at the eastern end of the wetland; these conditions extend westward, but near-surface sediment is unsaturated at the margins and at the western end of the wetland. Based on vegetation surveys conducted between 2017 and 2019, there appears to be recovery of cattails in the west end of the wetland, which had been largely dewatered when the outfall that discharged directly into the wetland was relocated further upstream to the current location of Outfall 001. Channel meandering and sediment redistribution, however, are resulting in the reestablishment and expansion of cattails in this area (LANL 2016, 601432). The volume of effluent entering the wetland has remained sufficiently high to maintain both the height of the water table and the area of wetland vegetation cover (LANL 2016, 601432). The wetland vegetation community is important in mitigating storm water–related mobilization of contaminants through root binding and physical trapping of suspended sediments.

1.2 Contamination in Wetland Sediment

Hexavalent chromium [Cr(VI)] was historically released into liquid effluent from the TA-03 power plant at the head of Sandia Canyon from 1956 to 1972. Some of the Cr(VI) made its way to the regional aquifer beneath Sandia and Mortandad Canyons, and Cr(VI) concentrations in the regional aquifer presently exceed NMED groundwater standards and U.S. Environmental Protection Agency (EPA) maximum contaminant levels (MCLs). Historical releases of PCBs from a one-time transformer storage area and PAHs from an asphalt batch plant also discharged to the wetland, which still contains an inventory of these contaminants. Sandia Canyon wetland performance monitoring is related to the overall chromium remediation project because a large portion of the original chromium inventory and other contaminants (i.e., PCBs and PAHs) are currently sequestered in the wetland sediment. The results of characterization work conducted to date in Sandia Canyon are described in the “Investigation Report for Sandia Canyon” (hereafter, the Phase I Investigation Report [IR]) (LANL 2009, 107453) and in the “Phase II Investigation Report for Sandia Canyon” (hereafter, the Phase II IR) (LANL 2012, 228624).

Detailed sediment mapping was performed during the Phase I investigations (LANL 2009, 107453). Canyon reach S-2, which contains the Sandia wetland, contains high concentrations and proportions of the originally released contaminant inventory. Reasons include

- proximity to contaminant sources,
- the large volume of sediment deposited during the period of active contaminant releases,
- the presence of high concentrations of organic matter in the wetland, and
- the presence of large amounts of silt and clay.

Contaminants commonly adsorb to, or can be precipitated with, sediment particles, clay, or organic matter. Chromium is the major inorganic contaminant of concern in the wetland that could be affected by both oxidation-reduction (redox) changes in the wetland and physical destabilization. Arsenic may also be released from wetland sediments upon dewatering (LANL 2009, 107453). Two groups of organic contaminants of concern, PCBs and PAHs, are primarily subject to physical transport in floods because of low solubility and a strong affinity for organic material and sediment particles. Important source areas for these contaminants are the former outfall for the power plant cooling towers in upper Sandia Canyon (chromium), a former transformer storage area along the south fork of Sandia Canyon (PCBs), and the former asphalt batch along the north fork of Sandia Canyon (PAHs) (LANL 2009, 107453).

The inventory of chromium contamination within the Sandia wetland exists primarily in the form of trivalent chromium [Cr(III)] because of reducing conditions. Alluvial saturation, along with significant amounts of solid organic matter produced from wetland vegetation, results in reducing alluvial aquifer conditions as indicated by high dissolved iron and manganese concentrations in alluvial groundwater. Oxidation by manganese oxides under aqueous conditions is the primary mechanism responsible for oxidation of Cr(III) to Cr(VI) (Rai et al. 1989, 249300). Complete oxidation of Cr(III) to Cr(VI) is likely to occur if the molar concentrations of manganese dioxide [Mn(IV)] exceed those of ferrous oxide [Fe(II)], Cr(III), and chromium binding sites on organic matter. This situation, however, is unlikely within the active Sandia wetland because concentrations of total iron, consisting mainly of Fe(II), and solid organic matter are present at much higher weight-percent concentrations than Mn(IV), which is usually present in the parts per million range (discussed in more detail in Appendix J of the Phase I IR) (LANL 2009, 107453). In addition, drying and leaching experiments conducted on Sandia wetland sediments to quantify the potential release of Cr(VI) during drying of the wetland material showed that Cr(III) appears to remain stable, suggesting insufficient Mn(IV) is produced to oxidize appreciable amounts of Cr(III) to Cr(VI) (LANL 2009, 107453). Dissolved chromium in leachates was primarily in the form of Cr(III), indicating that most chromium measured in a filtered wetland performance monitoring sample was resistant to oxidation and likely occurred as colloids. This explanation is supported by Sandia wetland analyses of Cr(VI), with results generally below the method detection limit (MDL) (LANL 2016, 601432).

Data from geochemical studies presented in the Phase I IR (LANL 2009, 107453) and previous Sandia wetland performance reports indicate that chromium in wetland sediments is predominantly geochemically stable as Cr(III) and is not likely to become a future source of chromium contamination in groundwater, especially if saturated conditions are maintained within the wetland. The frequent nondetections of Cr(VI) in alluvial water confirm that most if not all the chromium exists as Cr(III) (see results in section 3.0). Results from baseline monitoring of the wetland (LANL 2014, 257590) and from monitoring in 2014 (LANL 2015, 600399), 2015 (LANL 2016, 601432), 2016 (LANL 2017, 602341), 2017 (LANL 2018, 603022), 2018 (N3B 2019, 700415), 2019 (N3B 2020, 700810), and 2020 (N3B 2021, 701253) show that the Sandia wetland system is chemically and physically stable, with stable-to-increasing wetland vegetation cover in different parts of the system. Most importantly, results of storm water monitoring from gaging station E123 have shown a reduction of PCBs and chromium following the GCS installation.

1.3 Project Goals

Newport News Nuclear BWXT-Los Alamos, LLC (N3B) has prepared this document pursuant to the Compliance Order on Consent, signed June 24, 2016, and environmental surveillance at the Laboratory (LANL 2021, 701835). Specifically, the results presented in this report fulfill requirements set forth in the "Work Plan and Final Design for Stabilization of the Sandia Canyon Wetland" (LANL 2011, 207053). In that plan, the Laboratory proposed reporting Sandia wetland monitoring data to NMED by April 30 of each year. The requirement for designing a Sandia wetland monitoring program was previously set forth in NMED's "Approval with Modification, Interim Measures Work Plan for Stabilization of the Sandia Canyon Wetland" (NMED 2011, 203806) in response to the Laboratory's "Interim Measures Work Plan for Stabilization of the Sandia Canyon Wetland" (LANL 2011, 203454). The original monitoring plan was provided in the work plan (LANL 2011, 207053). Over the course of monitoring in the Sandia wetland area, NMED and N3B have periodically made updates to the monitoring plan based on an increased understanding of the system. The current monitoring plan is discussed in more detail in section 2.0. The monitoring plan is designed to identify physical or chemical changes in the Sandia wetland related to (1) the installation of a GCS at the terminus of the wetland (LANL 2013, 251743) and (2) changes in outfall chemistry and discharge volumes related to the SERF expansion (DOE 2010, 206433).

Specifically, monitoring efforts address the following questions:

- Are outfall volumes high enough to maintain the wetland?
- Is the physical stability of the wetland being maintained by the GCS?
- Is the GCS functioning to attenuate storm flow and prevent migration of contaminants?
- Is the wetland chemically stable?

2.0 METHODS

Monitoring was conducted in 2021 for surface water and alluvial groundwater. Data are assessed relative to baseline conditions presented in the "Sandia Wetland Performance Report, Baseline Conditions 2012–2014" (LANL 2014, 257590). The current year's data are also compared with previous years to identify any physical and geochemical changes during the monitoring period. Monitoring data include

- water levels and water chemistry from alluvial wells that monitor the alluvial groundwater in the wetland,
- surface water and storm water data from two gaging stations located upstream of the wetland and one gaging station located downstream,
- light detection and ranging (LiDAR) data to monitor vegetation and detect geomorphic change (triennially),
- annual post-monsoon walkdowns with NMED, and
- semiannual and greater-than-50 cubic feet per second (cfs) inspections of the GCS and the log-check dams on the tributary.

In the case of a large disturbance event (approximately 100 cfs at E123) additional monitoring will occur. This metric has been defined based on historical knowledge, which showed that approximately 100-cfs storm events have the potential to cause significant erosion. If discharge at gaging station E123 reaches this discharge value, N3B will consider this a large storm event that might warrant an aerial-based geomorphic and vegetation survey in advance of the routine third-year survey. If significant erosion or vegetation disturbance is observed after a scheduled field visit is performed, aerial surveys will be performed after/during the monsoon season (after for geomorphic surveys and during for vegetation surveys). If noteworthy features are identified in the aerial surveys, the features will be field-checked and additional ground-based survey methods may be implemented.

2.1 Changes to Monitoring in 2021

N3B did not make any changes to the monitoring plan in 2021 and followed the same plan as in 2019 and 2020. A detailed description of changes to monitoring that began in 2019 are included in the 2019 Sandia Wetland Performance Report (N3B 2020, 700810). Proposed changes to the monitoring plan for 2022 are outlined in section 2.3.

2.2 Monitoring Conducted in 2021

Quarterly sampling of Sandia wetland surface water and annual sampling of alluvial groundwater is coordinated with the Chromium Investigation monitoring group sampling, conducted under the "Interim Facility-Wide Groundwater Monitoring Plan for the 2021 Monitoring Year, October 2020–September 2021, Revision 1" (N3B 2020, 701041) and the "Interim Facility-Wide Groundwater Monitoring Plan for the 2022 Monitoring Year, October 2021–September 2022, Revision 1" (N3B 2021, 701672). In 2021, sampling was conducted at eight alluvial wells within the wetland (collocated with the piezometers where water was collected through 2016 [Table 2.2-1]), as well as at surface water gaging stations E121 and E122 (above the wetland) and E123 (below the wetland). (See Figure 1.0-1.)

Alluvial groundwater analytical results were screened against New Mexico Water Quality Control Commission groundwater standards (20.6.2 New Mexico Administrative Code [NMAC]), and base flow and storm water analytical results were screened against the appropriate surface water quality standards in 20.6.4 NMAC (see section 3.0). All analyses were performed off-site by U.S. Department of Energy Consolidated Audit Program–certified contract laboratories.

Analytical results meet the N3B minimum data quality objectives as outlined in N3B-PLN-SDM-1000: "Sample and Data Management Plan." N3B-PLN-SDM-1000 sets the validation frequency criteria at 100% Level 1 examination and Level 2 verification of data and at 10% minimum Level 3 validation of data. A Level 1 examination assesses the completeness of the data as delivered from the analytical laboratory, identifies any reporting errors, and checks the usability of the data based on the analytical laboratory's evaluation of the data. A Level 2 verification evaluates the data to determine the extent to which the laboratory met the analytical method and the contract-specific quality control and reporting requirements. A Level 3 validation includes Levels 1 and 2 criteria and determines the effect of potential anomalies encountered during analysis and possible effects on data quality and usability. A Level 3 validation is performed manually with method-specific data validation procedures. Laboratory analytical data are validated by N3B personnel as outlined in N3B-PLN-SDM-1000; N3B-AP-SDM-3000: "General Guidelines for Data Validation"; N3B-AP-SDM-3014: "Examination and Verification of Analytical Laboratory Data"; and additional method-specific analytical data validation procedures. All associated validation procedures have been developed, where applicable, from the EPA QA/G-8 "Guidance on Environmental Data Verification and Data Validation," the U.S. Department of Defense/Department of Energy "Consolidated Quality Systems Manual for Environmental Laboratories," the EPA National Functional Guidelines for data validation, and the American National Standards Institute/American Nuclear Society 41.5: "Verification and Validation of Radiological Data for Use in Waste Management and Environmental Remediation."

2.2.1 Surface Water Monitoring

Surface water gaging stations E121 and E122 are located in the upgradient western end of the Sandia Canyon watershed. Surface water gaging station E123 is located to the east immediately below the terminus of the wetland. Figure 1.0-1 shows the locations of the gaging stations and outfalls as well as the extent of the Sandia wetland. In 2021, gaging station E121 measured discharge from Outfall 001 and storm water runoff from approximately 50 acres of TA-03. With changes at SERF in September 2016, discharge from SCC cooling towers is primarily directed to Outfall 001, with Outfall 03A027 used only for maintenance and emergency discharge. Gaging station E122 measures discharge from Outfall 03A199 and storm water runoff from approximately 50 acres from TA-03. Gaging station E123 measures surface water flow below the wetland, including discharge from all outfalls and storm water runoff from approximately 185 acres, 100 acres of which are monitored by E121 and E122. Flow rates into and out of the wetland are measured at gaging stations E121, E122, and E123 during sample-triggering storm events as well as during base flow conditions. Appendix D (on CD and included with this document) provides analytical data and 5-min stage, discharge, and precipitation data.

In 2021, ISCO 3700 automated samplers attempted to collect storm water samples when discharge was greater than 5 cfs above base flow at gaging stations E121 and E123. After four sampling events at gaging station E123, the sampler trip level was raised to 50 cfs above base flow on June 28, 2021, for the remainder of the season. After five sampling events at gaging station E121, the sampler trip level was raised to 50 cfs above base flow on July 2, 2021, for the remainder of the season. At gaging station E122, the automated sampler trip level was inadvertently left at the 2020 level of 12 cfs from activation on May 14, 2021, to June 3, 2021. Storm events on May 30 and June 2, 2021, were not sampled at E122 because of the high trip level (Table 2.2-2). On June 3, 2021, the sampler trip level was set to 1 cfs above base flow. After five sampling events at gaging station E122, the trip level was raised to 19 cfs on July 2, 2021. Sampling trip levels are flexible (not arbitrary), are based on historical data, and are optimized to adapt to interannual flow conditions. Base flow and storm flow samples in 2021 were analyzed based on the suites presented in Table 2.2-3. Samplers E121 and E123 were activated on May 17, 2021, and Sampler E122 was activated on May 14, 2021. Sampler shutdowns occurred on November 3, 2021, at gaging stations E121, E122, and E123. Stations E121 and E123 are equipped with a Sutron 9210 data logger, a Microwave Data Systems, Inc., MDS 4710 radio transceiver, and a Sutron Accubar bubbler. Station E122 is equipped with a Sutron 9210 data logger, an MDS 4710 radio transceiver, and a VEGA Americas, Inc., VEGAPULS 61 radar sensor. Stage is recorded every 5 min and transmitted to a base station where it is archived in a database. All three gaging stations are equipped with two automated ISCO samplers: one with a 24-bottle set for suspended sediment concentration (SSC) analyses throughout the storm event, and one with a 12-bottle set for collection of chemistry samples (Table 2.2-4). Analytes other than those listed in Table 2.2-4 were sampled in storm flow in 2021 for purposes other than the monitoring of wetland performance (i.e., dissolved organic carbon, alkalinity, pH, gross alpha, and particle size). Only analytes required for the monitoring of wetland performance are presented in Table 2.2-3.

2.2.2 Alluvial System Monitoring

Monitoring of alluvial groundwater chemistry is accomplished with alluvial wells constructed of a 2-in.-inside diameter polyvinyl chloride (PVC) casing and a 2-in. slotted PVC casing to act as a screen surrounded by a filter pack consisting of 1/20 silica sand (Table 2.2-5). The current alluvial wells (prefix SWA) were installed to replace piezometers (prefix SCPZ) between 2014 and 2016. The alluvial wells were collocated with the old piezometers (data from shared locations are reported together in the section 3.4 figures). Table 2.2-1 provides a crosswalk of the piezometers and alluvial wells. Since 2017, only water from the alluvial wells has been sampled. Initially, there were 12 alluvial wells arranged in

4 transects bisecting the surface water channel. However, beginning in 2019, only the first and fourth transects, and wells SWA-2-4 and SWA-2-6 from the second transect, were sampled for a total of 8 wells (Figure 1.0-1).

The monitored alluvial well (piezometer) transects are as follows:

- Alluvial wells SWA-1-1 (SCPZ-1), SWA-1-2 (SCPZ-2/SWA-1), and SWA-1-3 (SCPZ-3) are located on a sand-and-gravel terrace near the active channel (c1 geomorphic unit) toward the western end of the wetland, which has experienced channel incision and dewatering relative to historical conditions. These alluvial systems are located on the c3 geomorphic unit, away from the active channel and associated inset terrace (c2a geomorphic unit), which are locations into which cattails have expanded since vegetation monitoring began in 2014. Well SWA-1-1 is screened toward the base of alluvial fill, while the tops of the screens in wells SWA-1-2 and SWA-1-3 are approximately 6 ft and 3 ft below ground surface (bgs), respectively (Table 2.2-5).
- Wells SWA-2-4 (SCPZ-4) and SWA-2-6 (SCPZ-6/SWA-2) form a transect in the widest portion of the wetland. The tops of the well screens are 2–3 ft bgs because the wetland water level is at or very near the surface at this transect. It is at these shallowest depths that changes in water-level and sediment oxidation, were they to occur, would be expected to manifest as a result of reduced effluent discharge. Similarly, the lateral margins of the wetland may dewater before the middle of the wetland as a result of reduced effluent volumes. This effect could be most pronounced where the wetland is widest and water flux is most spread out. It is also at such locations that preferential flow paths within the alluvium may form.
- The final transect of wells SWA-4-10 (SCPZ-10), SWA-4-11 (SCPZ-11B), and SWA-4-12 (SCPZ-12/SWA-4) have responded most to the rewatering that has occurred at the eastern terminus of the wetland because of the effect of the GCS. The wetland water level is at or near the surface at this transect. Water was routed around this area during GCS construction.

The 2021 sampling and analysis plan for the alluvial wells is provided in Table 2.2-3. Most of the analyses were designed as indicators of redox changes associated with potential dewatering of the wetland. Alluvial locations were instrumented with sondes for continuous monitoring of water levels, specific conductance, and temperature. Full suites were collected at all locations in October 2021. The field parameter data from the surface water and alluvial wells are provided in Table 2.2-6.

In 2021, all transducers in the Sandia wetland were replaced with In-Situ, Inc., Level TROLL 500 15 psi data loggers (Table 2.2-7). The three transducers in the easternmost transect (SWA-4-10, SWA-4-11, SWA-4-12) were replaced in January and the remaining five transducers were replaced in October. The Level TROLL 500 transducers are programmed to collect continuous measurements of water level, water pressure, and temperature every hour. The factory calibration for the Level TROLL 500 is rated for 18 months of accurate data collection. Data downloads are collected twice per year from the installation date. Each transducer will be replaced within 12 months of the installation date.

2.2.3 Geomorphic and Vegetation Monitoring

Beginning in 2019, a new aerial survey technique was used to replace ground-based Global Positioning System (GPS) survey methods used in prior years. The surveys were performed on the entire Sandia wetland area using airborne hyperspectral and LiDAR equipment to collect geomorphic and vegetation data. Aerial LiDAR surveys are planned to be performed every 3 yr. If a large storm event is determined to have caused significant geomorphic change during a year when a survey is not scheduled, then a LiDAR survey will be conducted. The LiDAR surveys provide a detailed digital elevation model of the area that can be compared with historical ground-based geomorphic survey data. A LiDAR survey of geomorphology was conducted in October 2021 and the results are discussed in detail in Appendix B.

In the Sandia wetland a large storm event is defined as flows exceeding 100 cfs at gaging station E123. In 2021, storm water peak discharge did not exceed 100 cfs at gaging station E123; hence, no additional visual inspection of the wetland to document qualitative geomorphic changes was warranted.

2.2.4 GCS Monitoring

The GCS is inspected biannually and following rain events with discharges at gaging stations greater than 50 cfs (LANL 2014, 600083). If erosion or any indications of instability are observed, appropriate actions will be taken to ensure continued stability and functionality of the GCS. The GCS inspections, with photographs of these drainage controls, are presented in Appendix C.

2.3 2022 Monitoring Plan

The 2022 monitoring plan will remain largely the same as the plan approved in March 2019 (N3B 2020, 700810). The only change that will occur is the reporting schedule for the geomorphic and vegetation data. The aerial-based geomorphic data from 2021 will be discussed in the current year’s report, but it will also be discussed in the 2022 report alongside the aerial-based vegetation data that will be collected in 2022. In 2025, the next survey year, vegetation data will be collected in August and geomorphic data will be collected in October and both will be included in the 2025 report. Presenting both the geomorphic and vegetation data together will provide a more complete picture of the physical condition of the wetland.

3.0 RESULTS AND DISCUSSION

Changes in any one metric do not necessarily represent a detriment to the overall function of the wetland and will not necessarily lead to contaminant release from wetland sediments. The wetland should be evaluated in terms of total system performance over time with multiple lines of evidence used to determine if the system is stable.

3.1 Inputs to and Hydrology of the Sandia Wetland

3.1.1 Outfalls

Outfall volumes from Outfall 001 were initially lower after SERF came online but have actually shown a slight increasing trend over the period of monitoring in the Sandia Wetland. Figure 1.1-1(B) shows there has been a significant increase in mean daily outfall volume per month since 2014, although the trend is relatively weak ($p = 0.0087$, linear regression). Mean daily volume of effluent per month back to 2006 is shown in Figure 1.1-1(A). Outfall volume per day back to 2010 is shown alongside mean daily discharge from E121, E122, and E123 in Figure 3.1-1. Outfall daily volumes in the beginning of 2021 were quite high and followed a similar annual pattern to 2020. The decrease in inputs to Outfall 001 in the summer months may have been due to the rerouting of blowdown water from the SCC to the power plant cooling towers before being discharged. This rerouting occurred to ensure effluent complied with the discharge temperature limit of 20°C. Outfall volumes continue to stay well above the 40,000 gpd needed to sustain the wetland. This is further supported by the gaging station and alluvial water-level data.

3.1.2 Precipitation and Gage Discharge

Precipitation in 2021 was below average, continuing an extended period of drought from 2020, with the exception of May and June 2021, when precipitation was average. Drought conditions persisted through the end of 2021. In 2021, there were no large-disturbance (greater than 50 cfs) events. For each sample-triggering storm event in 2021, Table 2.2-2 shows precipitation at rain gage RG121.9, storm water peak discharge, and whether a sample was collected at E121, E122, or E123 gaging station. Storm water discharge at E121 equaled or exceeded the trip level (5 cfs above the base flow at the beginning of the season and then changed to 50 cfs on June 28) five times in 2021, and samples were collected from five of those events. Discharge at E122 equaled or exceeded the lowered trip level (1 cfs above the base flow at the beginning of the sampling season, and then changed to 19 cfs above the base flow on July 2) seven times in 2021 and samples were collected from five of those events. Discharge at E123 exceeded the trip level (5 cfs above the base flow at the beginning of the season and then changed to 50 cfs) four times in 2021 and samples were collected from four of those events. Hydrographs of the sample-triggering storm events in 2021 are shown in Figure 3.1-2. In 2021, the average transmission time from E121 to E123 and from E122 to E123 was approximately 108 min for both (Table 3.1-1). This finding indicates that storm water flows from either gaging station E121 or gaging station E122 through the wetland to gaging station E123 in approximately the same amount of time. Base flow levels at E121 were generally lower during January–May 2021 in comparison with 2020 but comparable during the rest of the year. Base flow levels at E122 and E123 in 2021 were comparable with those in 2020 (Figure 3.1-1).

3.1.3 Alluvial Water Levels

Water-level monitoring continues as a means to determine how operational effluent releases and precipitation/snowmelt affect the overall wetland hydrology. Comparisons between the 2020 and 2021 water levels (shown in Figure 3.1-3) indicate they have been relatively stable. SWA-2-6 shows more daily variability in water level in 2021 compared with 2020, and the average water level is slightly reduced. However, note that the scale on the plot of the second transect of wells (including SWA-2-4 and SWA-2-6) is much smaller than those shown for the other two transects, so the actual variations are consistent with what is observed in the rest of the wetland. Seasonal decreases in water levels are observed in all wells, with the exception of SWA-2-4 and SWA-2-6, presumably as a result of high rates of evapotranspiration associated with warm temperatures and lower-magnitude precipitation events in the summers compared with those in the previous years. The water levels in the alluvial system tend to remain stable because of the relatively impermeable Bandelier Tuff bedrock base of the wetland, and an impermeable downgradient end (the GCS) keeps the water contained in the wetland. As long as water inputs exceed wetland evapotranspiration, even significantly reduced outfall discharge may be able to sustain water levels and sufficient saturation of wetland sediments. Decreased outfall discharge may manifest more in the surface water balance of the wetland than in alluvial groundwater levels. In addition, water temperatures were consistent, showing temporal changes with seasons and with less variation in wells located in the channel and wells at a depth greater than 10 ft (SWA-1-1) (Figure 3.1-3).

3.2 Physical Stability of the Wetland

The physical stability of the wetland was assessed via an aerial-based geomorphic survey in 2021. Raster-based change detection was calculated between the 2021 survey data and the 2018 survey data to determine areas of geomorphic change. However, the resulting geomorphic change results yielded much higher values than expected based on previous results and visual inspections (see Appendix C). Field verification and vegetation data will be incorporated into the 2022 report to correct the geomorphic change detection results.

Vegetation was not surveyed in 2021. The next aerial-based vegetation survey is schedule for 2022. Details and results from the current year's geomorphic survey can be found in Appendix B.

Table 3.2-1 summarizes geomorphic changes associated with large storm events that have occurred in the wetland since 2014. As in 2020, there were no significant events recorded for 2021.

3.3 GCS Performance in Containing Contamination

Inspection results from GCS monitoring, presented in Appendix C, indicate that the GCS is stable and does not require corrective or mitigating actions. As mentioned above, there were no significant flow events in Sandia Canyon in 2021. Inspections were performed in May and October 2021 and the post-monsoon walkdown of the wetland with NMED occurred on November 1, 2021. Maintenance that occurred in 2021 included removing a coir log that was leading to localized scour and removing debris from the canyon. Additionally, erosion and sediment migration in the western side channels, which were noted in the October inspection, were addressed by installing log berms and rock check dams. Photos and descriptions from the inspections and walkdown are included in Appendix C.

As noted in the baseline performance report (LANL 2014, 257590), similar base flow chemistry for many constituents between upgradient (E121) and downgradient (E123) locations indicates a relatively short residence time for surface water and little interaction (exchange) with alluvial groundwater. This finding is evident for chloride, nitrate plus nitrite, and silica, which are indicators of water quality in outfall discharge in the context of chemistry from Outfall 001 (Figures 1.1-3 to 1.1-5). Gaging station E121 is used as a monitoring point for discerning integrated impacts of changing input chemistry and decreasing effluent volumes from Outfall 001 in base flow. Generally, improvements in water chemistry discharged from Outfall 001 associated with the SERF expansion have been evident for chloride and silica (as inferred from post-SERF and post-GCS concentrations at E121) (Figures 1.1-3 and 1.1-5). Nitrate concentrations showed a smaller, although still notable, post-GCS decrease at E121 and E123 (Figure 1.1-4).

Analytical results from base flow and storm flow at the three gaging stations illustrate that the GCS is effective at minimizing the migration of contaminants out of the wetland (Figure 3.3-1). Gaging station E123, below the GCS, is the key integrating location of total wetland performance in mitigating discharges of contaminants of concern. Monitoring of storm water at E123 is used to evaluate if anomalously high levels of sediment and contaminants (e.g., chromium, PCBs, PAHs) are mobilized during floods because of a reduction in contaminant contact times with sediment, sorption capacity, or other chemical and/or physical stability in the wetland.

In the box-and-whisker plots in Figure 3.3-1, the median sediment content (measured as SSC) in base flow and storm flow are similar post-GCS. However, there is much less variability (and many fewer data points) in base flow sediment compared with storm flow. For example, the highest storm flow SSC in 2021 was approximately 100 times greater than the highest 2021 base flow samples. The effect of the GCS on base flow sediment cannot be evaluated because sediment pre-GCS was measured as total suspended sediment (TSS) rather than SSC. The United States Geological Survey (USGS) notes that significant bias in the relation of TSS and SSC exists and these methods should not be used interchangeably. USGS also recommends that SSC be used for monitoring natural waters (Gray et al. 2000, 255422). The SSC results at E123 show that the GCS does, in general, reduce SSC in storm flow. This is especially evident in 2021 (red triangles on the boxplots). This reduction is noteworthy because several contaminants in the wetland are strongly sorbed to sediments, and a reduction in SSC should be a good proxy for reduction of contaminant migration. Sediment volume for all of upper Sandia Canyon is positively correlated to runoff volume through the following relationship:

$$\textbf{sediment volume} = \mathbf{0.205} \times \textbf{runoff volume}^{\mathbf{0.927}} \qquad \textbf{Equation 1}$$

This model was built from calculated sediment volume and associated runoff volume data from storm events at the three gaging stations from 2014 through 2021 (Table 3.3-1). As illustrated in Figure 3.3-2, the relationship is quite strong ($R^2 = 0.60$). Figure 3.3-2 also shows that sediment volume was generally higher in 2014 compared with other years, and this may have been caused by disturbance associated with the construction of the GCS.

The ability of the GCS to attenuate storm flow is less clear, as shown in base flow and storm flow peak discharge data at E123 in Figure 3.3-1. The median peak discharges for base flow and storm flow at E123 are slightly lower after the GCS was constructed, although there is still high variability in both. Because base flow is an approximation and storm flow is classified as any discharge above base flow, this method of evaluating the GCS is less accurate than the measurements of SSC, PCBs, and chromium.

PCB concentrations in both base flow and storm flow at E123 are, on average, reduced since the GCS was constructed (Figure 3.3-1). While PCB concentrations in base flow and storm flow were higher downgradient of the wetland (relative to upgradient locations E121 and E122) before the GCS was built, the concentrations are closer in magnitude upgradient and downgradient of the wetland since the GCS was constructed. The trend in base flow PCB concentrations at all of the gaging stations indicates a general decrease from pre-GCS to post-GCS. This may be attributed to changes in outfall chemistry. However, in 2021 PCB concentrations in base flow at E122 show a higher variability than has been seen previously and the combined contributions of E121 and E122 are evident in the base flow results at E123. Despite this, base flow PCB concentrations at E123 continue to be much lower than pre-GCS concentrations. PCB concentrations in storm flow samples in 2021 tended to fall above the median post-GCS levels and were notably high at E121. However, storm flow PCB concentrations downstream at E123 were within the range observed in previous years.

Total dissolved chromium in base flow has shown a general decreasing trend at E121 post-GCS (Figure 3.3-1). This may be because of process improvements at SERF. Dissolved Cr(VI) is much higher at the upstream gaging stations than downstream at E123, demonstrating the reducing conditions present in the wetland [note that Cr(VI) is measured only in base flow]. Total dissolved chromium in storm flow has remained relatively stable at all locations post-GCS. Downstream, at E123, total chromium concentrations in storm flow continue to be much lower in 2021 than pre-GCS construction, demonstrating that the GCS is functioning to prevent migration of chromium downstream.

Total PAH concentrations were computed using the 19 most prominent PAHs, and nondetections were considered zero. PAHs were not analyzed in storm flow before the GCS was built. In base flow, all total PAH results were nondetections pre-GCS (Figure 3.3-1). In storm flow, total PAH concentrations are similar upgradient and downgradient of the wetland. Generally, higher concentrations of PAHs have been detected at E122 than at E121 and E123. This is likely the influence of the former asphalt batch plant near the northern fork of upper Sandia Canyon. However, in 2021, an exceedance of only one PAH, benzo(a)anthracene, was observed in the August base flow sample from E123. There were no PAH exceedances in the subsequent base flow samples collected in November (Table 3.3-2 and Table 3.3-3).

3.3.1 Base Flow and Storm Flow Exceedances

Base flow and storm water analytical results from gaging stations E121, E122, and E123 in 2021 were screened against the appropriate surface water quality criteria (SWQC) (Table 3.3-2). The two main sources of surface water that enter the wetland are discharges from outfalls and storm water runoff from the developed landscape within TA-03. This run-on sourced water influences the results from E121 and E122. Flow at E123 consists of a mix of waters from E121, E122, runoff through the Sandia wetland, and urban runoff from the Laboratory and Los Alamos County. The exceedances detected in storm water and base flow in 2021 include aluminum, benzo(a)anthracene, copper, dioxins, lead, total PCBs, and zinc. The dioxin criteria apply to the sum of the dioxin toxicity equivalents expressed as 2,3,7,8-tetrachlorodibenzo-p-dioxin. The dioxin exceedances are driven by concentrations of PCB congeners. Exceedances at E121 occurred primarily in storm water, with the exception of total PCBs, which exceeded in all four base flow samples. Construction and ongoing industrial activity in TA-03, upstream of E121, are likely the source of the high PCB results. Construction to expand Sigma Building (building 03-66) resulted in soil disturbance and soil relocation in the vicinity of Area of Concern (AOC) 03-052(b). AOC 03-052(b) is a former storm drain, which may have received contaminants from AOC 03-056(k), a container storage area and loading dock at building 03-66. PCBs may have been managed and released from 03-056(k). PCBs were analyzed for and detected in shallow soil samples (LANL 2015, 600912). These activities are being investigated further and PCB results within the wetland are being closely monitored. Exceedances at E122 were also primarily in storm water, with the exception of total PCBs, which exceeded in three of four base flow samples. As with the other two gaging stations, exceedances at E123 were mostly in storm water, although there was one base flow benzo(a)anthracene exceedance and total PCB exceedances in all four base flow samples. Although there are exceedances of total PCBs at E123, the high total PCB concentrations seen at E121 are not translated downstream of the wetland at E123 (Table 3.3-3).

3.4 Chemical Stability of the Wetland

The alluvial well array provides valuable water-level and alluvial groundwater chemistry data. These locations monitor potential changes associated with outfall volumes, evolving geomorphology, redistribution of reducing zones, and changes in chemistry of the outfall (in the case of more conservative constituents). The metrics for identifying deleterious impacts as monitored in the wells are (1) persistent increases in contaminant concentrations [e.g., Cr(VI)] and/or increases in oxidizing conditions as indicated by redox-sensitive species (e.g., dissolved iron) and (2) persistent decreases in water levels that have deleterious effects on obligate wetland vegetation.

Selected analytical results for water chemistry time-series data (filtered) from the alluvial sampling array are presented in Figures 3.4-1 to 3.4-4. Time-series plots are presented in the relative spatial distribution of the wells in the wetland, as follows:

- the upper plots are from the most northerly wells in each transect, ordered from west to east;
- the middle plots are from wells in the center of each transect, ordered from west to east; and
- the bottom plots are from the southernmost wells in each transect, in the same orientation.

The alluvial sampling array is composed of three transects running north to south and spread out along the length of the wetland. In addition, data for surface water entering the wetland at gaging station E121 and exiting the wetland at gaging station E123 are plotted at the western- and easternmost parts of the wetland, respectively, to provide a comparison of input and output base flow chemistry (Figure 1.0-1). Differences between base flow data and alluvial groundwater data may indicate subsurface processes (e.g., reduction) and provide information about residence times in the alluvial system. Key analytes plotted include redox-sensitive species (iron and manganese), and key contaminants (dissolved arsenic and chromium) (Figures 3.4-1 to 3.4-4). Table 2.2-6 details surface water base flow sampling and field parameters, respectively, for samples collected in CY 2021.

3.4.1 Redox-Sensitive Species

Redox-sensitive species provide information on the degree of reduction occurring in the wetland sediments. Concentrations of arsenic, manganese, and iron tend to be higher in the alluvial system than in surface water, indicating reducing conditions in the alluvial system owing to increased mobility of most reduced metals. Within the surface-water system, concentrations at E121 and E123 are similar for all redox-sensitive species (Figures 3.4-1 through 3.4-4).

Ferrous oxide, the reduced form of iron, is the predominant form present in alluvial waters of the wetland, plotting at the same level or just slightly below the total iron (Figure 3.4-1). Total-iron concentrations higher than Fe(II) are believed to be samples with colloidal ferric oxide [Fe(III)], or iron chelated by microbial or phyto-siderophores. Measurement of speciated iron stopped midway through 2018, although based on previous data, the majority of total iron is assumed to be Fe(II). Total iron concentrations in 2021 are similar to those measured in 2020. Alluvial samples continue to have much higher iron concentrations than those measured at the input and output gaging stations. The historically higher values for total iron in the easternmost transect are believed to be of colloidal iron, which has decreased as a result of the recovery from disturbance caused by the installation of the GCS, as suggested by other constituents. This decreasing trend has continued in 2021.

All the locations appear to be strongly reducing with respect to manganese at the depth of screen completion (Figure 3.4-2). Locations SWA-1-2 and SWA-1-3 have somewhat lower manganese concentrations, consistent with their shallow completion depths in sands and gravels. Most of the manganese is believed to be in its reduced form, with increases indicating increasing reducing conditions in alluvial sediment. Manganese concentrations measured in 2021 were relatively similar to those of previous years, with continually higher concentrations in the wetland compared with the gaging stations.

Arsenic can exist as arsenite [As(III)] or arsenate [As(V)]. Arsenite is relatively mobile and should predominate under reducing conditions. Within the range of analytical error, most of the total arsenic detected in analytical results from alluvial wells was As(III), confirming the reducing conditions of the wetland (Figure 3.4-3). In 2021, arsenic concentrations were consistent with those of previous years, continuing to demonstrate the reducing conditions in the wetland.

Dissolved total chromium concentrations in the wetland alluvial system are quite high (the NMED groundwater exceedance criterion for chromium is 50 ppb) (Table 3.4-1). There is significant spatial variation in chromium distribution (Figure 3.4-4). Given the varied environmental fate and transport of the different forms of chromium, including those in organo-metal moieties, it is difficult to make meaningful spatial comparisons of total chromium. However, locations SWA-1-2, SWA-1-3, SWA-4-10, SWA-4-11, and SWA-4-12 have higher concentrations on average, with concentrations at the latter three locations perhaps resulting from disturbance associated with GCS construction in the easternmost transect. This trend continued in 2021; the reason for higher Cr(III) in the westernmost transect remains unclear.

The concentrations of dissolved Cr(VI) measured in the alluvial system over the past 5 yr were nearly all at the detection limit or were nondetections (Figure 3.4-4). Seven out of the eight alluvial samples collected in 2021 were nondetections. Before 2017, samples analyzed for Cr(VI) were not filtered, with the exception of a few filtered test samples in 2013. Because reporting is to the dissolved chromium standard criterion, only the filtered data are shown. The consistently low or nondetected Cr(VI) concentrations reflect the strong reducing conditions in the wetland. The highest detections of Cr(VI) concentration were at E121 and E122 (Figure 3.3-1). These higher concentrations of Cr(VI) entering the wetland are believed to be from potable water derived from the regional aquifer and concentrated in the cooling towers. Station E123, at the terminus of the wetland, has Cr(VI) concentrations below or just at the detection limit, indicating the chromium exchange capacity and other abiotic immobilizing reductions in Cr(VI) as it moves through the wetland. Since analysis of dissolved Cr(VI) began in 2017, no samples have exceeded the New Mexico groundwater standards.

3.4.2 Alluvial Groundwater Exceedances

The alluvial system data from 2021 were screened to groundwater standards (Table 3.4-1). Exceedances in alluvial groundwater included total chromium, iron, and manganese. Iron and manganese exceedances were the most commonly observed and are expected because of the reducing wetland conditions, bringing these likely geology-derived metals into solution. Dissolved manganese is more persistent than iron because of manganese oxidation kinetics, and it has been observed in surface water at E123 in past surveys. There was one total chromium exceedance at SWA-1-2. This location showed exceedances in both 2019 and 2020 and has had consistently high chromium concentrations (Fig. 3.4-4). Most of the total chromium concentration in alluvial groundwater in the wetland is Cr(III); the measured Cr(VI) at the locations of the exceedances is at or below the MDL and has never exceeded New Mexico groundwater standards.

4.0 CONCLUSIONS

This performance period covers the eighth year following baseline monitoring. The monitoring performed during the performance period indicates that the Sandia wetland is stable and well-established following installation of the GCS. Yearly comparisons of analytical results indicate that the wetland is discharging lower concentrations of contaminants of concern in storm water since construction of the GCS. Even with periods of lower effluent volumes entering the wetland and seasonal evapotranspiration, the alluvial system remains stable and wetland sediments remain highly reducing, with no concerning temporal trends in chemistry noted.

Despite overall reduced effluent discharge volumes after SERF came online in 2012, water levels remain sufficiently high to sustain and promote healthy growth of the obligate wetland vegetation. Continuing vegetation monitoring in future years will be valuable in assessing wetland performance, with abundant wetland vegetation promoting sediment stability and preserving reducing conditions. No large-scale, systematic erosion has been noted in the wetland, and the system seems to be highly stable from a physical perspective. The aerial-based geomorphic survey data presented in this report will be combined with vegetation data and field verification data in the 2022 report to provide a comprehensive analysis of the physical stability of the wetland area.

The GCS has arrested headcutting at the terminus of the wetland. Planted wetland vegetation has rapidly established around the GCS, and wetland vegetation is stable in the upper portion of the system. Storm water data indicate that the GCS has had a positive impact on mitigation of contaminant transport. Suspended sediment, PCBs, and chromium concentrations have decreased at E123 post-GCS, presumably because of cessation of headcutting at the terminus of the wetland and conditions that promote immobilization. High concentrations of PCBs were measured this year at the upstream gaging station, E121, but did not translate to high results below the wetland at gaging station E123.

Ongoing monitoring will continue to allow assessment of changes within the Sandia wetland related to the GCS, changes in effluent chemistry, and decreases in effluent volumes and discharge rates. An adaptive management strategy will be employed should adverse changes be noted.

5.0 REFERENCES AND MAP DATA SOURCES

5.1 References

The following reference list includes documents cited in this report. Parenthetical information following each reference provides the author(s), publication date, and ERID, ESHID, or EMID. ERIDs were assigned by Los Alamos National Laboratory's (the Laboratory's) Associate Directorate for Environmental Management (IDs through 599999); ESHIDs were assigned by the Laboratory's Associate Directorate for Environment, Safety, and Health (IDs 600000 through 699999); and EMIDs are assigned by N3B (IDs 700000 and above).

DOE (U.S. Department of Energy), August 24, 2010. "Final Environmental Assessment for the Expansion of the Sanitary Effluent Reclamation Facility and Environmental Restoration of Reach S-2 of Sandia Canyon at Los Alamos National Laboratory, Los Alamos, New Mexico," U.S. Department of Energy document DOE/EA-1736, Los Alamos Site Office, Los Alamos, New Mexico. (DOE 2010, 206433)

EPA (U.S. Environmental Protection Agency), August 12, 2014. "NPDES Permit No. NM0028355 Final Permit Decision," U.S. Environmental Protection Agency Region 6, Dallas, Texas. (EPA 2014, 600257)

EPA (U.S. Environmental Protection Agency), March 27, 2015. "NPDES Permit No. NM0028355, Final Permit Decision for Permit Modification," U.S. Environmental Protection Agency Region 6, Dallas, Texas. (EPA 2015, 701237)

Gray, J.R., G.D. Glysson, L.M. Turcios, and G.E. Schwarz, August 2000. "Comparability of Suspended-Sediment Concentration and Total Suspended Solids Data," U.S. Geological Survey Water-Resources Investigations Report 00-4191, Reston, Virginia. (Gray et al. 2000, 255422)

Griffin, J., January 11, 2021. Outfall 001 and 03A199 Data Request [and attachment, N3B Request for Data, Updated Outfall 001 Flow Diagram, and Summary of Changes]. E-mail message to L. Marble (N3B) and A. Chan (N3B) from J. Griffin (LANL), Los Alamos, New Mexico. (Griffin 2021, 701199)

LANL (Los Alamos National Laboratory), October 2009. "Investigation Report for Sandia Canyon," Los Alamos National Laboratory document LA-UR-09-6450, Los Alamos, New Mexico. (LANL 2009, 107453)

LANL (Los Alamos National Laboratory), May 2011. "Interim Measures Work Plan for Stabilization of the Sandia Canyon Wetland," Los Alamos National Laboratory document LA-UR-11-2186, Los Alamos, New Mexico. (LANL 2011, 203454)

LANL (Los Alamos National Laboratory), September 2011. "Work Plan and Final Design for Stabilization of the Sandia Canyon Wetland," Los Alamos National Laboratory document LA-UR-11-5337, Los Alamos, New Mexico. (LANL 2011, 207053)

LANL (Los Alamos National Laboratory), March 2012. "100% Design Memorandum for Sandia Wetlands Stabilization Project," Los Alamos National Laboratory, Los Alamos, New Mexico. (LANL 2012, 240016)

LANL (Los Alamos National Laboratory), September 2012. "Phase II Investigation Report for Sandia Canyon," Los Alamos National Laboratory document LA-UR-12-24593, Los Alamos, New Mexico. (LANL 2012, 228624)

LANL (Los Alamos National Laboratory), December 2013. "Completion Report for Sandia Canyon Grade-Control Structure," Los Alamos National Laboratory document LA-UR-13-29285, Los Alamos, New Mexico. (LANL 2013, 251743)

LANL (Los Alamos National Laboratory), June 2014. "Sandia Wetland Performance Report, Baseline Conditions 2012–2014," Los Alamos National Laboratory document LA-UR-14-24271, Los Alamos, New Mexico. (LANL 2014, 257590)

LANL (Los Alamos National Laboratory), December 15, 2014. "2014 Annual Monitoring Report for Sandia Canyon Wetland Grade-Control Structure (SPA-2012-00050-ABQ)," Los Alamos National Laboratory letter and attachments (ENV-DO-14-0378) to K.E. Allen (USACE) from A.R. Grieggs (LANL), Los Alamos, New Mexico. (LANL 2014, 600083)

LANL (Los Alamos National Laboratory), April 2015. "Sandia Wetland Performance Report, Performance Period April 2014–December 2014," Los Alamos National Laboratory document LA-UR-15-22463, Los Alamos, New Mexico. (LANL 2015, 600399)

LANL (Los Alamos National Laboratory), September 2015. "Supplemental Investigation Report for Upper Sandia Canyon Aggregate Area, Revision 1," Los Alamos National Laboratory document LA-UR-15-26598, Los Alamos, New Mexico. (LANL 2015, 600912)

LANL (Los Alamos National Laboratory), April 2016. "2015 Sandia Wetland Performance Report," Los Alamos National Laboratory document LA-UR-16-22618, Los Alamos, New Mexico. (LANL 2016, 601432)

LANL (Los Alamos National Laboratory), April 2017. "2016 Sandia Wetland Performance Report," Los Alamos National Laboratory document LA-UR-17-23076, Los Alamos, New Mexico. (LANL 2017, 602341)

LANL (Los Alamos National Laboratory), April 2018. "2017 Sandia Wetland Performance Report," Los Alamos National Laboratory document LA-UR-18-23194, Los Alamos, New Mexico. (LANL 2018, 603022)

LANL (Los Alamos National Laboratory), September 2021. "ASER Annual Site Environmental Report 2020," Los Alamos National Laboratory document LA-UR-21-28555, Los Alamos, New Mexico. (LANL 2021, 701835)

LANL (Los Alamos National Laboratory), February 16, 2022. "Response to N3B Information Request for the 2021 Sandia Wetlands Report," Los Alamos National Laboratory letter (EPC-DO: 22-056) and attachments to E. Loechell (N3B) from S. Story (LANL), Los Alamos, New Mexico. (LANL 2022, 701910)

N3B (Newport News Nuclear BWXT-Los Alamos, LLC), April 2019. "2018 Sandia Wetland Performance Report," Newport News Nuclear BWXT-Los Alamos, LLC, document EM2019-0091, Los Alamos, New Mexico. (N3B 2019, 700415)

N3B (Newport News Nuclear BWXT-Los Alamos, LLC), March 2020. “2019 Sandia Wetland Performance Report,” Newport News Nuclear BWXT-Los Alamos, LLC, document EM2020-0020, Los Alamos, New Mexico. (N3B 2020, 700810)

N3B (Newport News Nuclear BWXT-Los Alamos, LLC), September 2020. “Interim Facility-Wide Groundwater Monitoring Plan for the 2021 Monitoring Year, October 2020–September 2021, Revision 1,” Newport News Nuclear BWXT-Los Alamos, LLC, document EM2020-0404, Los Alamos, New Mexico. (N3B 2020, 701041)

N3B (Newport News Nuclear BWXT-Los Alamos, LLC), March 2021. “2020 Sandia Wetland Performance Report,” Newport News Nuclear BWXT-Los Alamos, LLC, document EM2021-0053, Los Alamos, New Mexico. (N3B 2021, 701253)

N3B (Newport News Nuclear BWXT-Los Alamos, LLC), September 2021. “Interim Facility-Wide Groundwater Monitoring Plan for the 2022 Monitoring Year, October 2021–September 2022, Revision 1,” Newport News Nuclear BWXT-Los Alamos, LLC, document EM2021-0535, Los Alamos, New Mexico. (N3B 2021, 701672)

NMED (New Mexico Environment Department), June 9, 2011. “Approval with Modification, Interim Measures Work Plan for Stabilization of the Sandia Canyon Wetland,” New Mexico Environment Department letter to G.J. Rael (DOE-LASO) and M.J. Graham (LANL) from J.E. Kieling (NMED-HWB), Santa Fe, New Mexico. (NMED 2011, 203806)

Rai, D., L.E. Eary, and J.M. Zachara, October 1989. “Environmental Chemistry of Chromium,” *Science of the Total Environment,* Vol. 86, No. 1–2, pp. 15–23. (Rai et al. 1989, 249300)

5.2 Map Data Sources

Rain Gages; Los Alamos National Laboratory; ER-ES Surface Hydrology Group; 2017.

WQH NPDES Outfalls; Los Alamos National Laboratory, ENV Water Quality and Hydrology Group; Edition 2002.01; 01 September 2003.

Alluvial Well Locations; Los Alamos National Laboratory, Waste and Environmental Services Division; Locus EIM database pull; 2017.

Paved Road Arcs; Los Alamos National Laboratory, FWO Site Support Services, Planning, Locating and Mapping Section; 06 January 2004; as published 29 November 2010.

Grade Control Structure and Cascade Pool; Los Alamos National Laboratory; ER-ES Engineering Services; as published, project 14-0015; 2017.

Structures; Los Alamos National Laboratory, FWO Site Support Services, Planning, Locating and Mapping Section; 06 January 2004; as published 29 November 2010.

Former Los Alamos County Landfill; Los Alamos National Laboratory; ER-ES Engineering Services; as published, project 14-0015; 2017.

Canyon Reaches; Los Alamos National Laboratory, ENV Environmental Remediation and Surveillance Program, ER2002-0592; 1:24,000 Scale Data; Unknown publication date.

Technical Area Boundaries; Los Alamos National Laboratory, Site Planning & Project Initiation Group, Infrastructure Planning Office; September 2007; as published 13 August 2010.

Orthophotography, Los Alamos National Laboratory Site, 2014; Los Alamos National Laboratory, Site Planning and Project Initiation Group, Space and Site Management Office; 2014.

Contours, 20 and 5-ft intervals; as generated from 2014 LiDAR elevation data; Los Alamos National Laboratory, ER-ES; as published, project 14-0015; 2017.

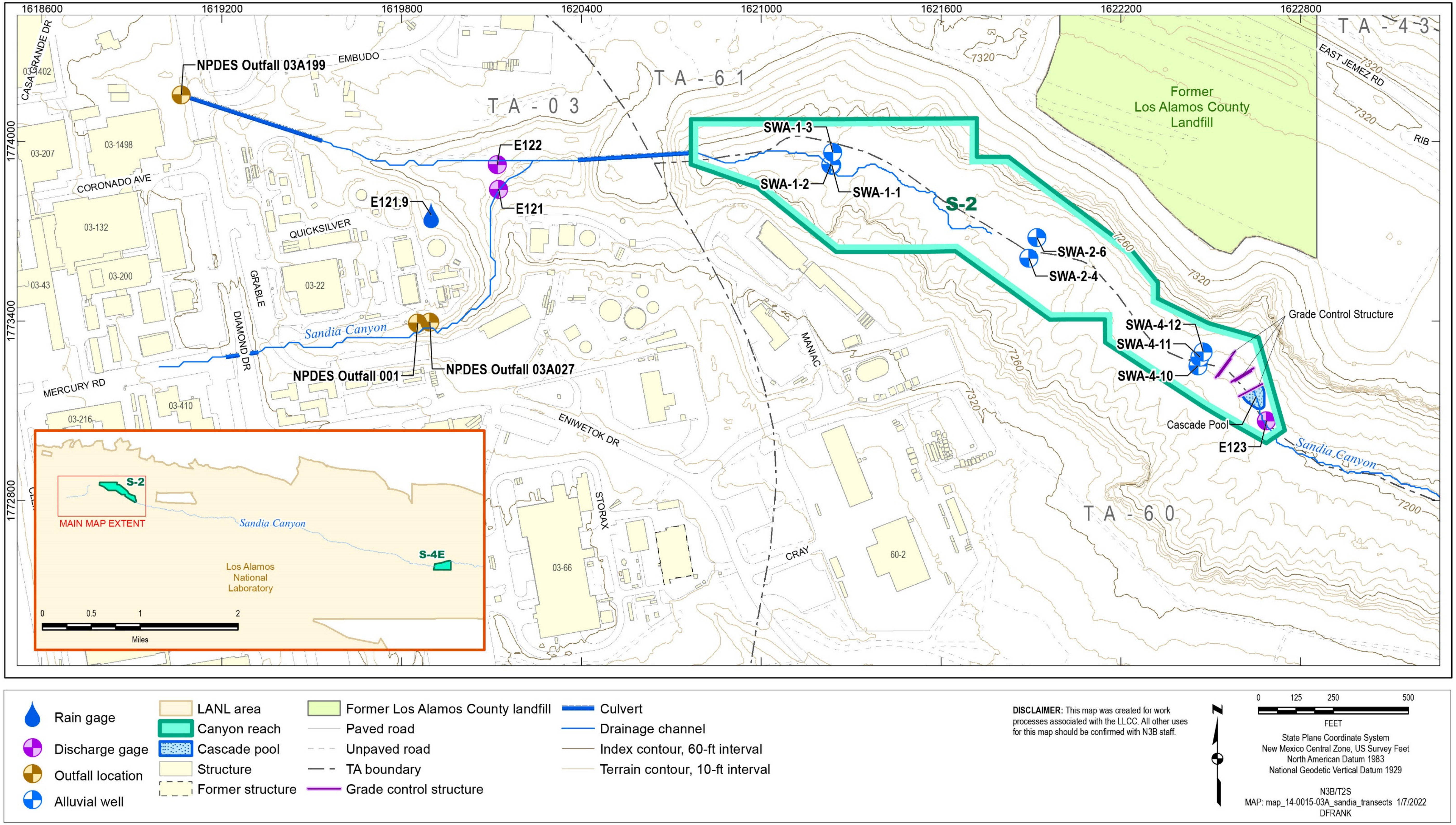

Note: Reach S-2 essentially encompasses the wetland. Reach S-4E is located approximately 3.4 mi downstream of S-2.

Figure 1.0-1 Locations of the Sandia GCS, National Pollutant Discharge Elimination System outfalls, precipitation gage E121.9, alluvial wells, surface and storm water gaging stations, former Los Alamos County landfill, surrounding technical areas, and reaches S-2 and S-4E

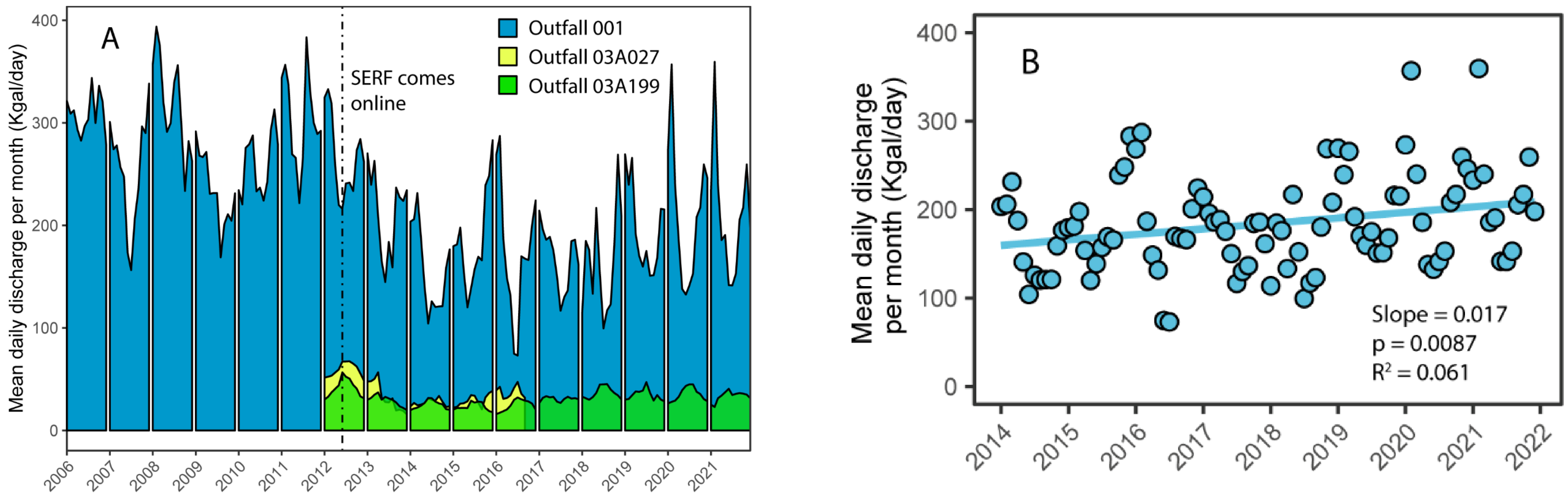

Notes: Monthly average effluent release volumes are shown for Outfall 001 from January 2006 through December 2021 (blue); for Outfall 03A027 from January 2012 through September 2016 (yellow); and for Outfall 03A199 from January 2012 through December 2021 (green). Note that no discharges to Outfall 03A027 have occurred since September 2016. Linear regression fitted to mean daily discharge per month data. There has been a small, but significant, increasing trend in mean daily discharge per month since 2014 ($p = 0.0087$, linear regression).

Figure 1.1-1 (a) Monthly average effluent release volumes (expressed as kgal./day) and (b) Linear regression fitted to mean daily discharge per month data

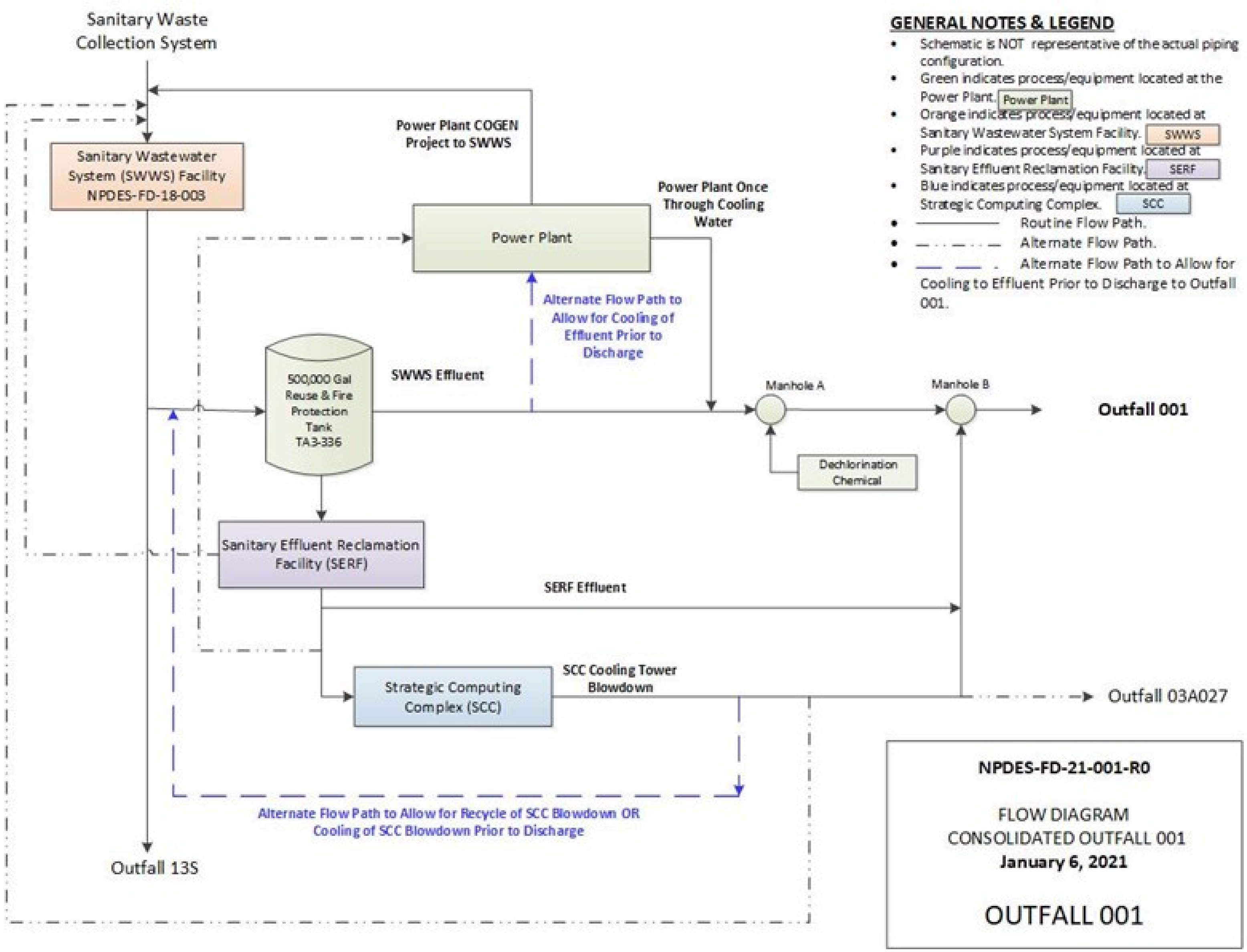

Figure 1.1-2 Updated process schematic for the power plant, SWWS, and SERF connections to Outfall 001 (current configuration)

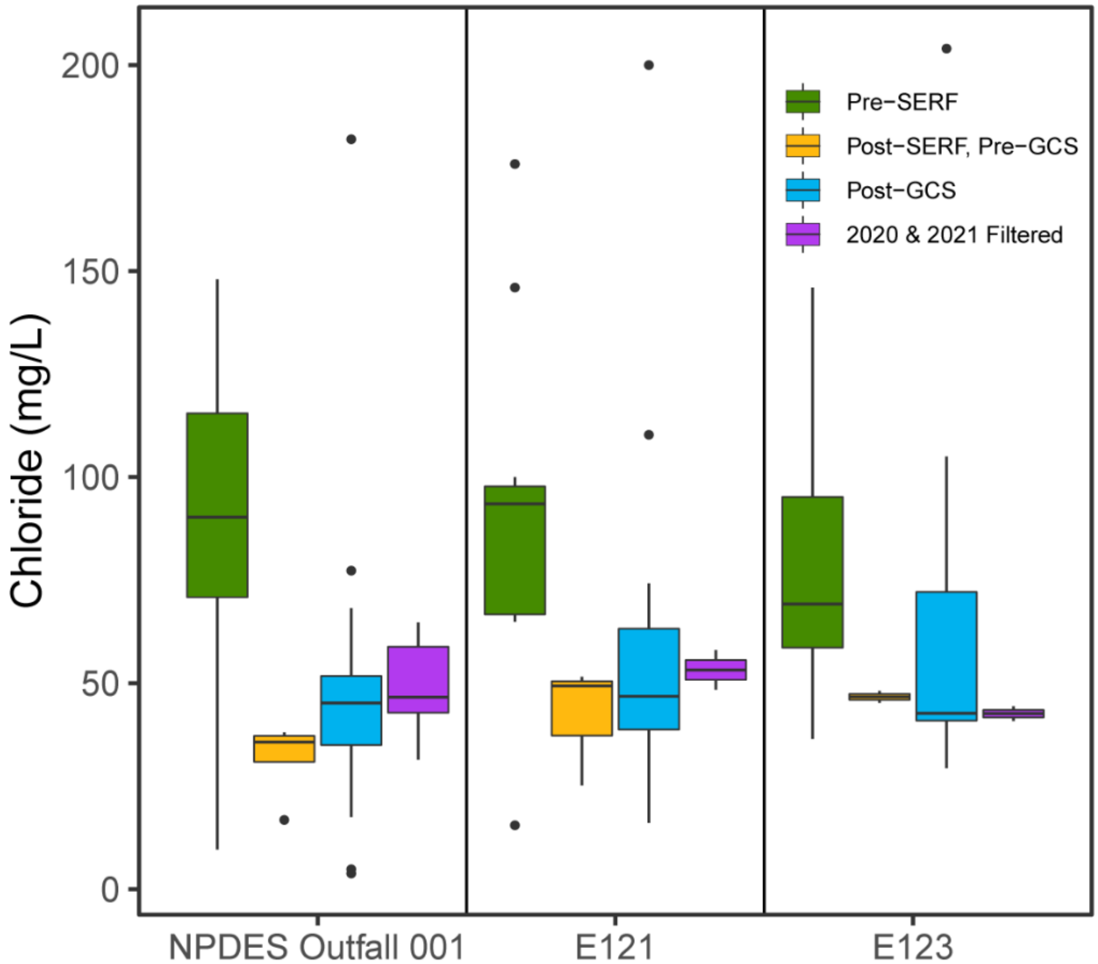

Notes: The lower and upper bounds of each box correspond to the first and third quartiles, respectively, and the thick black line in each box shows the median. Whiskers extend to the largest or smallest value, or at most 1.5 times +/- the interquartile range (the height of the box). Values above or below the whiskers are marked as outliers (solid black points). The post-GCS period includes data from 2014 to 2019. Note that because of differences in monitoring requirements at Outfall 001 compared with E121 and E123, concentrations before 2020 should not be compared across locations. Outfall 001 samples through 2019 were unfiltered, while data from gaging stations E121 and E123 have always been filtered. Beginning in 2020, Outfall 001 samples changed to being filtered, meaning the 2020 & 2021 Filtered boxplots can be compared across locations.

Figure 1.1-3 Box-and-whisker plots of chloride concentration, a water quality indicator, before and after SERF came online and before and after the GCS was constructed, at Outfall 001 and at gaging stations E121 and E123

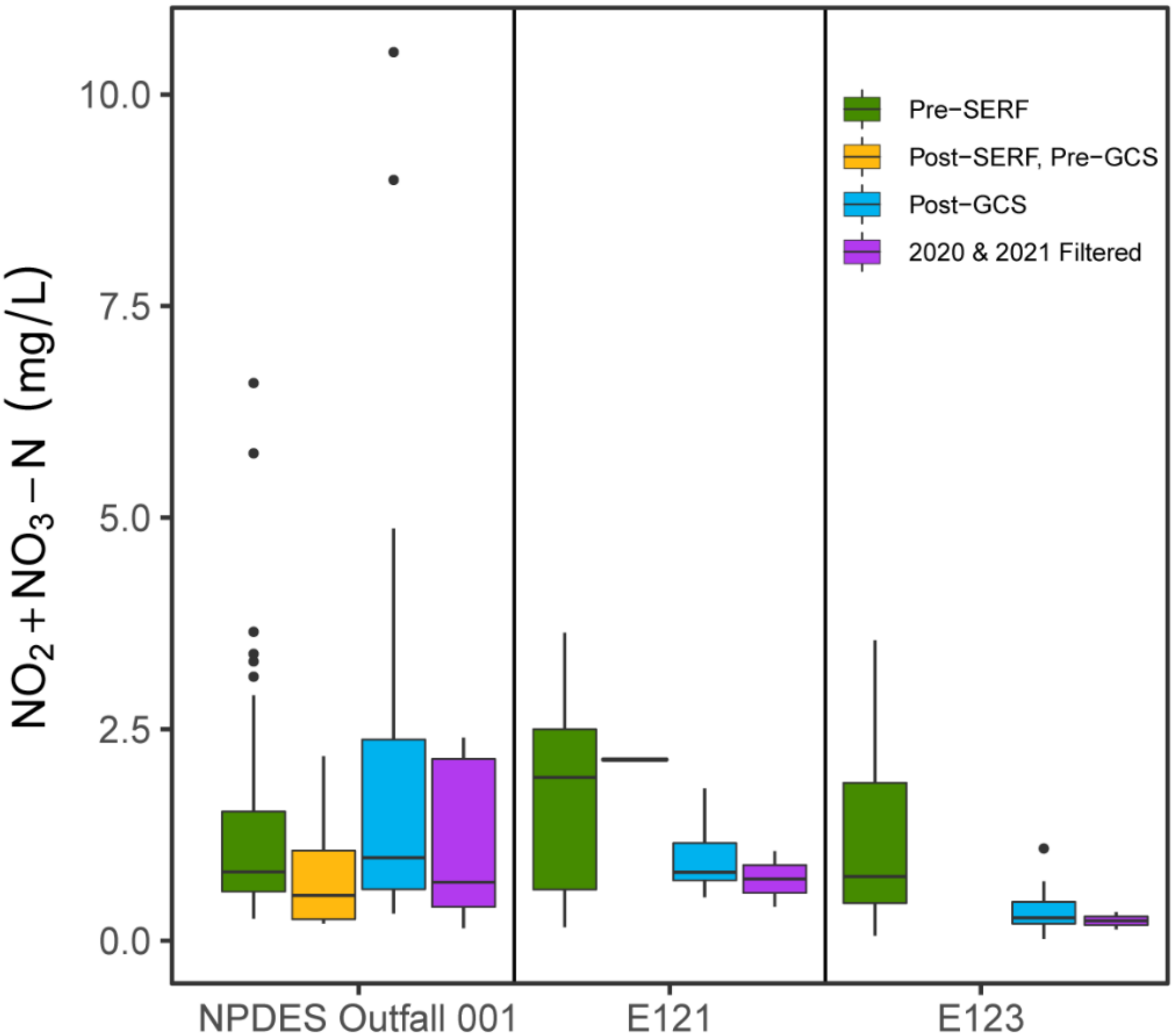

Notes: The lower and upper bounds of each box correspond to the first and third quartiles, respectively, and the thick black line in each box shows the median. Whiskers extend to the largest or smallest value, or at most 1.5 times +/- the interquartile range (the height of the box). Values above or below the whiskers are marked as outliers (solid black points). The post-GCS period includes data from 2014 to 2019. Note that because of differences in monitoring requirements at Outfall 001 compared with E121 and E123, concentrations before 2020 should not be compared across locations. Outfall 001 samples through 2019 were unfiltered, while data from gaging stations E121 and E123 have always been filtered. Beginning in 2020, Outfall 001 samples changed to being filtered, meaning the 2020 & 2021 Filtered boxplots can be compared across locations.

Figure 1.1-4 Box-and-whisker plots of nitrate plus nitrite as nitrogen concentration, a water quality indicator, before and after SERF came online and before and after the GCS was constructed, at Outfall 001 and at gaging stations E121 and E123

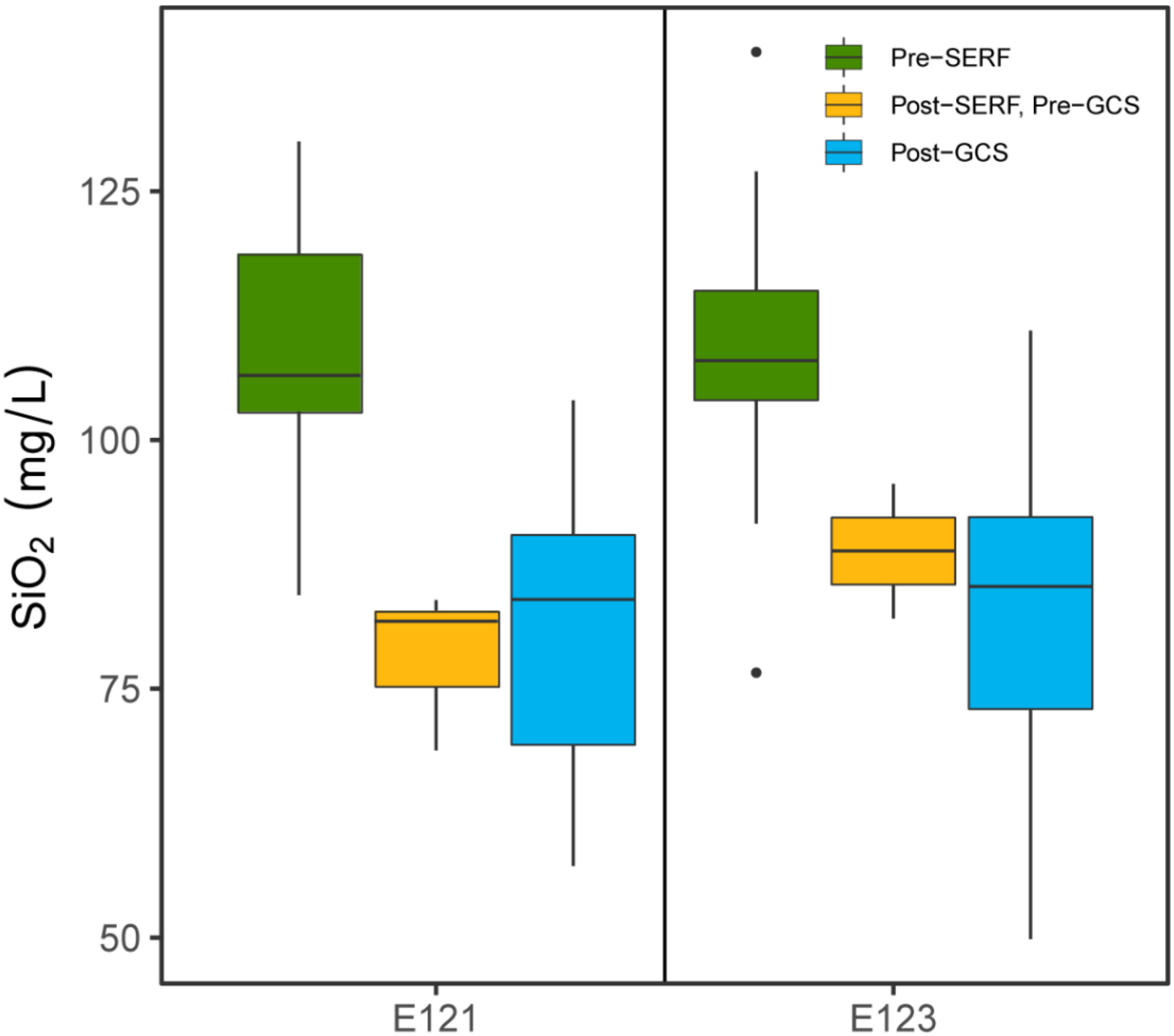

Notes: The lower and upper bounds of each box correspond to the first and third quartiles, respectively, and the thick black line in each box shows the median. Whiskers extend to the largest or smallest value, or at most 1.5 times +/- the interquartile range (the height of the box). Values above or below the whiskers are marked as outliers (solid black points). The post-GCS period includes data from 2014 to 2021.

Figure 1.1-5 Box-and-whisker plots of silicon dioxide concentration, a water quality indicator, before and after SERF came online and before and after the GCS was constructed, at gaging stations E121 and E123. Silicon dioxide is not measured at Outfall 001.

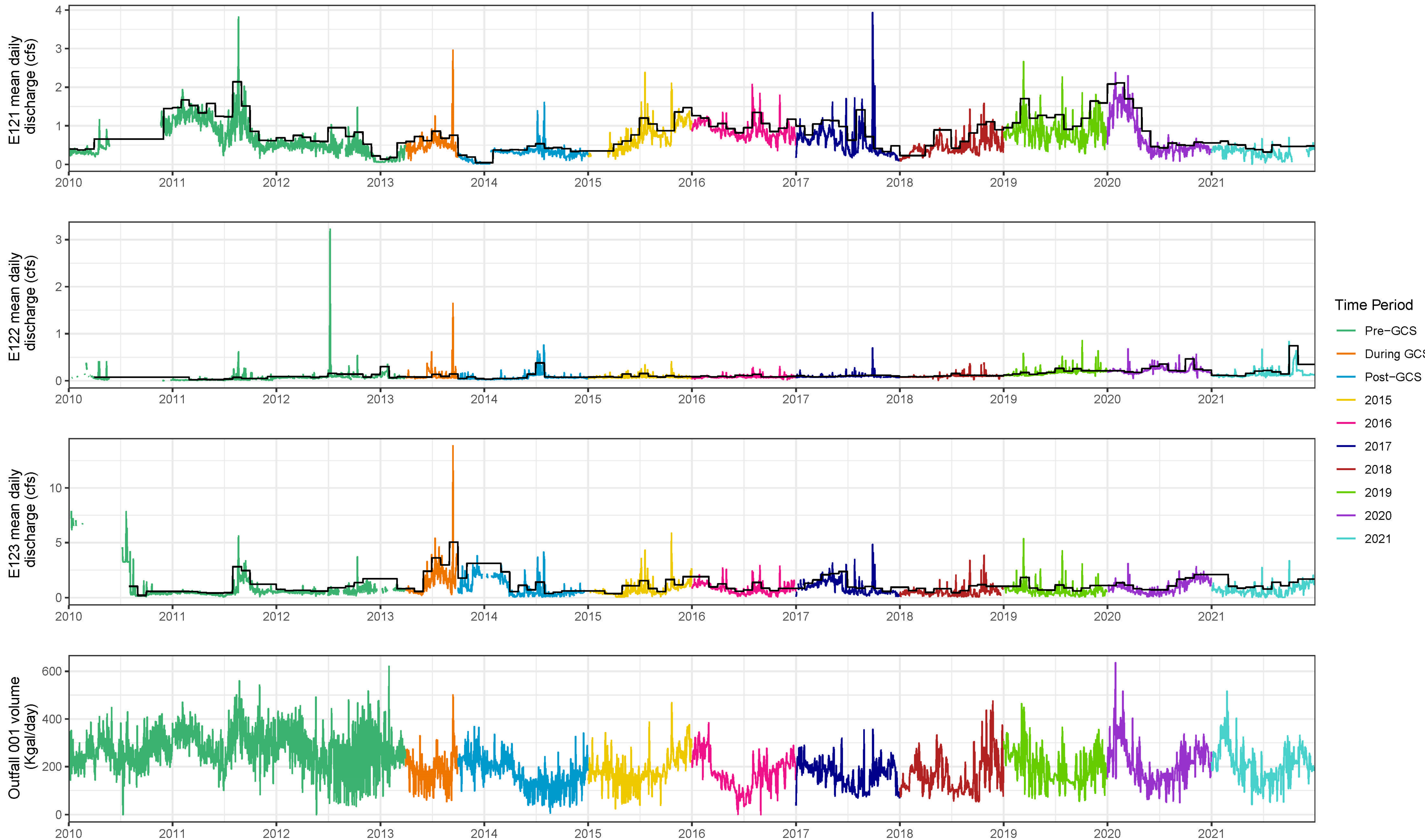

Note: Black lines show approximate base flow, calculated as the monthly median daily discharge plus 1.5 times the interquartile range.

Figure 3.1-1 Time series plots from 2010 to 2021 showing mean daily discharge at gaging stations E121, E122, and E123 and Outfall 001

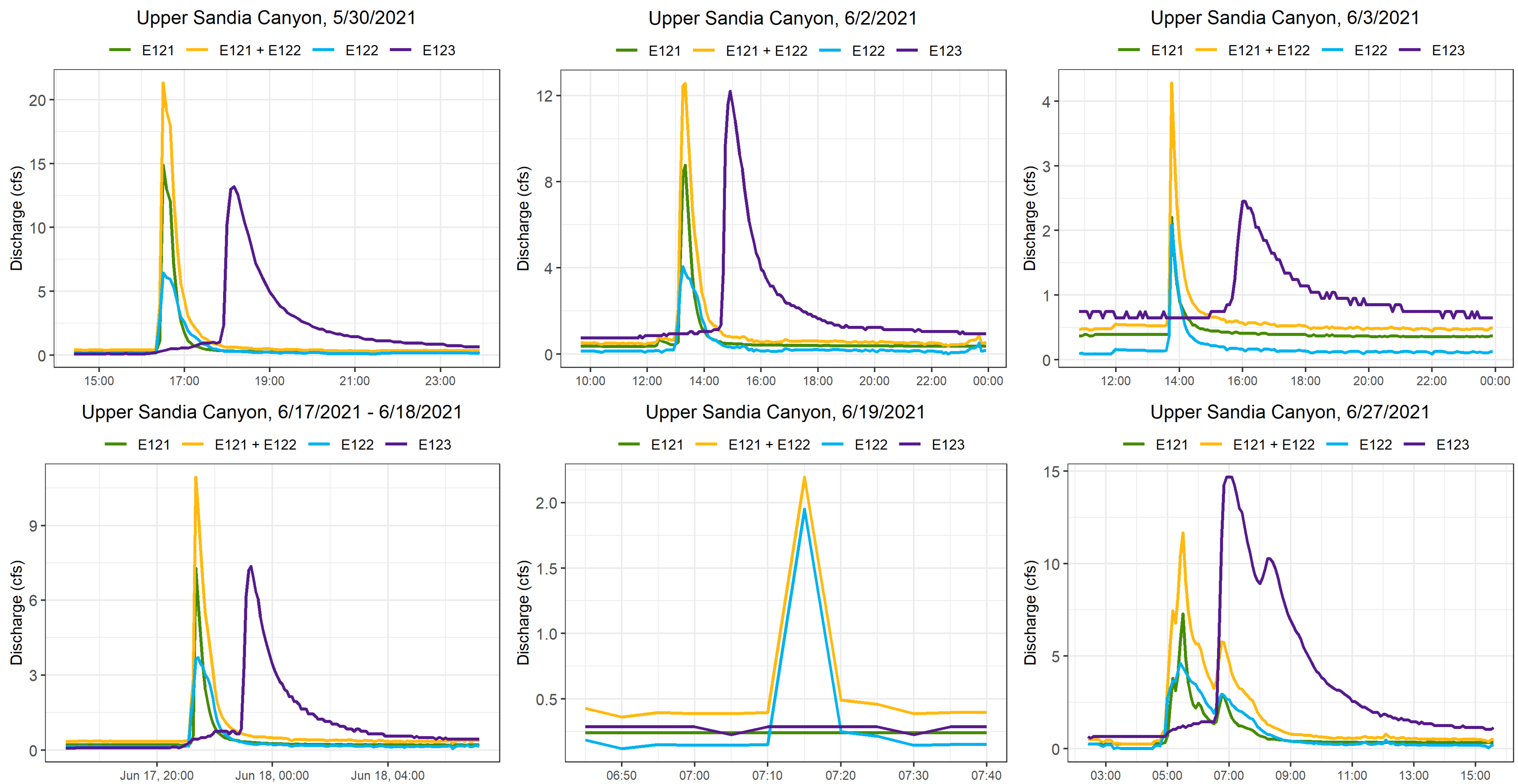

Notes: Not all gages were sampled during every storm event. Refer to Table 2.2-2 for details on each gage.

Figure 3.1-2 Hydrographs of storm water discharge at E121, E122, and E123 during each sample-triggering storm event in 2021

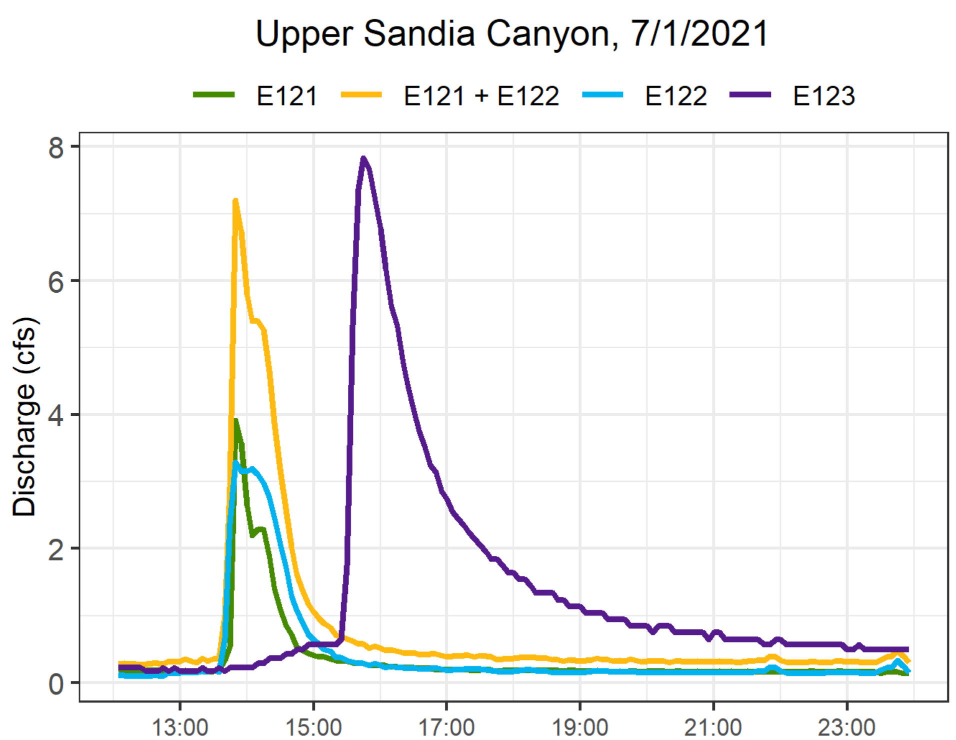

Notes: Not all gages were sampled during every storm event. Refer to Table 2.2-2 for details on each gage.

Figure 3.1-2 (continued) Hydrographs of storm water discharge at E121, E122, and E123 during each sample-triggering storm event in 2021

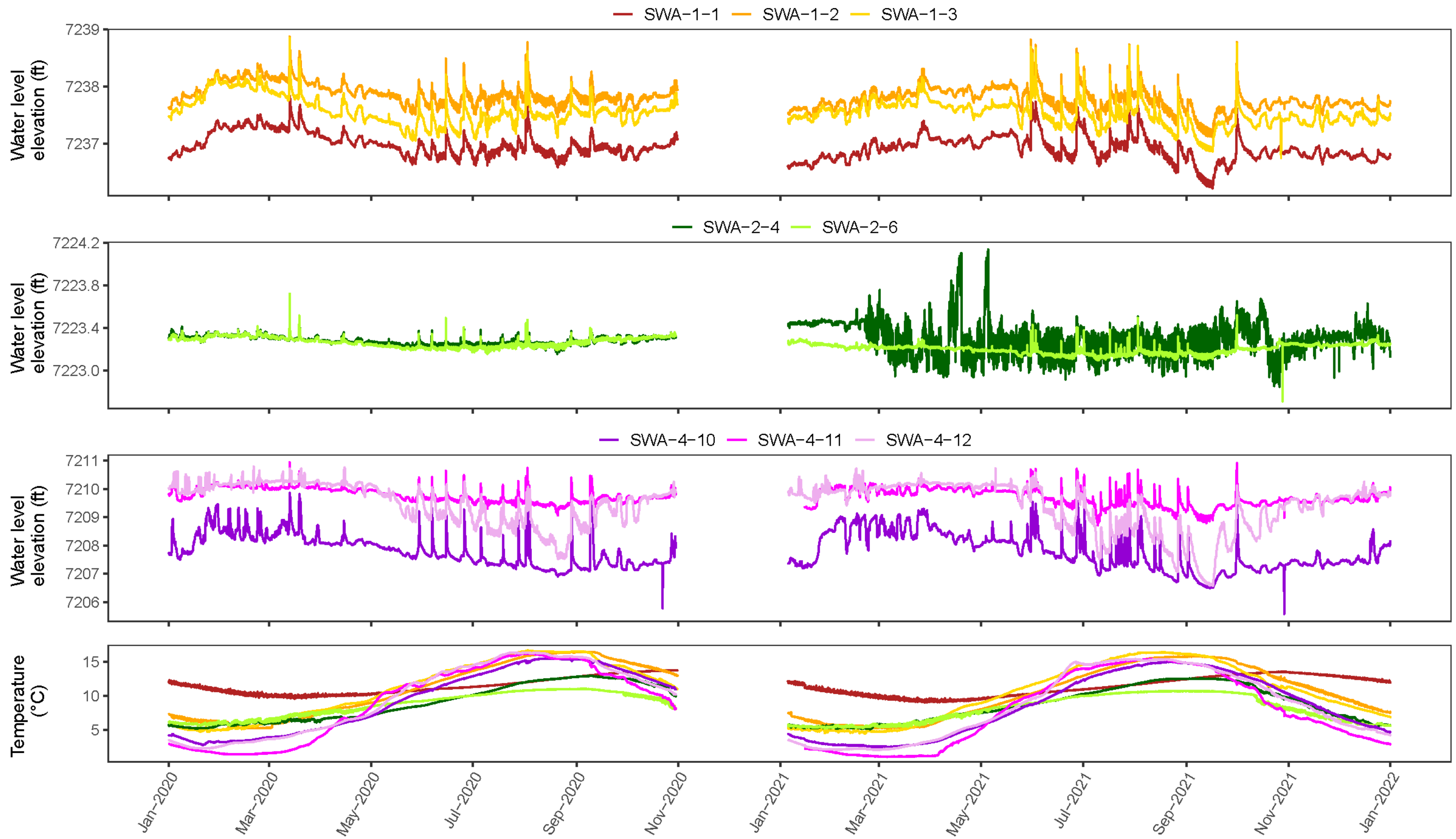

Note: Because of a programming error of the pressure transducers, there was a gap in data collection between approximately November 2020 and January 2021.

Figure 3.1-3 Alluvial water levels and alluvial water temperature in 2020 and 2021

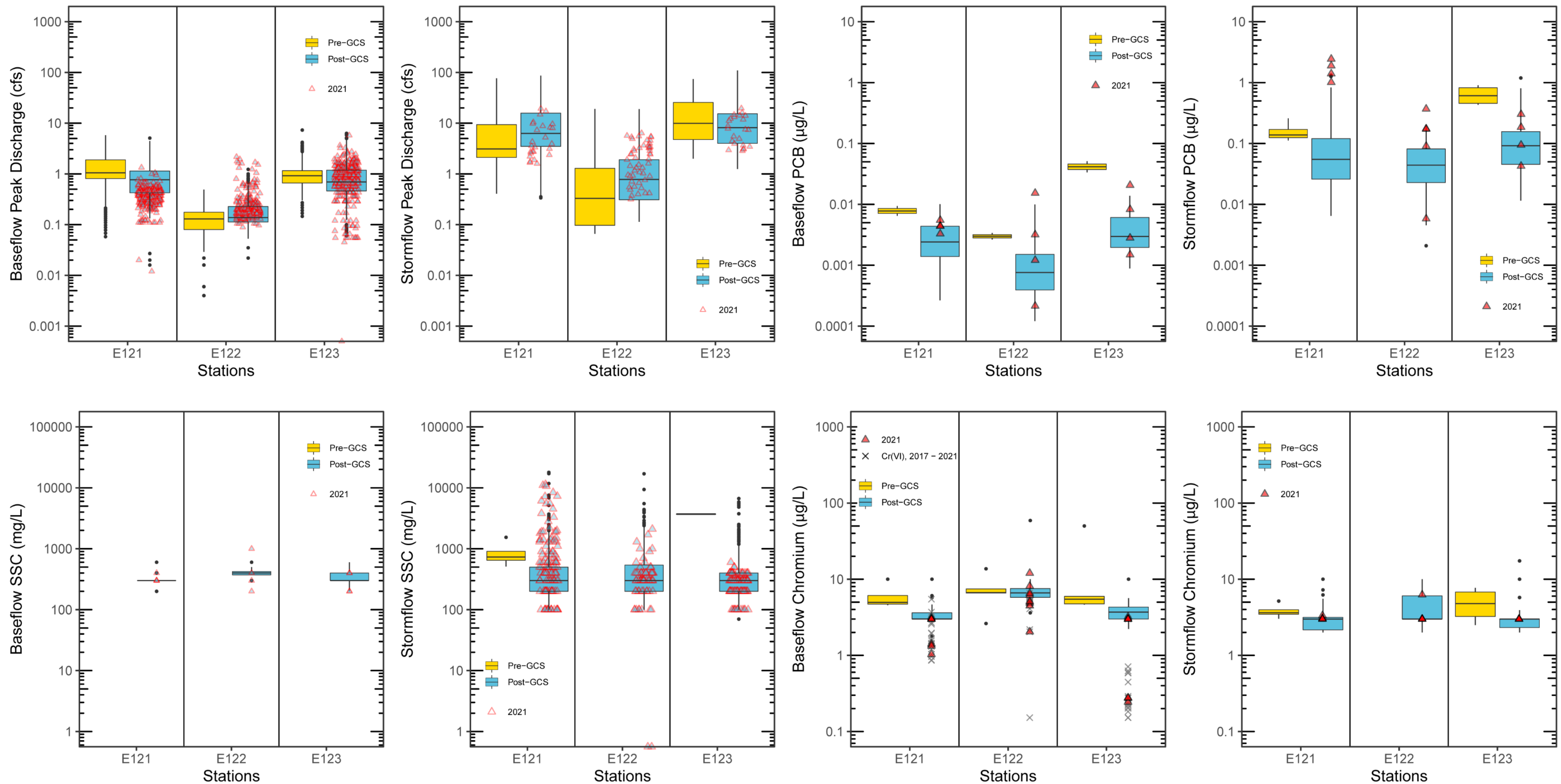

Notes: Data for 2021 are not included in the post-GCS boxplots and are only overlaid as triangles. Triangles falling directly on the x-axis represent zeros (the log-scale is not defined for zero). The lower and upper bounds of each box correspond to the first and third quartiles, respectively, and the thick black line in each box shows the median. Whiskers extend to the largest or smallest value, or at most 1.5 times +/- the interquartile range (the height of the box). Values above or below the whiskers are marked as outliers (solid black points). Before 2012, total suspended sediment (TSS) was measured rather than SSC; TSS data are not shown on the SSC plots as they are not comparable metrics. There were no pre-GCS base-flow data for SSC and limited pre-GCS storm-flow data. Cr(VI) has only been measured in base flow data since 2017.

Figure 3.3-1 Pre- and post-GCS box-and-whisker plots of peak discharge, SSC, total PCBs, dissolved chromium and Cr(VI), and PAHs for base flow and storm flow at gaging stations E121, E122, and E123

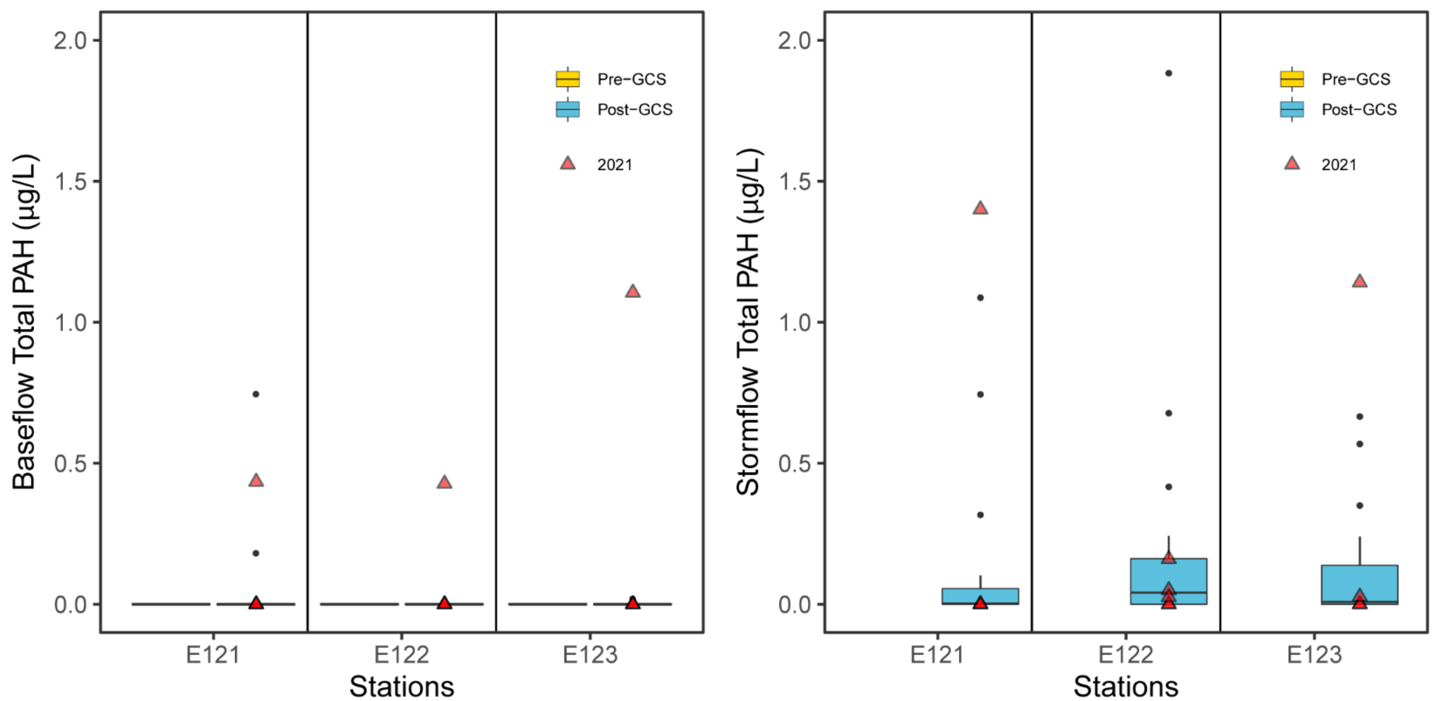

Notes: Data for 2021 are not included in the post-GCS boxplots and are only overlaid as triangles. Triangles falling directly on the x-axis represent zeros (the log-scale is not defined for zero). The lower and upper bounds of each box correspond to the first and third quartiles, respectively, and the thick black line in each box shows the median. Whiskers extend to the largest or smallest value, or at most 1.5 times +/- the interquartile range (the height of the box). Values above or below the whiskers are marked as outliers (solid black points). Before 2012, TSS was measured rather than SSC; TSS data are not shown on the SSC plots as they are not comparable metrics. There were no pre-GCS base-flow data for SSC and limited pre-GCS storm-flow data. Cr(VI) has only been measured in base flow data since 2017.

Figure 3.3-1 (continued) Pre- and post-GCS box-and-whisker plots of peak discharge, SSC, total PCBs, dissolved chromium and Cr(VI), and PAHs for base flow and storm flow at gaging stations E121, E122, and E123

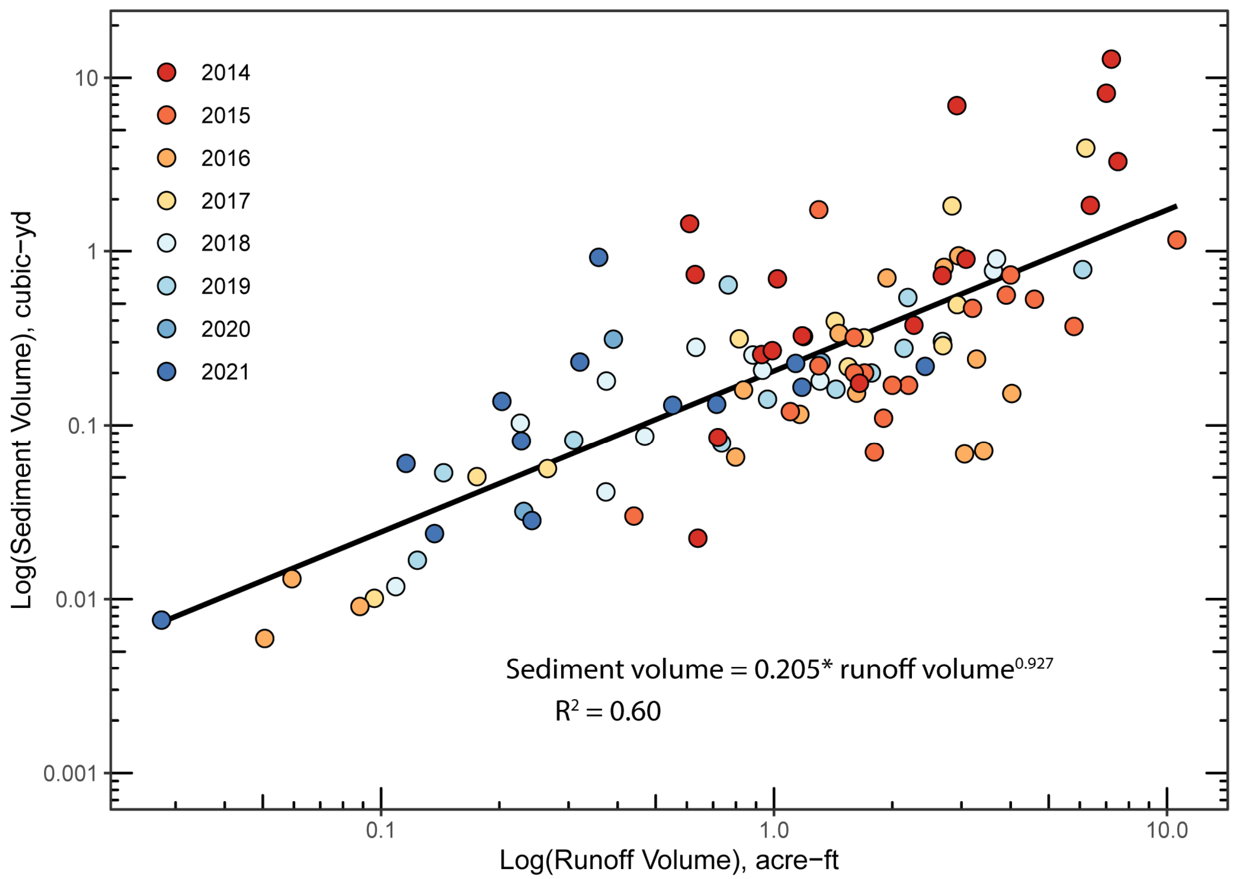

Notes: The best-fit line is shown in black. Note that the model generated is not linear because data are displayed on a log-scale. Sediment volume was not calculated for the storm event at E122 on 6/19/2021 because the 24-bottle ISCO did not collect samples. Therefore, there were not enough SSC samples to make an accurate calculation.

Figure 3.3-2 Log-log plot showing the relationship between sediment volume and runoff volume from storm events from 2014 through 2021 at gaging stations E121, E122, and E123

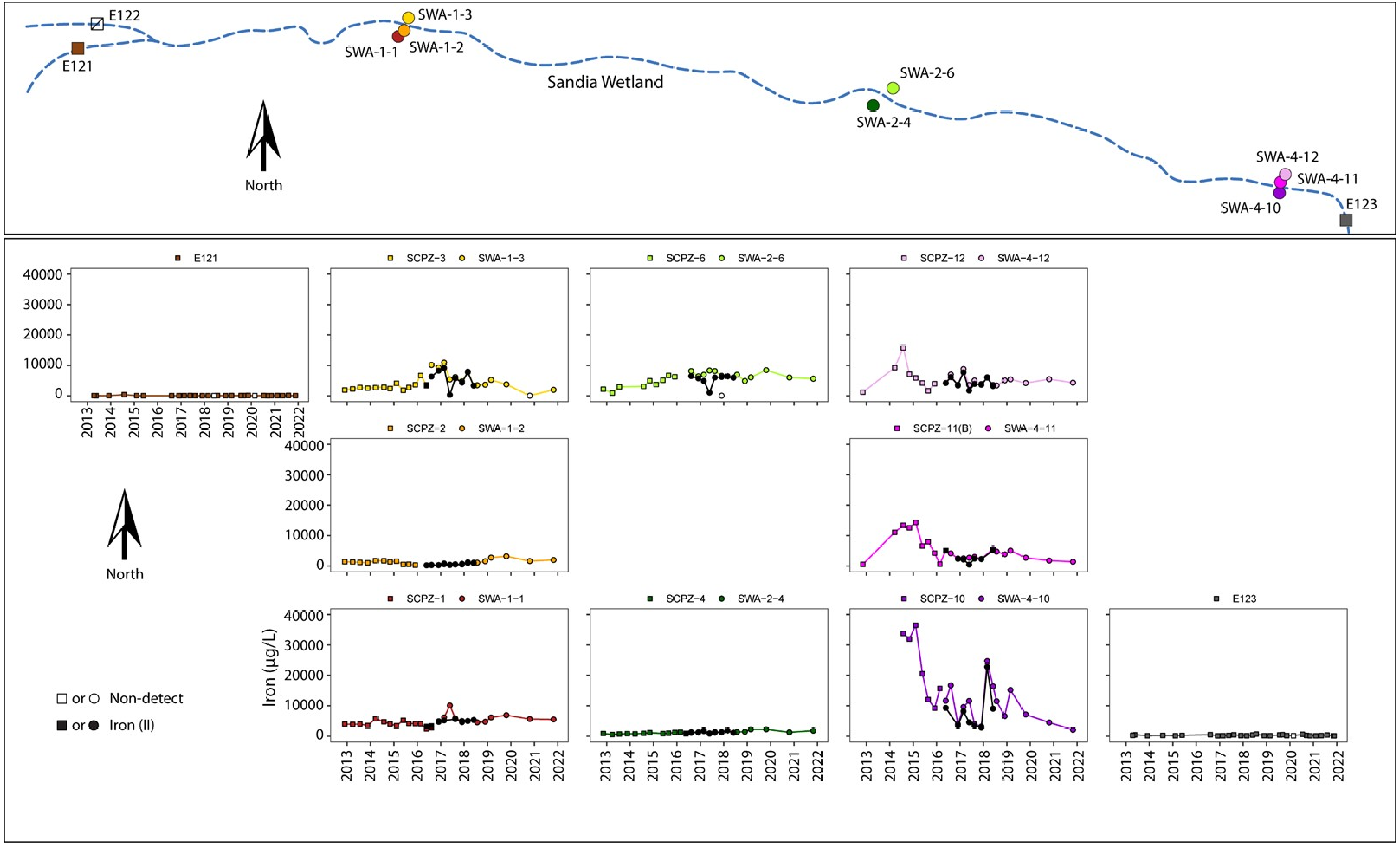

Notes: Surface water stations include E121, E122 (plot not shown), and E123. Piezometers are labeled with the prefix SCPZ (square symbols), and alluvial wells are labeled with the prefix SWA (circle symbols). The plots are arranged in three transects from west to east. Data are plotted for the full period of wetland monitoring. Nondetections are plotted as the MDL with open symbols. Total iron is represented with colored symbols and Fe(II) with black symbols. Monitoring at alluvial wells SWA-2-5, SWA-3-7, SWA-3-8, and SWA-3-9 was discontinued in 2019; data can be found in previous years' reports. The map above is not to scale but shows approximate sampling locations in relation to the approximate thalweg (blue dashed line).

Figure 3.4-1 Iron concentrations in Sandia wetland surface water and alluvial system

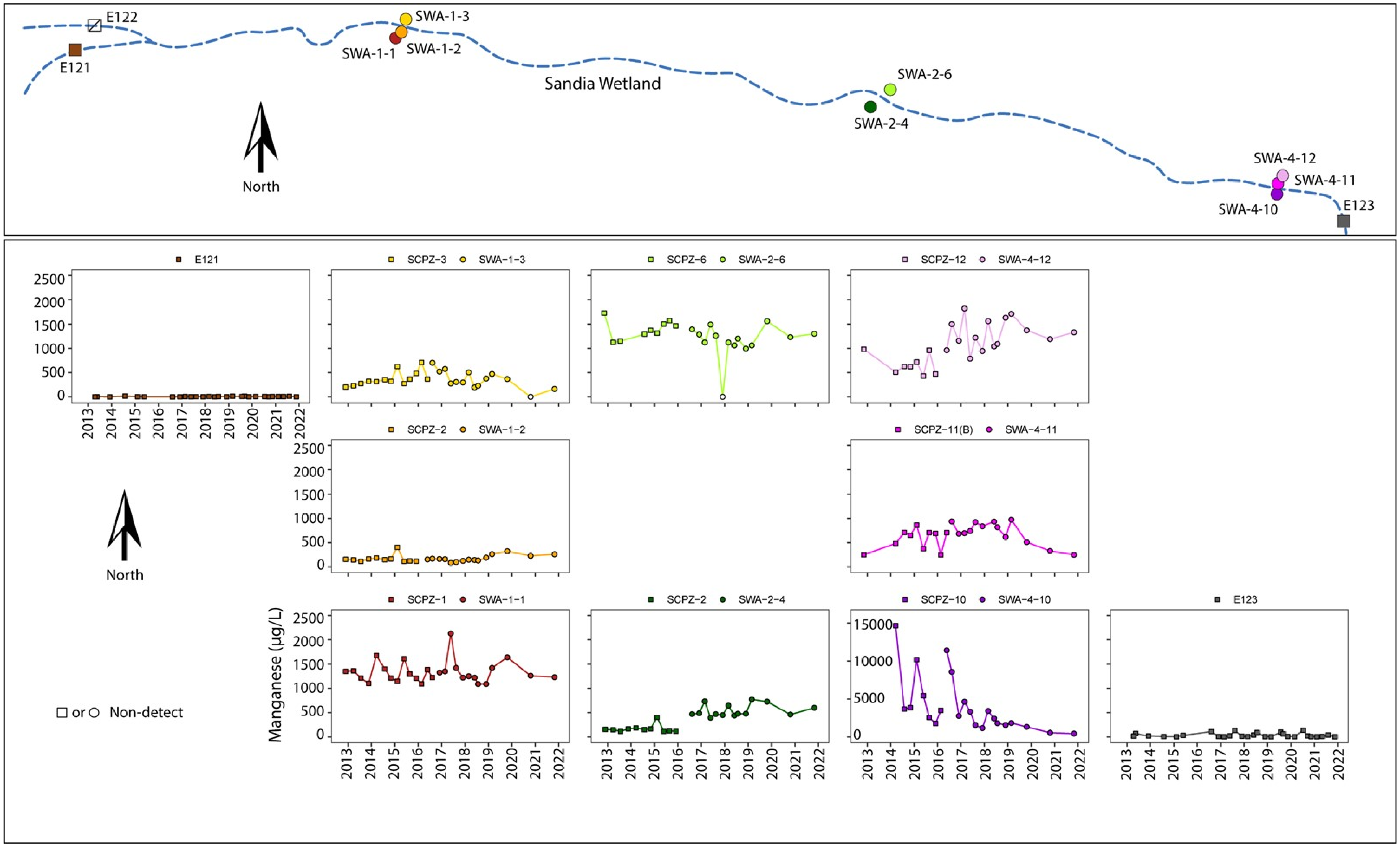

Notes: Surface water stations include E121, E122 (plot not shown), and E123. Piezometers are labeled with the prefix SCPZ (square symbols), and alluvial wells are labeled with the prefix SWA (circle symbols). The plots are arranged in three transects from west to east. Data are plotted for the full period of wetland monitoring. Nondetections are plotted as the MDL with open symbols. Monitoring at alluvial wells SWA-2-5, SWA-3-7, SWA-3-8, and SWA-3-9 was discontinued in 2019; data can be found in previous years' reports. The map above is not to scale but shows approximate sampling locations in relation to the approximate thalweg (blue dashed line).

Figure 3.4-2 Manganese concentrations in Sandia wetland surface water and alluvial system

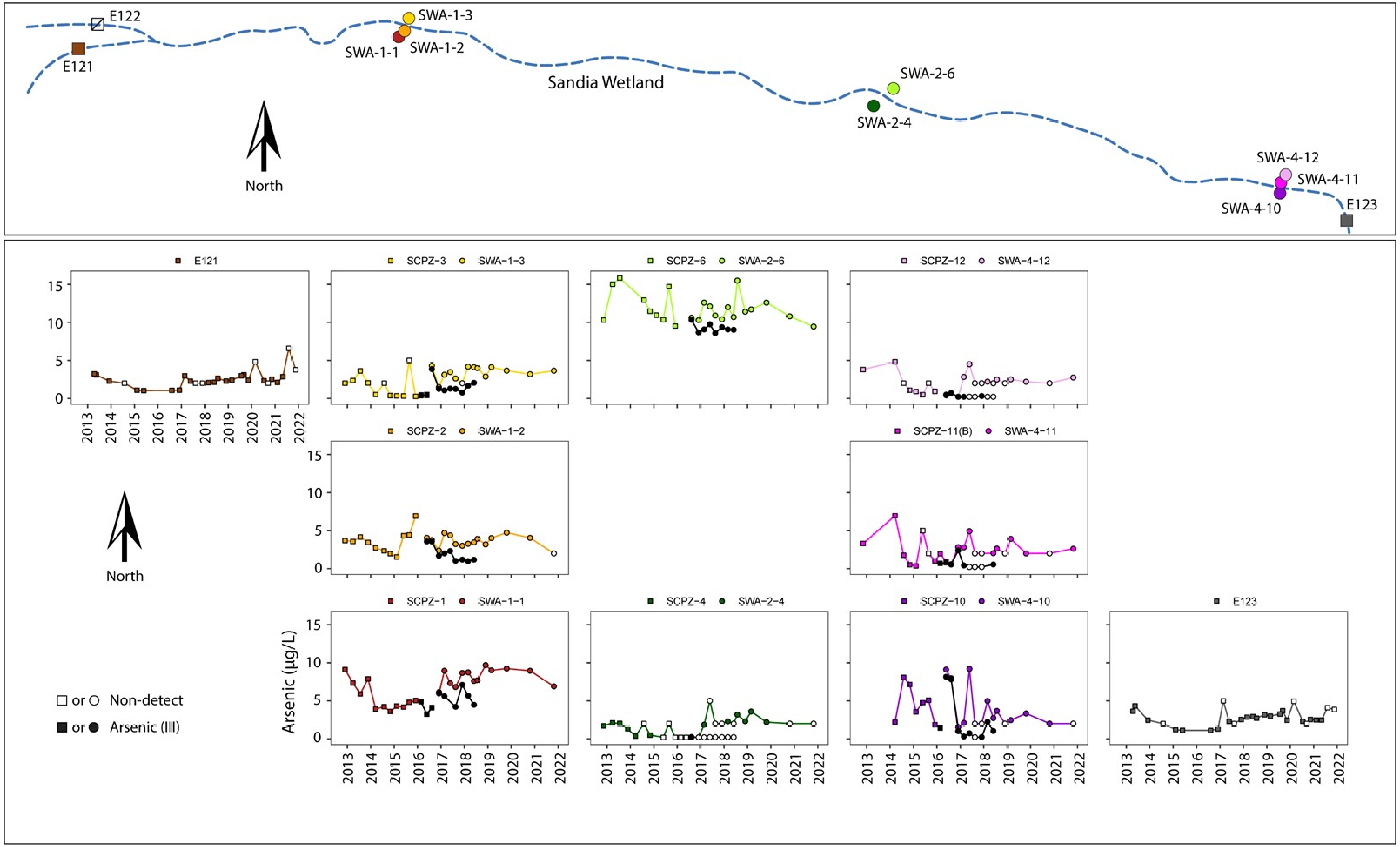

Notes: Surface water stations include E121, E122 (plot not shown), and E123. Piezometers are labeled with the prefix SCPZ (square symbols), and alluvial wells are labeled with the prefix SWA (circle symbols). The plots are arranged in three transects from west to east. Data are plotted for the full period of wetland monitoring. Nondetections are plotted as the MDL with open symbols. Total arsenic is represented with colored symbols and arsenite [As(III)] with black symbols. Monitoring at alluvial wells SWA-2-5, SWA-3-7, SWA-3-8, and SWA-3-9 was discontinued in 2019; data can be found in previous years' reports. The map above is not to scale but shows approximate sampling locations in relation to the approximate thalweg (blue dashed line).

Figure 3.4-3 Arsenic concentrations in Sandia wetland surface water and alluvial system

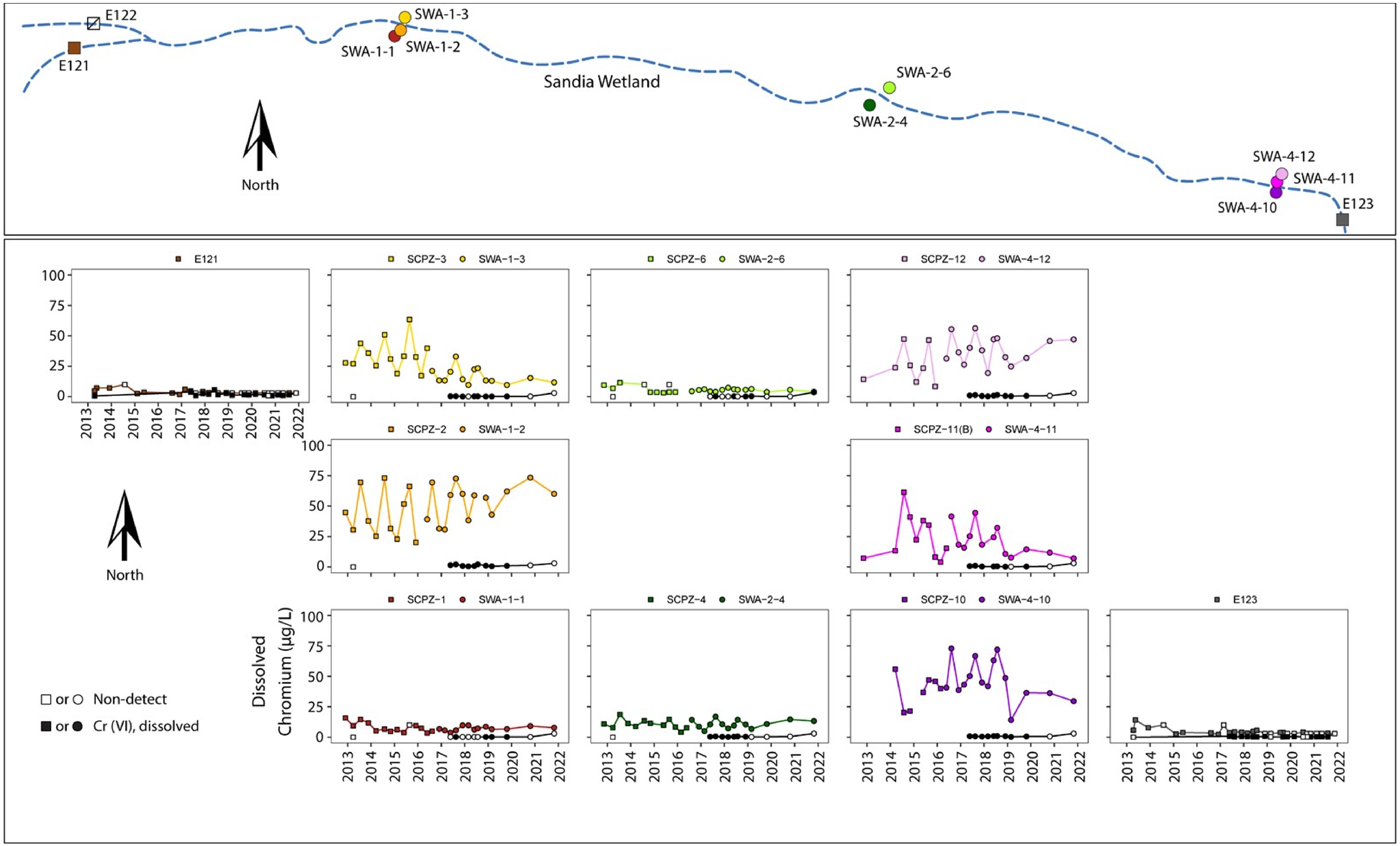

Notes: Surface water stations include E121, E122 (plot not shown), and E123. Piezometers are labeled with the prefix SCPZ (square symbols), and alluvial wells are labeled with the prefix SWA (circle symbols). The plots are arranged in three transects from west to east. Data are plotted for the full period of wetland monitoring. Nondetections are plotted as the MDL with open symbols. Total chromium is represented with colored symbols and Cr(VI) with black symbols. Monitoring at alluvial wells SWA-2-5, SWA-3-7, SWA-3-8, and SWA-3-9 was discontinued in 2019; data can be found in previous years' reports. The map above is not to scale but shows approximate sampling locations in relation to the approximate thalweg (blue dashed line).

Figure 3.4-4 Chromium concentrations in Sandia wetland surface water and alluvial system

Table 2.2-1
Schema Crosswalk: Past Piezometers and Current Alluvial Wells

Piezometer To	Alluvial Well	Date of Alluvial Well Installation
SCPZ-1	SWA-1-1	8/19/2016
SCPZ-2	SWA-1/SWA-1-2*	12/18/2014
SCPZ-3	SWA-1-3	7/21/2016
SCPZ-4	SWA-2-4	7/20/2016
SCPZ-6	SWA-2 / SWA-2-6*	12/16/2014
SCPZ-10	SWA-4-10	4/27/2016
SCPZ-11B	SWA-4-11	7/19/2016
SCPZ-12	SWA-4 / SWA-4-12*	12/15/2014

* SWA-1, SWA-2, and SWA-4 were pilot wells installed in December 2016; SWA-1-2, SWA-2-6, and SWA-4-12 are the same wells relabeled in 2015.

Table 2.2-2
Precipitation, Storm Water Peak Discharge, and Samples Collected at Gaging Stations E121, E122, and E123 for Each Sample-Triggering Storm Event in 2021

Storm Event Date	RG121.9 Total Precipitation (in.)	E121 Peak Discharge (ft^3/s)	E122 Peak Discharge (ft^3/s)	E123 Peak Discharge (ft^3/s)
5/30/2021	0.36	15 S[a]	6.4 NS[b]	13 S
6/2/2021	0.35	8.8 S	4.0 NS	12 S
6/3/2021	0[c]	2.2 BT[d]	2.0 S	2.4 BT
6/17/2021	0.20	7.3 S	3.6 S	7.4 S
6/19/2021	0.01	0.24 BT	1.9 S	0.29 BT
6/27/2021	0.64	7.3 S	4.6 S	15 S
7/1/2021	0.24	3.9 S	3.2 S	7.8 BT[e]

[a] S = Sample was collected. These discharge levels are shaded in green to emphasize those events for which discharge exceeded the trip level and samples were collected.

[b] NS = Trip level was exceeded at site but no samples were collected. This occurred at E122 when the activation trip level was left at the 2020 season value in error. The trip level was correct on 6/3/2021.

[c] No precipitation was recorded at RG121.9 on 6/3/21, but precipitation was recorded at other rain gages in the surrounding area, and all three gaging stations showed a flow response.

[d] BT = Flow was below the sampler trip level.

[e] Trip level at E123 was raised on 6/28/2021 after four samples were collected.

Table 2.2-3
2021 Sampling and Preservation Requirements for Sandia Wetland

Analytical Suite	Analytical Method	Sample Type[a]	Frequency	Filtered[b]	Preservation	Field Storage	Holding Time	Ideal Volume	Minimum Volume	Comment
Alluvial Wells[c]										
Cr(VI) speciation	IC-ICPMS:metals[d]	W	Annually	F	$NH_4OH/(NH_4)_2SO_4$ (liquid) buffer (1 mL to 100 mL of sample) to pH 9.3–9.7; ice	<4°C	28 days	125 mL	125 mL	—[e]
TAL[f] metals	SW-846:6010C and SW-846:6020 SW-846:7470A (Hg)	W	Annually	F	Nitric acid; ice	<4°C	6 months 28 days for Hg	1 L	300 mL	—
Surface Water Base Flow at Gages E121, E122, and E123										
PAH congeners	SW-846:8270D GC/MS-SIM[g]	WS	Quarterly	UF	Ice	<4°C	7 days	3 L	1 L	Amber glass with Teflon lid
PCB congeners	EPA:1668C	WS	Quarterly	UF	Ice	<4°C	1 yr	3 L	1L	Amber glass with Teflon lid
SVOC[h]	SW-846:8270D	WS	Quarterly	UF	Ice	<4°C	7 days	3 L	1 L	Amber glass with Teflon lid
TAL metals + total recoverable aluminum	SW-846:6010C and SW-846:6020 SW-846:7470A (Hg)	WS	Quarterly	F, UF, F10	Nitric acid; ice	<4°C	6 months 28 days for Hg	1 L	300 mL	—
Cr(VI) speciation	IC-ICPMS:metals	WS	Quarterly	F	$NH_4OH/(NH_4)_2SO_4$ (liquid) buffer (1 mL to 100 mL of sample) to pH 9.3–9.7; ice	<4°C	28 days	125 mL	125 mL	—
SSC	ASTM:D3977-97	WS	Quarterly	UF	Ice	No requirement	n/a[i]	1 L	1 L	—
Surface Water Storm Flow at Gages E121, E122, and E123										
PAH congeners	EPA:625 GCMS_SIM	WT	>10 cfs[j]	UF	Ice	<4°C	7 days	3 L	1 L	Amber glass with Teflon lid
PCB congeners	EPA:1668C	WT	>10 cfs	UF	Ice	<4°C	1 yr	3 L	1L	Amber glass with Teflon lid
SVOC	EPA:625	WT	>10 cfs	UF	Ice	<4°C	7 days	3 L	1 L	Amber glass with Teflon lid
TAL metals + total recoverable aluminum	EPA:200.7 and EPA:200.8 EPA:245.2 (Hg)	WT	>10 cfs	F, UF, F10	Nitric acid; ice	<4°C	6 months 28 days for Hg	1 L	300 mL	—
SSC	ASTM:D3977-97	WT	>10 cfs	UF	Ice	No requirement	n/a	1 L	1 L	—

[a] W = Alluvial groundwater samples; WS = base-flow water samples; WT = storm-flow water samples.
[b] F = Filtered using a 0.45-µm filter; UF = unfiltered; F10 = filtered using a 10-µm filter (for total recoverable aluminum only).
[c] Alluvial wells will be reduced to transect 1 (SWA-1-1, SWA-1-2, SWA-1-3), transect 4 (SWA-4-10, SWA-4-11, SWA-4-12), and wells SWA-2-4 and SWA-2-6.
[d] IC-ICPMS = Ion chromatography inductively coupled plasma mass spectrometry.
[e] — = None.
[f] TAL = Target analyte list.
[g] GC/MS-SIM = Gas chromatography/mass spectrometry–selective ion monitoring.
[h] SVOC = Semivolatile organic compound.
[i] n/a = Not applicable.
[j] >10 cfs = Greater than 10 cfs for E121 and E123 or greater than 1 cfs for E122; up to four samples.

Table 2.2-4
ISCO Bottle Configurations and Analytical Suites for the
2021 Storm Water Sampling Plan for E121, E122, and E123

Sample Bottle (1 L)	Start Time (min) 12-Bottle ISCO	Analytical Suites 12-Bottle ISCO	Start Time (min) 24-Bottle ISCO	Analytical Suites 24-Bottle ISCO
1	Peak+10	SSC; particle size	Trigger	SSC
2	Peak+12	PCBs (UF[a]) Part 1[b]	Trigger+2	SSC
3	Peak+14	DOC[c] (F[d]) + alkalinity (UF) + pH (UF)	Trigger+4	SSC
4	Peak+16	PCBs (UF) Part 2[b]	Trigger+6	SSC
5	Peak+18	TAL metals[e] + boron + uranium + hardness (F/UF) + total recoverable aluminum (F10µ[f])	Trigger+8	SSC
6	Peak+20	PAH (UF)	Trigger+10	SSC
7	Peak+22	SVOC[g] (UF)	Trigger+12	SSC
8	Peak+24	Gross alpha (UF)	Trigger+14	SSC
9	Peak+26	SSC	Trigger+16	SSC
10	Peak+28	Extra bottle	Trigger+18	SSC
11	Peak+30	Extra bottle	Trigger+20	SSC
12	Peak+32	Extra bottle	Trigger+22	SSC
13	n/a[h]	n/a	Trigger+24	SSC
14	n/a	n/a	Trigger+26	SSC
15	n/a	n/a	Trigger+28	SSC
16	n/a	n/a	Trigger+30	SSC
17	n/a	n/a	Trigger+50	SSC
18	n/a	n/a	Trigger+70	SSC
19	n/a	n/a	Trigger+90	SSC
20	n/a	n/a	Trigger+110	SSC
21	n/a	n/a	Trigger+130	SSC
22	n/a	n/a	Trigger+150	SSC
23	n/a	n/a	Trigger+170	SSC
24	n/a	n/a	Trigger+190	SSC

Notes: E121 = Sandia right fork at power plant, E122 = Sandia left fork at asphalt plant or south fork of Sandia at E122, and E123 = Sandia below wetland. The 12-bottle ISCO begins collection 10 min after the peak discharge (i.e., “Peak+10”) and the 24-bottle ISCO begins collection as soon as water is detected by the liquid level actuator (i.e., “Trigger”).

[a] UF = Unfiltered.

[b] Bottles 2 and 4 are to be sent to the analytical laboratory together for one PCB analysis.

[c] DOC = Dissolved organic carbon.

[d] F = Filtered through a 0.45-µm membrane.

[e] Target analyte list (TAL) metals are Ag, Al, As, Ba, Be, Ca, Cd, Co, Cr, Cu, Fe, Hg, K, Mg, Mn, Na, Ni, Pb, Sb, Se, Tl, V, and Zn; hardness is calculated from Ca and Mg, components of the TAL list.

[f] F10µ = Filtered through a 10-µm membrane.

[g] SVOC = Semivolatile organic compound.

[h] n/a = Not applicable.

Table 2.2-5
Completion Data for Alluvial Piezometers and Collocated Alluvial Wells

Piezometers									
	SCPZ-1	**SCPZ-2**	**SCPZ-3**	**SCPZ-4**	**SCPZ-6**	**SCPZ-10**	**SCPZ-11(A)**	**SCPZ-11(B)**	**SCPZ-12**
Total length (ft)	20.5	11.4	8.3	8.3	8.3	8.3	8.3	8.3	8.3
Stick up (ft)	4.36	3.26	3.19	3.16	3.18	4.01	3.8	4.48	3.77
Top of screen (ft bgs[a])	13.8	6.0	3	3	3	3	3	1	3
Total depth/bottom of screen (ft bgs)	16.2	8.3	5.4	5.4	5.4	5.4	5.4	5.4	5.4
Alluvial Wells									
	SWA-1-1	**SWA-1-2**	**SWA-1-3**	**SWA-2-4**	**SWA-2-6**	**SWA-4-10**		**SWA-4-11**	**SWA-4-12**
Ground elevation (ft amsl[b])	7239.90	7239.96	7239.23	7223.25	7222.90	7209.60	No collocated well	7210.70	7210.50
Total length (ft)	18.33	13.17	9.37	9.00	8.22	8.44		7.93	8.19
Stick up (ft)	3.03	4.57	3.37	3.23	2.86	3.46		3.37	2.54
Top of screen (ft bgs)	13.0	6.03	3.0	3.0	3.12	2.5		3.0	2.99
Bottom of screen (ft bgs)	15.5	8.53	5.5	5.5	5.62	5		5.5	5.49
Total depth (ft bgs)	16.0	9.03	6.0	6.0	6.12	5.5		6.0	5.99
Total depth (ft bTOC[c])	18.76	13.35	9.40	9.04	8.66	8.48		9.16	8.05

Note: Alluvial well shown below collocated piezometer.

[a] bgs = Below ground surface

[b] amsl = Above mean sea level.

[c] ft bTOC = feet below top of casing (measured in field and could vary).

Table 2.2-6
Field Parameter Data for Alluvial Locations and Surface Water Stations—2021 Sampling Events

Location Name	Date	Dissolved Oxygen (mg/L)	Oxidation-Reduction Potential (mV)	pH	Specific Conductance (µS/cm)	Temperature (°C)	Turbidity (NTU[a])
Surface Water Stations							
Sandia right fork at Pwr Plant (E121)	02/09/2021	8.79	ND[b]	8.19	443.6	8.7	1.19
	05/03/2021	8.11	ND	8.13	512.0	12.7	1.2
	08/03/2021	7.05	ND	8.01	497.8	19.3	1.16
	11/19/2021	8.39	ND	8.16	549.0	11.0	3.08
South fork of Sandia at E122	02/09/2021	5.51	ND	8.22	969.0	10.5	43.81
	05/03/2021	6.72	ND	8.04	353.7	16.0	105
	08/03/2021	5.63	ND	7.89	350.6	22.5	4.44
	11/19/2021	7.36	ND	8.23	284.3	14.9	1.38
Sandia below Wetlands (E123)	02/09/2021	10.30	ND	7.86	656.0	2.0	3.44
	05/03/2021	8.65	ND	7.84	499.7	8.9	1.55
	08/03/2021	7.03	ND	7.63	463.1	14.6	3.8
	11/19/2021	10.48	ND	7.75	538.0	2.8	1.13
Alluvial Wells							
SWA-1-1	10/28/2021	0.35	-150.7	7.12	560.0	13.4	2.78
SWA-1-2	10/29/2021	0.63	-98.2	7.08	447.9	12.9	3.67
SWA-1-3	10/27/2021	0.89	-84.1	7.00	446.9	10.9	4.59
SWA-2-4	10/28/2021	0.59	-83.9	6.76	496.3	10.2	5.77
SWA-2-6	10/28/2021	0.63	-143.8	7.14	584.0	9.7	11.65
SWA-4-10	10/29/2021	2.47	86	6.21	501.0	10.3	32.12
SWA-4-11	10/29/2021	0.74	-30.3	6.73	437.7	7.6	4.75
SWA-4-12	10/29/2021	0.64	-51.9	6.62	524.0	10.2	6.11

[a] NTU = Nephelometric turbidity unit.

[b] ND = No data.

Table 2.2-7
Installation and Calibration Information for Transducers in Alluvial Wells

Well	Installation Date	Transducer Calibration Date	Level TROLL 500 PSI Rating
SWA-1-1	10/19/2021	6/17/2021	15 psi
SWA-1-2	10/19/2021	6/22/2021	15 psi
SWA-1-3	10/19/2021	6/22/2021	15 psi
SWA-2-4	10/19/2021	6/7/2021	15 psi
SWA-2-6	10/25/2021	6/23/2021	15 psi
SWA-4-10	1/15/2021	7/30/2020	15 psi
SWA-4-11	1/15/2021	10/22/2020	15 psi
SWA-4-12	1/15/2021	10/21/2020	15 psi

Table 3.1-1
Travel Time of Flood Bore, Peak Discharge, Increase or Decrease in Peak Discharge, and Percent Change in Peak Discharge from Upgradient to Downgradient of the Wetland for Each Sample-Triggering Storm Event in 2021

Date	Travel Time from E121 to E123 (min)	Peak Discharge (cfs)				Travel Time from E122 to E123 (min)	Peak Discharge (cfs)			
		E121	E123	+/–[a]	%[b]		E122	E123	+/–[a]	%[b]
5/30/2021	100	15	13	-	13	100	6.4	13	+	103
6/2/2021	95	8.8	12	+	36	100	4.0	12	+	200
6/3/2021	135	2.2	2.4	+	9.1	135	2.0	2.4	+	20
6/17/2021	115	7.3	7.4	+	1.4	110	3.6	7.4	+	106
6/19/2021	no peak[c]	0.24	0.29	+	21	no peak	1.9	0.29	-	85
6/27/2021	85	7.3	15	+	105	90	4.6	15	+	226
7/1/2021	115	3.9	7.8	+	100	115	3.2	7.8	+	144
Min	85	0.24	0.29	n/a[d]	n/a	90	1.9	0.29	n/a	n/a
Mean	108	6.4	8.3	n/a	n/a	108	3.7	8.3	n/a	n/a
Max	135	15	15	n/a	n/a	135	6.4	15	n/a	n/a

[a] + = Increase; - = decrease.

[b] % = Percent change in peak discharge.

[c] For the 6/19/21 storm event, only E122 had a peak – there were no peaks at E121 and E123.

[d] n/a = Not applicable.

Table 3.2-1
Geomorphic Changes Associated with Large Storm Events

Date*	Station	Peak Discharge (cfs)	Noted Erosion in Geomorphic Surveying
9/13/2013	E123	108	Extensive repairs were required, including the design and construction of best management practice run-on control structures, replacement of boulders and repair of the cascade pool liner, removal of deposited sediments, and replanting of the lost vegetation in the GCS (section 3.4.2 of "Completion Report for Sandia Grade-Control Structure," (LANL 2013, 251743).
7/7/2014	E123	80	Overall, erosion within the system seems to be associated with scouring in small side channels outside the wetland proper or with channel rearrangement within the wetland proper. There is evidence of increased channelization in the lower part of the wetland and a new nick point, located upgradient of the most upstream sheet pile.
7/8/2014	E123	76	Overall, erosion within the system seems to be associated with scouring in small side channels outside the wetland proper or with channel rearrangement within the wetland proper. There is evidence of increased channelization in the lower part of the wetland and a new nick point, located upgradient of the most upstream sheet pile.

Table 3.2-1 (continued)

Date*	Station	Peak Discharge (cfs)	Noted Erosion in Geomorphic Surveying
7/31/2014	E123	109	Overall, erosion within the system seems to be associated with scouring in small side channels outside the wetland proper or with channel rearrangement within the wetland proper. There is evidence of increased channelization in the lower part of the wetland and a new nick point, located upgradient of the most upstream sheet pile.
7/26/2017	E121	87	Repeat GPS surveys in conjunction with field observations indicated that no significant geomorphic changes occurred in the wetland after the 2017 monsoon season. A small amount of deposition was detected in the plunge pool from storm runoff but has not affected the plunge pool area.
7/26/2017	E123	78	Repeat GPS surveys in conjunction with field observations indicated that no significant geomorphic changes occurred in the wetland after the 2017 monsoon season. A small amount of deposition was detected in the plunge pool from storm runoff but has not affected the plunge pool area.

* There were no large storm events in 2015, 2016, 2018, 2019, 2020, or 2021.

Table 3.3-1
Calculated Sediment Yield and Runoff Volume at Gaging Stations
E121, E122, and E123 for Each Sample-Triggering Storm Event from 2014 to 2021

Station	Date	Sediment Yield (ton)	Sediment Volume (yd^3)	Runoff Volume (acre-feet)	Peak Discharge (cfs)
2021					
E121	5/30/2021	0.52	0.23	0.32	15
E121	6/2/2021	2.06	0.92	0.36	8.8
E121	6/17/2021	0.31	0.14	0.20	7.3
E121	6/27/2021	0.29	0.13	0.55	7.3
E121	7/1/2021	0.13	0.06	0.12	3.9
E122	6/3/2021	0.02	0.01	0.03	2.0
E122	6/17/2021	0.18	0.08	0.23	3.6
E122	6/27/2021	0.05	0.02	0.14	4.6
E122	7/1/2021	0.06	0.03	0.24	3.2
E123	5/30/2021	0.51	0.23	1.14	13
E123	6/2/2021	0.37	0.17	1.18	12
E123	6/17/2021	0.30	0.13	0.71	7.4
E123	6/27/2021	0.49	0.22	2.42	15
2020					
E121	8/1/2020	0.70	0.31	0.39	19
E122	7/27/2020	0.07	0.03	0.02	2.1
E123	8/2/2020	0.51	0.23	1.3	14

Table 3.3-1 (continued)

Station	Date	Sediment Yield (ton)	Sediment Volume (yd^3)	Runoff Volume (acre-feet)	Peak Discharge (cfs)
2019					
E121	7/2/2019	1.43	0.64	0.8	25
E121	7/7/2019	0.17	0.08	0.7	16
E121	7/15/2019	0.72	0.32	1.2	33
E121	7/25/2019	0.32	0.14	1.0	34
E121	7/26/2019	1.21	0.54	2.2	36
E122	7/2/2019	0.12	0.05	0.1	3.7
E122	7/13/2019	0.04	0.02	0.1	1.8
E122	7/15/2019	0.18	0.08	0.3	5.2
E123	7/7/2019	0.36	0.16	1.4	12
E123	7/15/2019	0.62	0.28	2.1	24
E123	7/25/2019	0.45	0.20	1.8	29
E123	7/26/2019	1.75	0.78	6.1	40
2018					
E121	7/15/2018	0.09	0.04	0.4	14
E121	7/17/2018	0.46	0.21	0.9	29
E121	8/7/2018	0.19	0.09	0.5	18
E121	8/9/2018	0.63	0.28	0.6	21
E121	8/15/2018	0.57	0.25	0.9	42
E121	9/4/2018	0.40	0.18	1.3	38
E122	7/15/2018	0.03	0.01	0.1	3.3
E122	8/9/2018	0.23	0.10	0.2	3.8
E122	9/4/2018	0.40	0.18	0.4	4.3
E123	7/17/2018	1.72	0.77	3.6	31
E123	9/3/2018	0.68	0.30	2.7	21
E123	9/4/2018	2.02	0.90	3.7	35
2017					
E121	6/6/2017	0.70	0.31	0.8	26
E121	6/25/2017	0.71	0.32	1.7	21
E121	7/18/2017	0.48	0.22	1.5	36
E121	7/26/2017	4.09	1.83	2.8	87
E121	7/29/2017	0.88	0.40	1.4	30
E122	7/18/2017	0.11	0.05	0.2	5
E122	7/27/2017	0.02	0.01	0.1	2
E122	7/29/2017	0.13	0.06	0.3	5
E122	8/21/2017	<0.01	<0.01	0.2	2
E123	6/25/2017	1.10	0.49	2.9	30
E123	7/26/2017	8.79	3.94	6.2	78
E123	7/29/2017	0.64	0.29	2.7	29

Table 3.3-1 (continued)

Station	Date	Sediment Yield (ton)	Sediment Volume (yd^3)	Runoff Volume (acre-feet)	Peak Discharge (cfs)
2016					
E121	7/1/2016	0.36	0.16	0.8	22
E121	7/15/2016	0.26	0.12	1.2	22
E121	7/31/2016	1.80	0.81	2.7	47
E121	8/3/2016	0.34	0.15	1.6	37
E121	8/27/2016	1.57	0.70	1.9	51
E121	9/6/2016	0.75	0.34	1.5	40
E121	11/4/2016	0.15	0.07	0.8	8.4
E122	10/3/2016	0.02	0.01	0.1	22
E122	10/8/2016	0.01	0.01	0.1	22
E122	11/4/2016	0.03	0.01	0.1	47
E123	7/31/2016	0.34	0.15	4.0	46
E123	8/3/2016	2.10	0.94	2.9	13
E123	8/27/2016	0.54	0.24	3.3	28
E123	9/6/2016	0.15	0.07	3.1	18
E123	11/5–11/6/2016	0.16	0.07	3.4	15
2015					
E121	6/1/2015	0.45	0.20	1.7	20
E121	6/26/2015	3.88	1.74	1.3	18
E121	7/3/2015	0.71	0.32	1.6	30
E121	7/15–7/16/2015	0.50	0.22	1.3	39
E121	7/20–7/21/2015	1.62	0.73	4.0	50
E121	7/29–7/30/2015	0.38	0.17	2.2	14
E121	7/31/2015	0.27	0.12	1.1	9.2
E121	8/17/2015	0.45	0.20	1.6	36
E121	10/23–10/24/2015	0.38	0.17	2.0	28
E122	10/23–10/24/2015	0.07	0.03	0.4	5.1
E123	7/3/2015	1.26	0.56	3.9	35
E123	7/20–7/21/2015	2.58	1.16	10.6	64
E123	7/29–7/30/2015	0.84	0.37	5.8	29
E123	8/8/2015	0.15	0.07	1.8	16
E123	8/17/2015	1.06	0.47	3.2	38
E123	10/20/2015	0.25	0.11	1.9	16
E123	10/23/2015	1.19	0.53	4.6	48

Table 3.3-1 (continued)

Station	Date	Sediment Yield (ton)	Sediment Volume (yd^3)	Runoff Volume (acre-feet)	Peak Discharge (cfs)
2014					
E121	7/7/2014	0.84	0.38	2.3	63
E121	7/14–7/15/2014	0.19	0.09	0.7	4.8
E121	7/15–7/16/2014	1.64	0.73	0.6	10
E121	7/19/2014	3.22	1.44	0.6	11
E121	7/27–7/28/2014	0.57	0.26	0.9	29
E121	7/31/2014	15.4	6.91	2.9	66
E122	7/8/2014	0.60	0.27	1.0	10
E122	7/27–7/28/2014	0.05	0.02	0.6	6.2
E122	7/29/2014	0.73	0.33	1.2	12
E122	7/31/2014	1.55	0.69	1.0	19
E123	5/23/2014	1.62	0.73	2.7	18
E123	7/7/2014	4.12	1.84	6.4	80
E123	7/8/2014	18.2	8.14	7.0	76
E123	7/15–7/16/2014	2.01	0.90	3.1	20
E123	7/19/2014	0.39	0.17	1.7	18
E123	7/29/2014	7.36	3.30	7.5	62
E123	7/31/2014	28.6	12.8	7.2	109

Note: Sediment yield and volume were not calculated for the storm events at E122 on 6/19/2021 or 7/17/2020 because the 24-bottle ISCO did not collect samples. Therefore, there were not enough SSC samples to make an accurate calculation.

Table 3.3-2
Analytical Exceedances in Surface Water at Gaging Stations E121, E122, and E123

Gage	Sample Date	Analyte	Field Prep Code[b]	Sample Type[c]	Result	MDL[d]	PQL[e]	Unit[f]	Hardness Used[g]	Exceedance Ratio[a]				
										LW[h]	WH[i]	AAL[j]	CAL[k]	HH-OO[l]
E121	02/09/2021	Total PCB	UF	WS	0.00439	—[m]	—	µg/L	—	—	0.03	<0.01	0.03	6.86
E121	05/03/2021	Total PCB	UF	WS	0.00443	—	—	µg/L	—	—	0.03	<0.01	0.03	6.92
E121	05/30/2021	Aluminum	F10µ	WT	1370	19.3	50.0	µg/L	24.1	—	—	2.81	7.02	—
E121	05/30/2021	Copper	F	WT	5.45	0.300	2.00	µg/L	24.1	0.01	—	1.55	2.05	—
E121	05/30/2021	Dioxin[n]	UF	WT	4.94E-05	—	—	µg/L	—	—	—	—	—	968
E121	05/30/2021	Lead	F	WT	1.04	0.500	2.00	µg/L	24.1	0.01	—	0.08	2.00	—
E121	05/30/2021	Total PCB	UF	WT	2.44	—	—	µg/L	—	—	174	1.22	174	3813
E121	05/30/2021	Zinc	F	WT	33.8	3.30	20.0	µg/L	24.1	<0.01	—	0.77	1.02	<0.01
E121	06/02/2021	Aluminum	F10µ	WT	1870	19.3	50.0	µg/L	17.7	—	—	5.86	14.62	—
E121	06/02/2021	Copper	F	WT	4.25	0.300	2.00	µg/L	17.7	0.01	—	1.62	2.08	—
E121	06/02/2021	Dioxin	UF	WT	1.19E-06	—	—	µg/L	—	—	—	—	—	23.41
E121	06/02/2021	Total PCB	UF	WT	1.4	—	—	µg/L	—	—	100	0.70	100	2188
E121	06/17/2021	Aluminum	F10µ	WT	505	19.3	50.0	µg/L	29.1	—	—	0.80	2.00	—
E121	06/17/2021	Copper	F	WT	10.5	0.300	2.00	µg/L	29.1	0.02	—	2.50	3.37	—
E121	06/17/2021	Zinc	F	WT	61.2	3.30	20.0	µg/L	29.1	<0.01	—	1.18	1.55	<0.01
E121	06/27/2021	Aluminum	F10µ	WT	738	19.3	50.0	µg/L	12.1	—	—	3.89	9.71	—
E121	06/27/2021	Copper	F	WT	3.42	0.300	2.00	µg/L	12.1	0.01	—	1.86	2.32	—
E121	06/27/2021	Dioxin	UF	WT	7.80E-07	—	—	µg/L	—	—	—	—	—	15.29
E121	06/27/2021	Total PCB	UF	WT	1.01	—	—	µg/L	—	—	72.1	0.51	72.1	1578
E121	06/27/2021	Zinc	F	WT	25.7	3.30	20.0	µg/L	12.1	<0.01	—	1.10	1.45	<0.01
E121	07/01/2021	Aluminum	F10µ	WT	532	19.3	50.0	µg/L	21.5	—	—	1.28	3.19	—
E121	07/01/2021	Copper	F	WT	6.15	0.300	2.00	µg/L	21.5	0.01	—	1.95	2.55	—
E121	07/01/2021	Dioxin	UF	WT	1.52E-06	—	—	µg/L	—	—	—	—	—	29.72

Table 3.3-2 (continued)

Gage	Sample Date	Analyte	Field Prep Code[b]	Sample Type[c]	Result	MDL[d]	PQL[e]	Unit[f]	Hardness Used[g]	Exceedance Ratio[a]				
										LW[h]	WH[i]	AAL[j]	CAL[k]	HH-OO[l]
E121	07/01/2021	Total PCB	UF	WT	1.89	—	—	μg/L	—	—	135	0.95	135	2953
E121	08/03/2021	Total PCB	UF	WS	0.00551	—	—	μg/L	—	—	0.39	<0.01	0.39	8.61
E121	11/19/2021	Total PCB	UF	WS	0.00329	—	—	μg/L	—	—	0.24	<0.01	0.24	5.14
E122	02/09/2021	Total PCB	UF	WS	0.0153	—	—	μg/L	—	—	1.09	0.01	1.09	23.9
E122	06/03/2021	Aluminum	F10μ	WT	555	19.3	50.0	μg/L	33.5	—	—	0.73	1.81	—
E122	06/03/2021	Copper	F	WT	7.86	0.300	2.00	μg/L	33.5	0.02	—	1.64	2.23	—
E122	06/03/2021	Dioxin	UF	WT	7.92E-06	—	—	μg/L	—	—	—	—	—	155
E122	06/03/2021	Total PCB	UF	WT	0.0905	—	—	μg/L	—	—	6.46	0.05	6.46	141
E122	06/03/2021	Zinc	F	WT	66.4	3.30	20.0	μg/L	33.5	<0.01	—	1.12	1.48	<0.01
E122	06/17/2021	Aluminum	F10μ	WT	472	19.3	50.0	μg/L	26.6	—	—	0.85	2.11	—
E122	06/17/2021	Copper	F	WT	20.3	0.300	2.00	μg/L	26.6	0.04	—	5.26	7.03	—
E122	06/17/2021	Dioxin	UF	WT	1.46E-05	—	—	μg/L	—	—	—	—	—	286
E122	06/17/2021	Total PCB	UF	WT	0.369	—	—	μg/L	—	—	26.4	0.18	26.4	577
E122	06/17/2021	Zinc	F	WT	89.7	3.30	20.0	μg/L	26.6	<0.01	—	1.87	2.47	<0.01
E122	06/19/2021	Total PCB	UF	WT	0.0058	—	—	μg/L	—	—	0.41	<0.01	0.41	9.06
E122	06/27/2021	Aluminum	F10μ	WT	544	19.3	50.0	μg/L	12.3	—	—	2.80	7.00	—
E122	06/27/2021	Copper	F	WT	8.15	0.300	2.00	μg/L	12.3	0.02	—	4.37	5.54	—
E122	06/27/2021	Dioxin	UF	WT	1.42E-05	—	—	μg/L	—	—	—	—	—	279
E122	06/27/2021	Lead	F	WT	0.74	0.500	2.00	μg/L	12.3	0.01	—	0.12	3.06	—
E122	06/27/2021	Total PCB	UF	WT	0.173	—	—	μg/L	—	—	12.4	0.09	12.4	270
E122	06/27/2021	Zinc	F	WT	40.8	3.30	20.0	μg/L	12.3	<0.01	—	1.71	2.26	<0.01
E122	07/01/2021	Aluminum	F10μ	WT	809	19.3	50.0	μg/L	18.2	—	—	2.44	6.09	—
E122	07/01/2021	Copper	F	WT	6.95	0.300	2.00	μg/L	18.2	0.01	—	2.57	3.33	—
E122	07/01/2021	Dioxin	UF	WT	9.40E-06	—	—	μg/L	—	—	—	—	—	184
E122	07/01/2021	Lead	F	WT	0.628	0.500	2.00	μg/L	18.2	0.01	—	0.06	1.66	—
E122	07/01/2021	Total PCB	UF	WT	0.174	—	—	μg/L	—	—	12.4	0.09	12.4	272

Table 3.3-2 (continued)

Gage	Sample Date	Analyte	Field Prep Code[b]	Sample Type[c]	Result	MDL[d]	PQL[e]	Unit[f]	Hardness Used[g]	Exceedance Ratio[a]				
										LW[h]	WH[i]	AAL[j]	CAL[k]	HH-OO[l]
E122	07/01/2021	Zinc	F	WT	40.8	3.30	20.0	µg/L	18.2	<0.01	—	1.20	1.59	<0.01
E122	08/03/2021	Total PCB	UF	WS	0.00318	—	—	µg/L	—	—	0.23	<0.01	0.23	4.97
E122	11/19/2021	Total PCB	UF	WS	0.00121	—	—	µg/L	—	—	0.09	<0.01	0.09	1.89
E123	02/09/2021	Total PCB	UF	WS	0.0206	—	—	µg/L	—	—	1.47	0.01	1.47	32.2
E123	05/03/2021	Total PCB	UF	WS	0.00281	—	—	µg/L	—	—	0.20	<0.01	0.20	4.39
E123	05/30/2021	Aluminum	F10µ	WT	1190	19.3	50.0	µg/L	29.9	—	—	1.82	4.54	—
E123	05/30/2021	Copper	F	WT	8.18	0.300	2.00	µg/L	29.9	0.02	—	1.90	2.56	—
E123	05/30/2021	Dioxin	UF	WT	4.95E-06	—	—	µg/L	—	—	—	—	—	97.0
E123	05/30/2021	Total PCB	UF	WT	0.185	—	—	µg/L	—	—	13.2	0.09	13.2	289
E123	06/02/2021	Aluminum	F10µ	WT	1300	19.3	50.0	µg/L	32.0	—	—	1.81	4.52	—
E123	06/02/2021	Copper	F	WT	6.05	0.300	2.00	µg/L	32.0	0.01	—	1.32	1.79	—
E123	06/02/2021	Dioxin	UF	WT	6.25E-06	—	—	µg/L	—	—	—	—	—	123
E123	06/02/2021	Total PCB	UF	WT	0.302	—	—	µg/L	—	—	21.6	0.15	21.6	472
E123	06/17/2021	Copper	F	WT	9.74	0.300	2.00	µg/L	46.6	0.02	—	1.49	2.09	—
E123	06/17/2021	Dioxin	UF	WT	7.71E-08	—	—	µg/L	—	—	—	—	—	1.51
E123	06/17/2021	Total PCB	UF	WT	0.0425	—	—	µg/L	—	—	3.04	0.02	3.04	66.4
E123	06/27/2021	Aluminum	F10µ	WT	700	19.3	50.0	µg/L	19.3	—	—	1.95	4.86	—
E123	06/27/2021	Copper	F	WT	5.32	0.300	2.00	µg/L	19.3	0.01	—	1.87	2.42	—
E123	06/27/2021	Dioxin	UF	WT	1.20E-07	—	—	µg/L	—	—	—	—	—	2.36

Table 3.3-2 (continued)

Gage	Sample Date	Analyte	Field Prep Code[b]	Sample Type[c]	Result	MDL[d]	PQL[e]	Unit[f]	Hardness Used[g]	Exceedance Ratio[a]				
										LW[h]	WH[i]	AAL[j]	CAL[k]	HH-OO[l]
E123	06/27/2021	Total PCB	UF	WT	0.0944	—	—	μg/L	—	—	6.74	0.05	6.74	148
E123	08/03/2021	Benzo(a)anthracene	UF	WS	0.34	0.300	1.00	μg/L	—	—	—	—	—	1.89
E123	08/03/2021	Total PCB	UF	WS	0.00828	—	—	μg/L	—	—	0.20	<0.01	0.20	4.39
E123	11/19/2021	Total PCB	UF	WS	0.00149	—	—	μg/L	—	—	0.11	<0.01	0.11	2.33

[a] Analytical results are normalized by calculating an exceedance ratio. This ratio is defined as the analytical result divided by the applicable water quality standard. Thus, results exceeding the standard will be greater than an exceedance ratio of 1.0.

[b] Field preparation code: UF = unfiltered; F10μ = filtered to 10 μm; F = filtered to 0.45 μm.

[c] Sample type: WS = base flow; WT = storm water.

[d] MDL = Method detection limit.

[e] PQL = Practical quantitation limit or uncertainty.

[f] Unit applies to result, MDL, PQL, and screening level.

[g] The hardness measured during the storm event was used to calculate hardness-based screening levels. Hardness units are mg/L.

[h] LW = Livestock watering.

[i] WH = Wildlife habitat.

[j] AAL = Acute aquatic life.

[k] CAL = Chronic aquatic life.

[l] HH-OO = Human health-organism only.

[m] — = Not provided by the analytical laboratory or not applicable.

[n] The dioxin criteria apply to the sum of the dioxin toxicity equivalents expressed as 2,3,7,8-tetrachlorodibenzo-p-dioxin. The exceedances are driven by PCB concentrations.

Table 3.3-3
Summary of 2021 Base Flow and Storm Water Surface Water Quality Criteria Exceedances

Location	Media Type	Filtration	Analyte	Total Samples	Number of Samples Exceeding SWQC[a]	Average of Sample Results Exceeding SWQC	Maximum Sample Results Exceeding SWQC	Unit
E121	Storm water	F10μ[b]	Aluminum	5	5	1003	1870	μg/L
E122	Storm water	F10μ	Aluminum	5	4	595	809	μg/L
E123	Storm water	F10μ	Aluminum	4	3	1063	1300	μg/L
E123	Base flow	UF[c]	Benzo(a)anthracene	4	1	0.34	0.34	μg/L
E121	Storm water	F[d]	Copper	5	5	5.95	10.5	μg/L
E122	Storm water	F	Copper	5	4	10.8	20.3	μg/L
E123	Storm water	F	Copper	4	4	7.32	9.74	μg/L
E121	Storm water	UF	Dioxin[e]	4	4	1.32E-05	4.94E-05	μg/L
E122	Storm water	UF	Dioxin	5	4	1.15E-05	1.46E-05	μg/L
E123	Storm water	UF	Dioxin	4	4	2.85E-06	6.25E-06	μg/L
E121	Storm water	F	Lead	5	1	1.04	1.04	μg/L
E122	Storm water	F	Lead	5	2	0.684	0.740	μg/L
E121	Storm water	UF	Total PCB	4	4	1.69	2.44	μg/L
E122	Storm water	UF	Total PCB	5	5	0.16	0.37	μg/L
E123	Storm water	UF	Total PCB	4	4	0.16	0.30	μg/L
E121	Base flow	UF	Total PCB	4	4	0.00441	0.00551	μg/L
E122	Base flow	UF	Total PCB	4	3	0.00656	0.01530	μg/L
E123	Base flow	UF	Total PCB	4	4	0.00830	0.02060	μg/L
E121	Storm water	F	Zinc	5	3	40.2	61.2	μg/L
E122	Storm water	F	Zinc	5	4	59.4	89.7	μg/L

[a] SWQC = Surface water quality criteria.
[b] F10μ = Filtered to 10 μm.
[c] UF = Unfiltered.
[d] F = Filtered to 0.45 μm.
[e] The dioxin criteria apply to the sum of the dioxin toxicity equivalents expressed as 2,3,7,8-tetrachlorodibenzo-p-dioxin. The exceedances are driven by PCB concentrations.

Table 3.4-1
Analytical Exceedances in the Alluvial System

Location	Sample Date	Parameter Name	Field Prep Code	Sample Usage Code	Sample Purpose	Report Result	Limit Unit	Screening Value	Screening Value Type
SWA-1-1	10/27/2021	Iron	F[a]	INV	REG	5520	µg/L	1000	NM GW STD[b]
SWA-1-1	10/27/2021	Manganese	F	INV	REG	1230	µg/L	200	NM GW STD
SWA-1-2	10/27/2021	Chromium	F	INV	REG	60.1	µg/L	50	NM GW STD
SWA-1-2	10/27/2021	Iron	F	INV	REG	1980	µg/L	1000	NM GW STD
SWA-1-2	10/27/2021	Manganese	F	INV	REG	262	µg/L	200	NM GW STD
SWA-1-3	10/27/2021	Iron	F	INV	REG	1960	µg/L	1000	NM GW STD
SWA-2-4	10/28/2021	Iron	F	INV	REG	1820	µg/L	1000	NM GW STD
SWA-2-4	10/28/2021	Manganese	F	INV	REG	600	µg/L	200	NM GW STD
SWA-2-6	10/28/2021	Iron	F	INV	REG	5610	µg/L	1000	NM GW STD
SWA-2-6	10/28/2021	Manganese	F	INV	REG	1300	µg/L	200	NM GW STD
SWA-4-10	10/29/2021	Iron	F	INV	REG	2110	µg/L	1000	NM GW STD
SWA-4-10	10/29/2021	Manganese	F	INV	REG	445	µg/L	200	NM GW STD
SWA-4-11	10/29/2021	Iron	F	INV	REG	1390	µg/L	1000	NM GW STD
SWA-4-11	10/29/2021	Iron	F	QC	FD	1440	µg/L	1000	NM GW STD
SWA-4-11	10/29/2021	Manganese	F	INV	REG	251	µg/L	200	NM GW STD
SWA-4-11	10/29/2021	Manganese	F	QC	FD	266	µg/L	200	NM GW STD
SWA-4-12	10/29/2021	Iron	F	INV	REG	4310	µg/L	1000	NM GW STD
SWA-4-12	10/29/2021	Manganese	F	INV	REG	1330	µg/L	200	NM GW STD

Note: All results have a dilution factor of 1.0.

[a] F = Filtered.

[b] NM GW STD = New Mexico Water Quality Control Commission groundwater standard.

Appendix A

Acronyms and Abbreviations,
Metric Conversion Table, and Data Qualifier Definitions

A-1.0 ACRONYMS AND ABBREVIATIONS

AAL	acute aquatic life
amsl	above mean sea level
AOC	area of concern
As(III)	arsenite
As(V)	arsenate
bgs	below ground surface
bTOC	below top of casing
CAL	chronic aquatic life
cfs	cubic foot per second
Cr(III)	trivalent chromium
Cr(VI)	hexavalent chromium
CY	calendar year
DC	direct current
DEM	digital elevation model
DOC	dissolved organic carbon
EPA	Environmental Protection Agency (U.S.)
F	filtered
Fe(III)	ferric oxide
Fe(II)	ferrous oxide
GC/MS-SIM	gas chromatography/mass spectrometry–selective ion monitoring
GCS	grade-control structure
gpd	gallons per day
GPS	Global Positioning System
HH-OO	human health-organism only
IC-ICPMS	ion chromatography inductively coupled plasma mass spectrometry
IR	investigation report
LANL	Los Alamos National Laboratory
LiDAR	light detection and ranging
LW	livestock watering
MCL	maximum contaminant level
MDL	method detection limit
Mn(IV)	manganese dioxide

N3B	Newport News Nuclear BWXT-Los Alamos, LLC
ND	no data
NMAC	New Mexico Administrative Code
NMED	New Mexico Environment Department
NPDES	National Pollutant Discharge Elimination System
NTU	nephelometric turbidity unit
PAH	polycyclic aromatic hydrocarbon
PCB	polychlorinated biphenyl
PQL	practical quantitation limit
PVC	polyvinyl chloride
redox	oxidation-reduction
SCC	Strategic Computing Complex
SERF	Sanitary Effluent Reclamation Facility
SSC	suspended sediment concentration
SVOC	semivolatile organic compound
SWQC	surface water quality criteria
SWWS	Sanitary Waste Water System
TA	technical area
TAL	target analyte list
TSS	total suspended sediment
UF	unfiltered
USGS	U.S. Geological Survey
WH	wildlife habitat

A-2.0 METRIC CONVERSION TABLE

Multiply SI (Metric) Unit	by	To Obtain U.S. Customary Unit
kilometers (km)	0.622	miles (mi)
kilometers (km)	3281	feet (ft)
meters (m)	3.281	feet (ft)
meters (m)	39.37	inches (in.)
centimeters (cm)	0.03281	feet (ft)
centimeters (cm)	0.394	inches (in.)
millimeters (mm)	0.0394	inches (in.)
micrometers or microns (µm)	0.0000394	inches (in.)
square kilometers (km^2)	0.3861	square miles (mi^2)
hectares (ha)	2.5	acres
square meters (m^2)	10.764	square feet (ft^2)
cubic meters (m^3)	35.31	cubic feet (ft^3)
kilograms (kg)	2.2046	pounds (lb)
grams (g)	0.0353	ounces (oz)
grams per cubic centimeter (g/cm^3)	62.422	pounds per cubic foot (lb/ft^3)
milligrams per kilogram (mg/kg)	1	parts per million (ppm)
micrograms per gram (µg/g)	1	parts per million (ppm)
liters (L)	0.26	gallons (gal.)
milligrams per liter (mg/L)	1	parts per million (ppm)
degrees Celsius (°C)	9/5 + 32	degrees Fahrenheit (°F)

A-3.0 DATA QUALIFIER DEFINITIONS

Data Qualifier	Definition
U	The analyte was analyzed for, but not detected.
J	The analyte was positively identified, and the associated numerical value is estimated to be more uncertain than would normally be expected for that analysis.
J+	The analyte was positively identified, and the result is likely to be biased high.
J-	The analyte was positively identified, and the result is likely to be biased low.
UJ	The analyte was not positively identified in the sample, and the associated value is an estimate of the sample-specific detection or quantitation limit.
R	The data are rejected as a result of major problems with quality assurance/quality control (QA/QC) parameters.

Appendix B

2021 Geomorphic Changes in Sandia Canyon Reach S-2

B-1.0 INTRODUCTION

This appendix evaluates geomorphic changes that occurred in Sandia Canyon reach S-2 between 2018 and 2021. Geomorphic changes were evaluated using light detecting and imaging (LiDAR) data collected over the entire Sandia wetland area. This methodology, in which LiDAR surveys are planned to occur every 3 yr, was originally outlined in the “2018 Sandia Wetland Performance Report” (N3B 2019, 700415) and replaced previously implemented ground-based Global Positioning System survey methods. Aerial-derived data sets from 2018 and 2021 are compared to depict geomorphic variability with the aim of evaluating the stability of the Sandia wetland within Los Alamos National Laboratory (LANL or the Laboratory).

B-2.0 DIGITAL ELEVATION MODEL GENERATION AND GEOMORPHIC CHANGE ESTIMATION PROCEDURES

Surveys of the entire Sandia wetland area of interest were performed using LiDAR equipment to collect geomorphic data. A baseline LiDAR aerial survey was performed in November 2018 and new aerial LiDAR data were collected in October 2021. A detailed digital elevation model (DEM) of the entire active channel within the wetland area and surrounding canyon was developed from each set of LiDAR data.

The 2018 LiDAR data were collected with a RIEGL 1560i LiDAR sensor and a Phase One digital frame camera mounted on a fixed-wing aircraft. LiDAR was acquired with a point density of 6 points per square meter; Figure B-2.0-1 presents the point density for this survey in the Sandia wetland. See Attachment B-1 for a detailed description the LiDAR collection process in 2018. The 2021 LiDAR data were collected with a Teledyne Optech Galaxy T2000 LiDAR sensor mounted on a fixed-wing aircraft; Figure B-2.0-2 presents the point density (points per square meter) for the 2021 survey in the Sandia wetland. The Galaxy T2000 scanner collects points at a density of 6.8 points per square meter; to ensure point-density thresholds were met, double coverage was planned into the LiDAR flights. See Attachment B-2 for a detailed description of coverage over the area of interest and the flight plan. Ground points were collected to accompany the aerial survey. The ground survey points serve as calibration and check points. The complete summary of the ground survey and the survey points is included as Attachment B-3. Attachment B-2 provides details as to how the ground points were used to calibrate and quality-check the LiDAR flights.

Two different techniques, a raster-based and a vector-based technique, were used for geomorphic change detection. The raster-based change detection approach used DEM differencing by comparing elevations from 2018 and 2021 (Figure B-2.0-3). The change detection DEM represents the vertical difference between the 2021 ground elevations and the 2018 ground elevations; further detail of the data processing is included in Attachment B-2. Elevation changes from -0.5 ft to +0.5 ft are set to “transparent” as a threshold. These thresholds are based on the absolute vertical accuracy of LiDAR Quality Level 1 data, which is approximately 10 cm. However, when change detection is calculated between two data sets, the vertical accuracy decreases to about 14 cm (or approximately 0.5 ft) because of error propagation. In highly vegetated areas, such as wetlands, small changes are more difficult to detect and there are more false positives, which can result in large geomorphic changes being detected that are actually due only to variation in vegetation height. In 2022, an aerial vegetation survey will be conducted; the combination of the vegetation and geomorphic data (to be included in the 2022 annual report) will more accurately characterize change in the Sandia wetland.

The vector-based change detection approach was completed for the 2018 and 2021 data sets as well. This approach only used the “ground” classified points from the LiDAR point cloud and implemented a vertical threshold of 0.5 ft of change and a point cluster size of 100 ft^2. The vertical and point size clusters were selected to avoid false positives from change related to either vertical or horizontal error. This approach indicated several areas of change within the Sandia wetland (Figure B-2.0-4). Additional details regarding the collection of LiDAR data, developments of surface and change detection DEMs, and change detection vector data can be found in the LiDAR Mapping Project 2018 Collection Data Delivery Report (Attachment B-1) and LiDAR Mapping Project 2021 Collection Data Delivery Report (Attachment B-2).

B-3.0 HYDROLOGIC EVENTS DURING THE 2021 MONSOON SEASON

In 2021 there were seven sample-triggering storm events, presented in Table B-3.0-1. The largest runoff-producing event in 2021 at stream gaging stations E121 and E122 (upstream of reach S-2) and E123 (downstream of the wetland and grade-control structure [GCS]) occurred on May 30, 2021 (section 3.0 of the main text presents additional details). The 24-hour rainfall total measured by the E121.9 rain gage in Sandia Canyon (upstream of reach S-2) on May 30 was 0.36 in. The maximum measured discharge at each gaging station occurred on May 30 at E121 (15 cubic feet per second [cfs]); on May 30 at E122 (6.4 cfs); and on June 27 at E123 (16 cfs) (Table B-3.0-1). The largest storm event occurred on June 27, 2021, and measured 0.64 in. of rainfall in 24-hr. The 2021 peak discharge was similar to the 2020 peak discharge at all gaging stations and slightly below (E122) or well below (E121 and E123) the mean for the 10-yr period of record.

B-4.0 MONITORING RESULTS

The monsoon season of 2021 resulted in minor annual changes to morphology of monitored features and caused no significant geomorphic changes within reach S-2.

B-4.1 Thalweg and Stream Bank

In 2018 the thalweg was ground-surveyed. In 2021, because of dense vegetation and braided channels, the LiDAR-derived thalweg was difficult to distinguish; this area will be ground-truthed in 2022 to verify the thalweg.

Stream banks in the reach between the plunge pool and the GCS (Figure B-4.1-1) show minimal changes from 2018 to 2021. Differences between the bank characterizations may be attributed to error in the DEM and likely do not reflect significant erosion or deposition within the Sandia wetland. This is supported by recent field visits to the wetland where no significant bank changes were noted; this will also be confirmed in field visits to the wetland in 2022.

B-4.2 Plunge Pool

The plunge pool is the uppermost feature of the Sandia wetland area and serves to dissipate flow energy before it enters the wetland. It is located downstream of a culvert that conveys outfall discharge from Technical Area 03. Discharge from the culvert maintains the water level in the plunge pool. The plunge pool area has been surveyed using ground-based techniques since 2013 (N3B 2019, 700415). In 2021 the LiDAR DEM was used to digitize the plunge pool perimeter.The ground-based surveys of the plunge pool in past years, and the LiDAR data in 2021, have shown minimal change, indicating that the plunge pool is stable (Table B-4.2-1 and Figure B-4.2-1).

B-4.3 Ground-Truth Field Verification

Areas of geomorphic change identified in the change detection DEM will be field-verified in 2022. There is geomorphic change in the Sandia wetland greater than 0.5 ft vertically and an area larger than 100 ft^2; these areas are shown in Figure B-2.0-4. The presence of dense vegetation within the wetland area, which can have a high variability in height between years, can make it difficult to accurately model the ground surface. Thus the current change detection results are likely overestimating geomorphic change in the wetland. The 2022 vegetation survey will also help correct the error, wherein changes in vegetation can be combined with changes in geomorphology to identify significant geomorphic change versus change in vegetation.

Additionally, the plunge pool perimeter, thalweg, and bank tops will be surveyed using ground-based techniques in 2022. The ground-based survey techniques in combination with the geomorphic change detection and the vegetation data will help to present a complete picture of current conditions and recent change in the Sandia wetland. These findings will be presented in the 2022 report.

B-5.0 CONCLUSIONS AND RECOMMENDATIONS

In 2021, storm water peak discharge did not exceed 100 cfs at gaging station E123; therefore, no additional visual inspection of the wetland to document qualitative geomorphic changes was warranted. However, an annual walkdown with the New Mexico Environment Department (NMED) was performed in 2021, as discussed in section 3.3 of the main text, and minimal change was identified.

The 2018 to 2021 raster-based change detection exhibits greater geomorphic change than is expected (when compared with the 2016 raster-based change detection given the absence of any large hydrologic events in the timeframes evaluated). This is likely due to the absence of an error correction applied to account for the dense vegetation present in the wetland. High variability in vegetation height is most likely contributing to the majority of change currently being detected using the raster-based change detection technique. In 2022, change detected in the 2018 to 2021 change detection DEM will be field verified and compared with the aerial vegetation surveys. Field verification and vegetation data will determine which changes detected were geomorphic change and which were due to vegetation changes. This information will be presented in the 2022 report.

If no large storm events that create significant geomorphic and/or vegetative change occur, aerial surveys will be performed every third year. The next vegetation survey is scheduled to occur in the summer of 2022. Beginning in the 2022 annual report, the vegetation and geomorphic data will be presented together. This will allow for a more comprehensive analysis of the stability of the wetland area. The vegetation surveys assess the extent and species composition of wetland vegetation as well as the overall health of the vegetation and vegetation height. The stability of wetland vegetation is intricately linked to geomorphic stability. Being able to display these data together will be especially helpful in interpreting the geomorphic change detection results, as vegetation is likely impacting the accuracy of that analysis. In the future, the vegetation and geomorphic surveying will be performed during the same year in order to align the wetland change detection methods. The next aerial-based survey is scheduled for 2025.

B-6.0 REFERENCES AND MAP DATA SOURCES

B-6.1 Reference

The following reference list includes documents cited in this appendix. Parenthetical information following each reference provides the author(s), publication date, and ERID, ESHID, or EMID. ERIDs were assigned by Los Alamos National Laboratory's (the Laboratory's) Associate Directorate for Environmental Management (IDs through 599999); ESHIDs were assigned by the Laboratory's Associate Directorate for Environment, Safety, and Health (IDs 600000 through 699999); and EMIDs are assigned by N3B (IDs 700000 and above).

N3B (Newport News Nuclear BWXT-Los Alamos, LLC), April 2019. "2018 Sandia Wetland Performance Report," Newport News Nuclear BWXT-Los Alamos, LLC, document EM2019-0091, Los Alamos, New Mexico. (N3B 2019, 700415)

B-6.2 Map Data Sources

Structures; Los Alamos National Laboratory, KSL Site Support Services, Planning, Locating and Mapping Section; 06 January 2004; as published 29 November 2010.

Hillshade; N3B/T2S, As published, GIS projects folder; \\n3b-fs01\n3b-shares) (Q: GIS DATA) 2014; BareEarth; BareEarth_DEM_Mosaic_Overviews; BareEarth_DEM_Mosaic.gdb

Sandia Wetlands 2019 Boundary; Sandia 2019 Wetlands Vegetation Density; N3B/T2S, As published, GIS projects folder; \\n3b-fs01\n3b-shares) (Q: GIS DATA) Project: 19-0056; project_data.gdb; sandia_density raster data set; 2020.

Contours, 20 and 2-ft interval; N3B/T2S, As published, GIS projects folder; \\n3b-fs01\n3b-shares) (Q: GIS DATA) Project: 19-0056; project_data.gdb; line feature data set; site_contour feature class; 2020.

2017 GPS Thalweg; N3B/T2S, As published, GIS projects folder; \\n3b-fs01\n3b-shares) (Q: GIS DATA) Project: 19-0056; project_data.gdb; line feature data set; T2017_Sandia_Thalweg_ln feature class; 2020.

2019 Aerial plunge pool; N3B/T2S, As published, GIS projects folder; \\n3b-fs01\n3b-shares) (Q: GIS DATA) \LANL Hyperspectral Data\Species_Distribution\West_AOI\W_Surface_Water.shp 2020.

2019 Bank top; N3B/T2S, As published, GIS projects folder; \\n3b-fs01\n3b-shares) (Q: GIS DATA) Project: 19-0056; project_data.gdb; line feature data set; T2018_Sandia_Canyon_BankTops_Line feature class; 2020.

2019 Plunge Pool; 3B/T2S, As published, GIS projects folder; Q:\LANL Hyperspectral Data\Species_Distribution\West_AOI\W_Surface_Water.shp 2020.

Surrounding Land: As published; N3B GIS project folder: Q:\16-Projects\16-0033\project_data.gdb\polygon\pline_lab_county; October 2019.

TA Boundary: As published; Triad SDE Spatial Geodatabase: GISPUBPRD1\PUB.Boundaries\PUB.Tecareas; October 2019.

Major Road: As published; Q:\16-Projects\16-0033\project_data.gdb\line\major_road; October 2019.

LANL Boundary: As published; Triad SDE Spatial Geodatabase: GISPUBPRD1\PUB.Boundaries\PUB.lanlarea; December 2021.

Tech Areas: As published; Triad SDE Spatial Geodatabase: GISPUBPRD1\PUB.Boundaries\PUB.tecareas; December 2020.

2019 Sandia Wetlands: As published, N3B/T2S, GIS projects folder; \\N3B-fs01\N3B-shares) (Q: GIS DATA) Project: 22-0004; project_data.gdb; poly feature dataset; wetland_outline_2019_revise; Information assumed to have originated from TPMC and was transferred to N3B/T2S sometime during the 2018 timeframe. Data as published, February 2022.

Buildings: As published, County of Los Alamos GIS Server: (https://gis.losalamosnm.us/securegis/rest/services/basemaps/basemap/FeatureServer); February 2022.

Drainage features: As published; Triad SDE Spatial Geodatabase: GISPUBPRD1\PUB.Hydrology\PUB.EM_sw_watercourse; February 2022.

Index and Terrain Contours (All Intervals): As published, N3B/T2S, GIS projects folder; \\N3B-fs01\N3B-shares) (Q: GIS DATA) Project: 22-0004; project_data.gdb; line feature dataset; site_contour; All contours generated from the 2021 Geotiff data as collected and processed by TetraTech's Geoinformatics Group; N3B/T2S, GIS projects folder; \\N3B-fs01\N3B-shares) Q:\GIS Drive\Lidar_2021\2021\03_DEM (change detection area)\NAVD88\GeoTIFF\. February 2022.

Grade-control structure: As published, N3B/T2S, GIS projects folder; \\N3B-fs01\N3B-shares) (Q: GIS DATA) Project: 12-Projects\12-0019\shp\dissolve_cad_export.shp; Information assumed to have originated from TPMC and was transferred to N3B/T2S sometime during the 2018 timeframe. Data as published, 2019.

Canyon Reaches: As published; Triad SDE Spatial Geodatabase: GISPUBPRD1\PUB.regulatory\PUB.canyon_reaches; February 2022.

Cascade Pool: As published, N3B/T2S, GIS projects folder; \\N3B-fs01\N3B-shares) (Q: GIS DATA) Project: 14-0015\shp\sandia_wetlands\cascade_pool.shp; Information assumed to have originated from TPMC and was transferred to N3B/T2S sometime during the 2018 timeframe. Data as published, February 2022.

Sandia wells (point features): As published; EIM data pull, February 2022.

Culvert: As published, N3B/T2S, GIS projects folder; \\N3B-fs01\N3B-shares) (Q: GIS DATA) Project: 14-0015\shp\sandia_wetlands\site_culverts.shp; Data as published, February 2022.

Paved Road: As published; Triad SDE Spatial Geodatabase: GISPUBPRD1\PUB.Infrastructure\PUB.paved_rds_arc; February 2022.

Unpaved Road: As published; Triad SDE Spatial Geodatabase: GISPUBPRD1\PUB.Infrastructure\PUB.paved_rds_arc, February 2022.

Thalweg 2018: As published, N3B/T2S, GIS projects folder; \\N3B-fs01\N3B-shares) (Q: GIS DATA) Project: 22-0004; project_data.gdb; line feature dataset; thalweg_2018_2021; Information assumed field collected/verified by handheld GPS sometime during or before 2018. As published, February 2022.

Thalweg 2021: As published, N3B/T2S, GIS projects folder; \\N3B-fs01\N3B-shares) (Q: GIS DATA) Project: 22-0004; project_data.gdb; line feature dataset; thalweg_2018_2021; As published, February 2022.

Fences: As published; Triad SDE Spatial Geodatabase: GISPUBPRD1\PUB.Infrastructure\PUB.fences_arc; December 2020.

Paved Parking: As published; Triad SDE Spatial Geodatabase: GISPUBPRD1\PUB.Infrastructure\PUB.paved_prkg_arc; February 2022.

2018 2021 change detection in elevation: As published, N3B/T2S, GIS projects folder; \\N3B-fs01\N3B-shares) (Q: GIS DATA) Lidar_2021\2021\04_Change_Detection\dz_difference. Data as collected and processed by TetraTech's Geoinformatics Group, February 2022.

Former Los Alamos County landfill: As published, N3B/T2S, GIS projects folder; \\N3B-fs01\N3B-shares) (Q: GIS DATA) Project: 14-0015; project_data.gdb; former_LA_landfill; February 2022.

2021 GeoTiff: As published, N3B/T2S, GIS projects folder; \\N3B-fs01\N3B-shares) (Q: GIS DATA). Data as collected and processed by TetraTech's Geoinformatics Group; N3B/T2S, GIS projects folder; \\N3B-fs01\N3B-shares) Q:\GIS Drive\Lidar_2021\2021\03_DEM (change detection area)\NAVD88\GeoTIFF\. February 2022.

Gage stations (point features): As published; EIM data pull, February 2022.

Banktop (2018, 2019, 2021): As published, N3B/T2S, GIS projects folder; \\N3B-fs01\N3B-shares) (Q: GIS DATA) Project: 22-0004; project_data.gdb; line feature dataset; banktops_2018_2019_2021, February 2022.

2018 plunge pool: As published, N3B/T2S, GIS projects folder; \\N3B-fs01\N3B-shares) (Q: GIS DATA) Project: 22-0004; project_data.gdb; poly feature dataset; T2018_Sandia_Canyon_Plunge_Poly, February 2022.

Watershed: As published; Triad SDE Spatial Geodatabase: GISPUBPRD1\PUB.Hydrology\PUB.Watersheds, February 2022.

Site orthophoto (NMLOSA18_Delivery.ecw): As published, N3B/T2S, GIS projects folder; \\N3B-fs01\N3B-shares) (Q: GIS DATA) GIS Drive\Aerial\2018\ECW\NMLOSA18_Delivery.ecw, February 2022.

2018 LiDAR point density feature class: As published, N3B/T2S, GIS projects folder; \\N3B-fs01\N3B-shares) (Q: GIS DATA) Project: 22-0004; project_data.gdb; poly feature dataset; point_info_point_density, February 2022.

2021 LiDAR point density feature class: As published, N3B/T2S, GIS projects folder; \\N3B-fs01\N3B-shares) (Q: GIS DATA) Project: 22-0004; project_data.gdb; poly feature dataset; outfile_point_info_2021, February 2022.

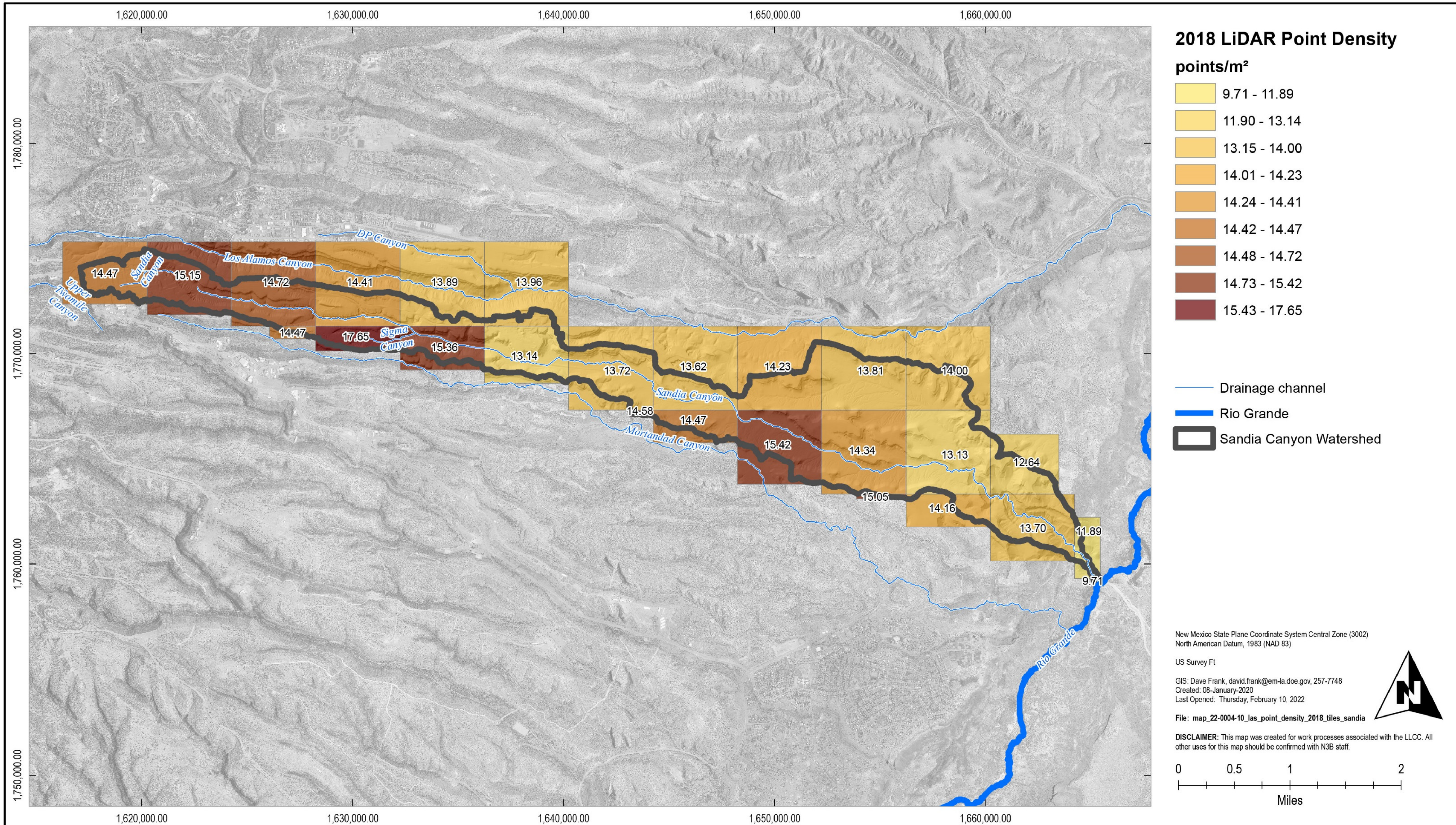

Figure B-2.0-1 2018 LiDAR survey point density in the Sandia Canyon watershed

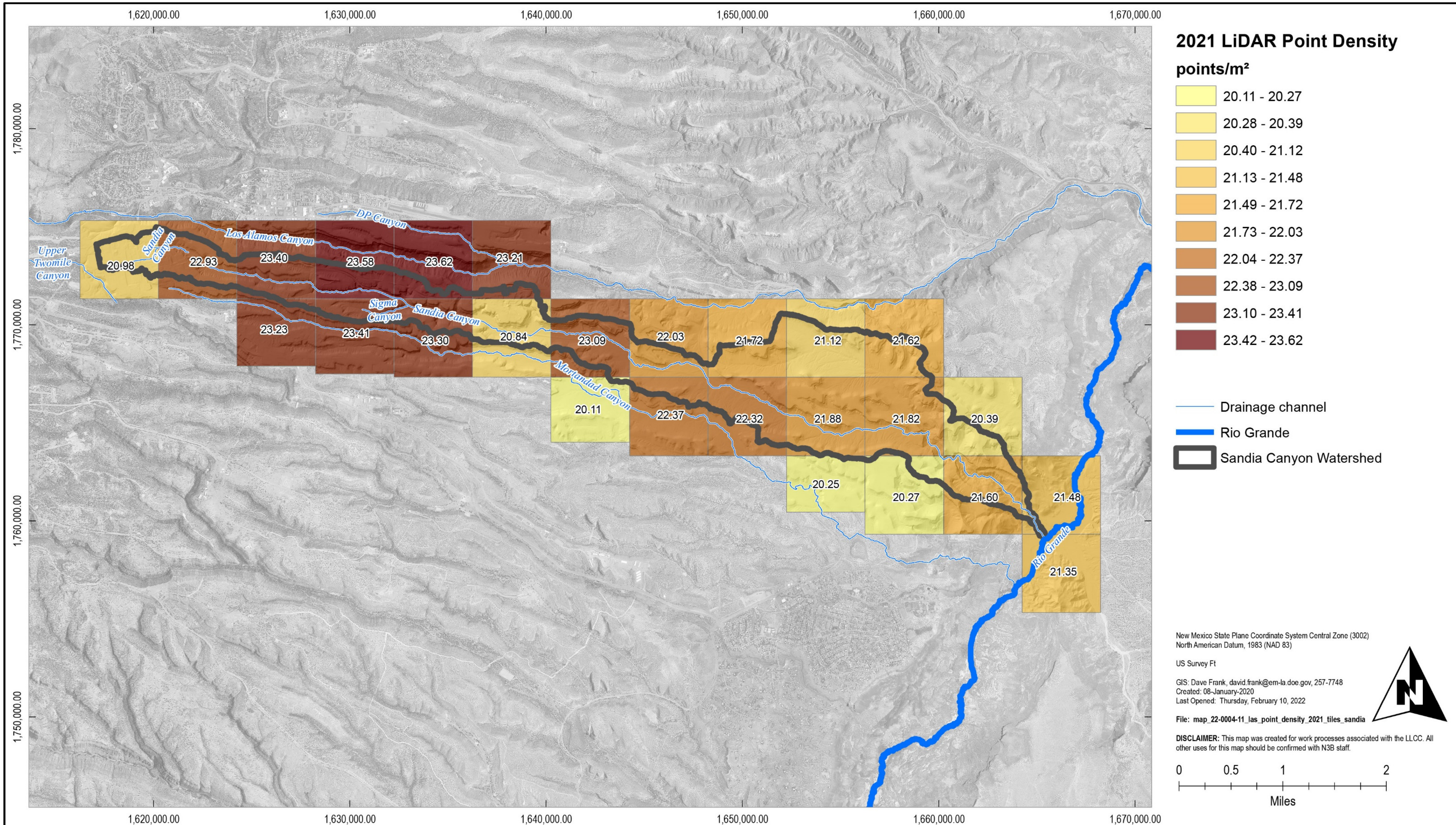

Figure B-2.0-2 2021 LiDAR survey point density in the Sandia Canyon watershed

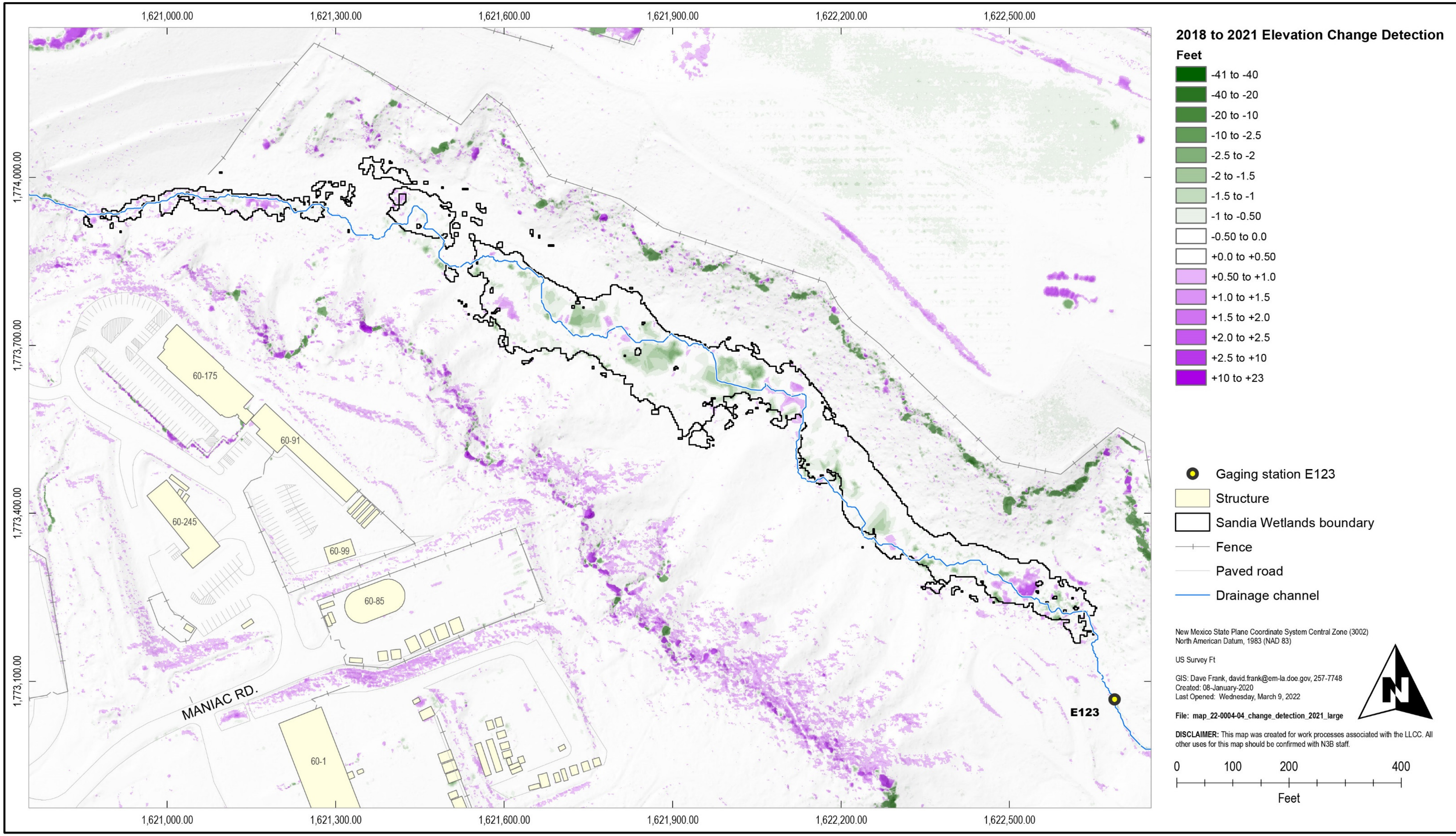

Figure B-2.0-3 2018 to 2021 LiDAR change detection DEM in the Sandia Wetland

Figure B-2.0-4 2018 to 2021 LiDAR vector change detection in the Sandia wetland

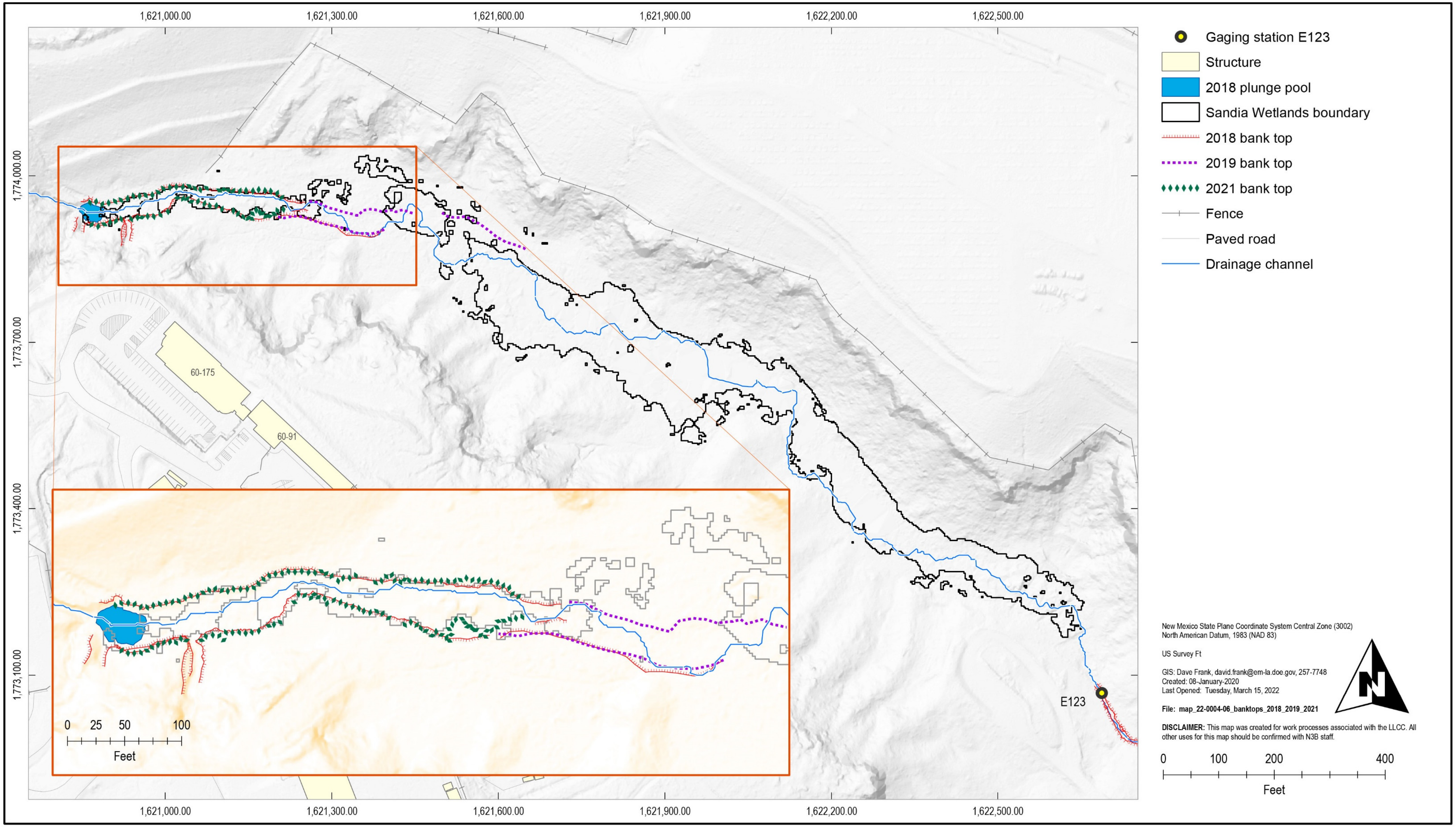

Figure B-4.1-1 2018 to 2021 bank top comparison

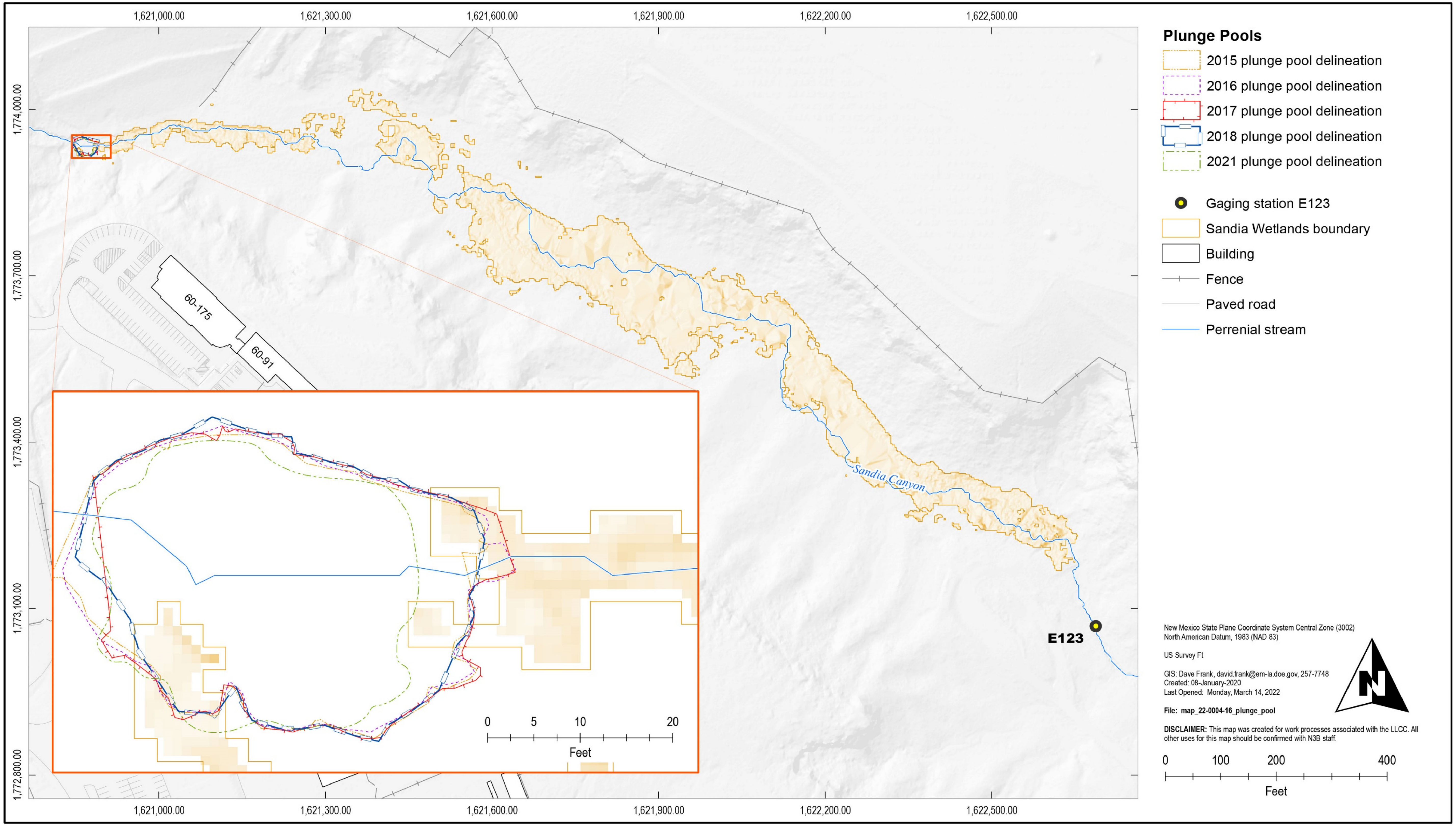

Figure B-4.2-1 2015 to 2021 plunge pool perimeter in Sandia Canyon

Table B-3.0-1
All Precipitation Events in 2021 Resulting in a Discharge Exceeding the Sampling Trip Level at Gaging Stations within the Sandia Wetland Reach S-2

Storm Event Date	RG121.9 Total Precipitation (in.)	E121 Peak Discharge (cfs)	E122 Peak Discharge (cfs)	E123 Peak Discharge (cfs)
5/30/2021	0.36	15 S[a]	6.4 NS[b]	15 S
6/2/2021	0.35	8.8 S	4.1 NS	14 S
6/3/2021	0	2.2 BT[c]	2.1 S	3.2 BT
6/17/2021	0.2	7.3 S	3.7 S	8.5 S
6/19/2021	0.01	0.26 NS	2.5 S	0.9 NS
6/27/2021	0.64	8.0 S	4.6 S	16 S
7/1/2021	0.24	3.9 S	3.3 S	9.0 NS

[a] S = Sample was collected.

[b] NS = Previous sample had not yet been retrieved so sample could not be collected.

[c] BT = Below trip level.

Table B-4.2-1
Plunge Pool Area and Growth Assessment

Year	Area (ft^2)	Area (m^2)	Percent Change in Area from Previous Survey
2021	867.6	80.6	18.8
2018	1067.7	99.2	5.03
2017	1124.2	104.4	1.9
2016	1103.4	102.5	2.4
2015	1077.9	100.1	3.4
2014	1042.5	96.9	18.5
2013[a]	879.5	81.7	n/a[b]

[a] 2013 is the baseline survey year for plunge pool perimeter mapping.

[b] n/a = Not applicable.

Attachment B-1

Los Alamos National Laboratory
LiDAR Mapping Project 2018 Collection Data Delivery Report
(on CD included with this document)

Attachment B-2

Los Alamos National Laboratory
LiDAR Mapping Project Data Delivery Report
(on CD included with this document)

Attachment B-3

Survey Report Summary for
35 Check Point LiDAR Support Project
(on CD included with this document)

Appendix C

2021 Watershed Mitigation Inspections

C-1.0 INTRODUCTION

Watershed storm water controls and grade-control structures (GCSs) are inspected biannually and after greater than 50–cubic foot per second (cfs) flow events. After large disturbance events (approximately 100 cfs at gaging station E123), additional inspections and monitoring will occur, including a walkdown of the channel. No large disturbance events occurred in 2021.

Inspections are completed to ensure watershed mitigations are functioning properly and to determine if maintenance is required. Examples of items evaluated during inspections include

- debris/sediment accumulation that could impede operation;
- water levels behind retention structures;
- physical damage of structure or failure of structural components;
- undermining, piping, flanking, settling, movement, or breeching of structure;
- vegetation establishment and vegetation that may negatively impact structural components;
- rodent damage;
- vandalism; and
- erosion.

The photographs in this appendix show the first and second 2021 inspections of watershed mitigations in Sandia Canyon. Each group of photographs is associated with a specific feature (e.g., standpipe, weir, upstream, downstream, vegetated cover) that could develop issues. Photographs of features were taken to replicate previous inspection photos as closely as possible.

In 2021, the Sandia GCS downstream gage did not record significant flow events. Two regular inspections were conducted in May and October of 2021. The post-monsoon walkdown of the Sandia wetland with the New Mexico Environment Department (NMED) took place on November 1, 2021. Recommended and completed maintenance is listed in the table below with photographs in section C-3.0.

Table C-1.0-1
Sandia Wetlands Maintenance

Maintenance	Date Recommended	Date Completed	Corresponding Photos
Remove coir log downstream of log check dams to address local scour.	11/4/2020	5/13/2021	C-3.0-1, C-3.0-2
Remove tire and debris from canyon.	11/4/2020	5/13/2021	C-3.0-3
Install log berms and rock check dams to address erosion and sediment migration from western side drainages.	10/19/2021	12/3/2021	C-3.0-4, C-3.0-5, C-3.0-6, C-3.0-7, C-3.0-8

The photographs in section C-2.0 illustrate the health of the wetland in and around the GCS, revegetation of adjacent slopes, and the best management practices put in place to help maintain the integrity of the GCS and its associated wetland vegetation.

Additional data on the position of the channel thalweg in the area of the GCS can be found in Appendix B of this report. Quantitative data from vegetation perimeter mapping in and around the GCS can be found in Appendix B of the 2019 Sandia Wetland Performance Report (N3B 2020, 700810).

C-2.0 SANDIA CANYON GRADE-CONTROL STRUCTURE INSPECTION PHOTOGRAPHS

C-2.1 Grade-Control Structure South Bank Vegetation

Photo C-2.1-1 May 13, 2021 – South bank vegetation, looking upstream/west

Photo C-2.1-2 October 19, 2021 – South bank vegetation, looking upstream/northwest

C-2.2 Grade-Control Structure North Bank Vegetation

Photo C-2.2-1 October 19, 2021 – North bank vegetation, looking upstream/southwest (no May photo)

C-2.3 Upper Grade-Control Structure

Photo C-2.3-1 May 13, 2021 – Upper grade-control structure, looking north

Photo C-2.3-2 October 19, 2021 – Upper grade-control structure, looking north

C-2.4 Middle Grade-Control Structure

Photo C-2.4-1 May 13, 2021 – Middle grade-control structure, looking north

Photo C-2.4-2 October 19, 2021 – Middle grade-control structure, looking north

C-2.5 Lower Grade-Control Structure

Photo C-2.5-1 May 13, 2021 – Lower grade-control structure, looking north

Photo C-2.5-2 October 19, 2021 – Lower grade-control structure, looking south

C-2.6 Cascade Structure

Photo C-2.6-1 May 13, 2021 – Cascade structure, looking upstream/northwest

Photo C-2.6-2 October 19, 2021 – Cascade structure, looking upstream/northwest

C-2.7 Run-On Defense Cell Barriers

Photo C-2.7-1 May 13, 2021 – Lower run-on cell barrier, looking west. Sediment level at 3 to 4 ft below top of spillway

Photo C-2.7-2 October 19, 2021 – Lower run-on cell barrier, looking west. Sediment level at 3 to 4 ft below top of spillway

C-2.8 Log Check Dams and Flow Spreader

Photo C-2.8-1 May 13, 2021 – Channel upgradient of upper log check dam, looking west

Photo C-2.8-2 October 19, 2021 – Channel upgradient of upper log check dam, looking south

Photo C-2.8-3 May 13, 2021 – Upper log check dam, looking west

Photo C-2.8-4 October 19, 2021 – Upper log check dam, looking southwest

Photo C-2.8-5 May 13, 2021 – Lower log check dam, looking south

Photo C-2.8-6 October 19, 2021 – Lower log check dam, looking southwest

Photo C-2.8-7 May 13, 2021 – Flow spreader, looking southwest

Photo C-2.8-8 October 19, 2021 – Flow spreader, looking east

C-3.0 MAINTENANCE PHOTOGRAPHS

Photo C-3.0-1 May 13, 2021 – Coir log recommended for removal to address local scour, looking south

Photo C-3.0-2 May 13, 2021 – Coir log removed, looking southeast

Photo C-3.0-3 May 13, 2021 – Trash removal

Photo C-3.0-4 October 19, 2021 – Sediment migrating into wetlands from side drainage. Recommend controls be installed to mitigate

Photo C-3.0-5 October 19, 2021 – Sediment migrating into wetlands from side drainage. Recommend controls be installed to mitigate

Photo C-3.0-6 December 22, 2021 – Log berms installed to address sediment migration from side drainage

Photo C-3.0-7 December 22, 2021 – Log berms installed to address sediment migration from side drainage

Photo C-3.0-8 December 22, 2021 – Rock check dam installed to address sediment migration from side drainage

Appendix D

Analytical Gaging Station, Alluvial Well,
and Sediment Data; Water-Level Data;
and 5-Min Stage, Discharge, and Precipitation Data
(on CD included with this document)